Molecular Dynamics Simulation of Interfacial Properties of Carbon Nanotube Reinforced Polymer Composites

A

Thesis

Submitted to

For the award of

DOCTOR OF PHILOSOPHY (Ph.D)

in

MECHANICAL ENGINEERING

by

Manish Dhawan

(41400175)

Supervised By

Dr. Raja Sekhar Dondapati

LOVELY FACULTY OF TECHNOLOGY AND SCIENCES
LOVELY PROFESSIONAL UNIVERSITY
PUNJAB
2019

`

DECLARATION

I declare that the thesis entitled **"Molecular Dynamics Simulation of Interfacial Properties of Carbon Nanotube Reinforced Polymer Composites"** has been prepared by me under the guidance of **Dr. Raja Sekhar Dondapati,** Associate Professor, School of Mechanical Engineering, Lovely Professional University, Phagwara, Punjab, India. No part of this thesis has formed the basis for the award of any degree or fellowship previously.

Manish Dhawan
Regd. No 41400175
Department of Mechanical Engineering,
Lovely Professional University
Phagwara, Punjab

DATE:

`

CERTIFICATE

I certify that **Manish Dhawan** bearing Regd. Number **41400175** has prepared his thesis entitled **"Molecular Dynamics Simulation of Interfacial Properties of Carbon Nanotube Reinforced Polymer Composites"** for the award of Ph. D degree of Lovely Professional University**,** under my guidance. He has carried out the work at the School of Mechanical Engineering, Lovely Professional University.

Dr. Raja Sekhar Dondapati
Associate Professor,
School of Mechanical Engineering,
Lovely Professional University, Phagwara, Punjab, India,
DATE:

`

PREFACE

The aim of present research work has been to study the Molecular Dynamics Simulation of Interfacial Properties of Carbon Nanotube Reinforced Polymer Composites. The study focuses on to find the effect of chirality, Nanotube length and diameter on properties of Carbon Nanotube (CNT) polymer composite using Molecular Dynamics (MD) simulation. The author also studied the damping and variation of damping loss factor with fiber volume fraction and fiber ratio and thermal conductivity of CNT reinforced polymers. The research work also include analysis of the effect of Stone-Wales and vacancy defects on thermo-mechanical properties The entire work carried out for this investigation has been presented in nine chapters.

Chapter-1 introduces Carbon Nano Tubes (CNT's), types of CNT's their properties, production, purification and applications along with introduction to polymers and Natural rubber, CNT defects and functionalized CNT Polymer composites. Chapter-2 begins with exhaustive survey of literature regarding CNT's, properties and applications of CNT's and CNT polymer composites. After comprehensive literature review problem formulation, scope and objectives of the study has been described. Chapter-3 describes about the materials under investigation and the methodologies employed. The parameters used for the present investigation has also been described in this chapter. Chapter-4 includes the findings and discussions of the study regarding the effect of chirality, nanotubes length and diameter on the interfacial properties of CNT reinforced polymer (NR) composites. Chapter-5 contains the results prediction of mechanical properties of CNT reinforced composites with fiber volume fraction and fibre ratio using MD simulation along with discussion of results. Chapter-6 includes the results and discussion regarding effect of Stone-Wales and vacancy defects on thermo-mechanical properties of CNT reinforced polymer nanocomposites. Chapter-7 deals with the results and discussion of the effect of functionalization of CNT's on the modulus of CNT composites and also predicted the thermal conductivity of the functionalized SWCNT/NR composite. Chapter-8 includes the prediction of damping of CNT's reinforced polymer composites using MD simulation. Chapter-9 contains the salient conclusions of the study regarding the study and the future scope of the study.

`

ACKNOWLEDGEMENTS

The author has great privilege to express his immense sense of gratitude to Dr. Raja Sekhar Dondapati, Associate Professor, School of Mechanical Engineering, Lovely Professional University, Phagwara, for his valuable guidance and untiring efforts throughout the tenure of this work. He has been an inspiring force where targets appeared to be difficult during the course of work. His timely help, constructive criticism and painstaking efforts made the author capable to compile the thesis in its present form.

It is a matter of great privilege and pride for me to express my sincere thanks and immense gratitude to Dr. Sumit Sharma, Assistant Professor, Mechanical Engineering Department, National Institute of Technology, Jalandhar for his valuable and intellectual guidance throughout the tenure of this work. His involvement, unflinching encouragement, amiable nature and easy accessibility have been immensely helpful to me.

Deep sense of gratitude is expressed to authorities of Lovely Professional University, Phagwara, for permitting the author to pursue his research work and extending necessary facilities during the experimental and analysis work. I also express my sincere thanks to Dr. Gurpreet Singh Phull, Head, School of Mechanical Engineering Lovely Professional University, Phagwara, for their cooperation and support. I would also acknowledge the support extended by IIT Delhi, IIT Roorkee and IIT Ropar for providing computational facilities in order to complete the simulations.

I wish to thank my friends and colleagues, for their moral support and help to keep things in perspective. Thanks are due to Dr. Rajeev Sobti, Professor & Dean, School of Computer Engineering Lovely Professional University, Phagwara, Mr. Navdeep Singh, Associate Professor & Dean, Division of Examination Lovely Professional University, Phagwara, and Mr. Raj Chawla for their everlasting support. Author is highly obliged and wishes to owe thanks to the technical staff of Lovely Professional University, Phagwara. The path towards this thesis spans several years of work, the author acknowledges his debt to all those who have helped along the way and seek apology that he could not mention personally one by one.

I humbly dedicate this work to my father, Late Sh. Mulkh Raj Dhawan, my mother Mrs. Adarsh Dhawan and parents-in-law, who are the source of inspiration and encouragement behind this research work. The author sincerely acknowledges the help

`

extended by them during the tenure of this work by sacrificing their comforts. At the same time, a sense of forgiveness is recorded for inability to provide probable help and attention they required during the entire duration. I would like to express my reverence and great admiration for brothers, sisters, brother-in-laws, sister-in-laws, nephews and nieces for their continual support and encouragement during the course of this work.

A sense of apology is due from my son, Naman Dhawan, who probably missed many precious moments of his childhood from fatherly love and affection. The wife of author, Deepika Dhawan, deserves special thanks and appreciation for him persistent moral support and giving her best to the growing son during the tenure of this work by sacrificing her comforts. Author is falling short of words to express gratitude to her for the determination shown to bear extra household responsibilities during the tenure of this work.

Above all, author is highly indebted to Great and Gracious Almighty God who blessed him with spiritual support and courage at each and every stage of this work.

MANISH DHAWAN

`

LIST OF FIGURES

`

`

`

`

`

LIST OF TABLES

`

`

LIST OF ABBREVIATIONS

CNT	Carbon nanotube
COMPASS	Condensed Phase Optimized Molecular Potential for Atomistic Simulation Studies
CVD	Carbon Vapour Deposition
EMD	Equilibrium Molecular Dynamics
FVF	Fiber Volume Fraction
ISS	Interfacial Shear Strength
LAMMPS	Large-scale Atomic/Molecular Massively Parallel Simulator
MD	Molecular Dynamics
MWCNT	Multi-Walled Carbon Nanotube
NEMD	Non-equilibrium Molecular Dynamics
NEMS	Nanoelectromechanical systems
NPT	Isothermal-Isobaric ensemble
NT	Nanotube
NVE	Micro-canonical ensemble
NVT	Canonical ensemble
PMMA	Poly-methyl metha-acrylate
PmPV	Poly m-phenylene vinylene
PP	Polypropylene
PVC	Polyvinyl chloride
PVT	Pressure Volume Temperature
SW	Stone-Wales
SWCNT	Single-Walled Carbon Nanotube

`

LIST OF SYMBOLS

$\mathbf{E_{11}}$	Longitudinal Young's modulus of composite
$\mathbf{E_{22}}$	Transverse Young's modulus of composite
$\mathbf{E_f}$	Young's modulus of fiber
$\mathbf{E_m}$	Young's modulus of matrix
$\mathbf{E_c}$	Young's modulus of composite
l/d	Aspect ratio of CNT/CNF
V_f	Volume fraction of fiber
$\boldsymbol{\tau}$	Surface density
$\boldsymbol{\gamma}$	Interfacial Shear Stress
$\mathbf{F_{II}}$	Pull-out forces

`

ABSTRACT

The discovery of CNT in 1991, started a new era in the world of materials science. The light-weight and ultra-tough materials replaced many other existing reinforcements to generate light weight composite materials with extraordinary mechanical properties. The purpose of this research is an investigation of the interfacial properties and mechanical properties of carbon nanotube reinforced Natural rubber composites as well as the different factors which affect the properties. The present study predicts the interfacial properties of the single-walled carbon nanotube (SWCNT) reinforced Natural rubber (NR) nanocomposites by using a series of pullout simulation using Molecular Dynamics (MD). Material Studio 2017© has been used as the tool for predicting all the properties. The variations in the potential energy and the pull-out force for the SWCNT reinforced NR nanocomposites was determined and the effects of nanotube length and diameter were studied for the pullout. In addition, the interfacial shear stress (ISS) and the surface density (γ) were predicted. The results showed that the incremental energy change increased sharply to a peak value at a specified displacement in the first stage and remained steady between specified peak values in the second stage. The average energy increment in the second stage (ΔE_{II}) was found to be independent of the nanotube length. ISS and γ decreased with increasing SWCNT diameter and converged at 113.47 MPa and 0.11 N/m.

Pristine carbon nanotubes (CNTs) exhibit exceptionally high mechanical properties. However, defects such as Stone-Wales (SW) and vacancy, which appears during manufacturing process, affect the performance of CNTs. In this study, armchair type single-walled CNT was considered and 1, 2, 4, 6, 8 and 10 vacancy defects and SW defects were introduced. Molecular Dynamics (MD) simulation was performed for investigating the effect of point and SW defects. All the defects follow the symmetric pattern for single walled carbon nanotube. Simulation has been done with CNTs packed in Natural rubber (NR) and mechanical properties were obtained. It is observed that as the number of vacancy defects or Stone Wales defects increases, the Young's modulus for CNT/Natural rubber composite successively degraded. However, in both the cases, the rate of decrease in young's moduli observed. Comparative study leads to a better design for NR-CNT composites. Further, a computational study based on Molecular Dynamics simulation is used to predict the mechanical and thermal behavior of carbon nanotubes (CNT) reinforced Natural rubber (NR) composites. A single-walled (5,5)

`

armchair type CNT is employed for this purpose. In this study, a comparison has been made between pristine and functionalized CNTs. The functionalization groups used in this study were carboxylic (-COOH), ester (-$COOCH_3$) and hydroxyl (-OH). The studies showed improvement in elastic properties of developed composites in the presence of functionalization group. In addition, the effect of volume fraction and 1-25% addition of functionalization group has been studied. The obtained simulation results show better load-transfer capacity in developed polymer system and improved elastic modulus. Thermal properties of developed composite systems were studied by non-equilibrium Molecular Dynamics method (NEMD). The addition of functionalized CNTs shows enhanced mechanical and thermal properties. Despite the different types of theoretical studies conducted on the macroscopic elastic behavior of CNTs, there remain the controversial issues regarding damping characteristics. Now a day, the damping properties of single walled carbon nanotubes were explored with great interest. Vibration produced in the structures due to dynamic loading creates unsafe operating conditions for the operator. It is essential to find the damping capacity of the material. Therefore, the damping loss factor has been calculated. With the addition of small percentage of CNTs, damping capacity of the material is improved due to the stick slip phenomena. It has been observed that the damping loss factor decreases with the increase in volume fraction and aspect ratio due to the slippery and curvy nature of single walled carbo nanotube reinforced polymer.

`

CONTENTS

`

Chapter 1

Introduction

In simple words, Carbon nanotube (CNT) is depicted as graphene sheet molded into a cylinder. In structural form, CNT is constructed from hexagonal rings of carbon. They can either be single layered or multi layered, and from this layering we derive its types, i.e. if CNT is single layered it is called as Single walled carbon nanotube (SWNT), or if it is multi layered it is called as Multi walled carbon nanotube (MWNT). A simple classification of CNT is shown in Figure 1.1[1]. Till now CNTs have fascinated many researchers because of their distinguished properties including physical properties as well as mechanical, thermal and electrical properties. CNTs were unknown three decades ago. Carbon Nanotubes are thin, as well as long hollow cylinders of carbon. It was the year 1991 when CNTs were discovered by Iijima [2]. As of late, greater fervor has been started for their comprehension and a lot of study has been performed. Still, the physical properties are yet being explored and researched upon. An unrestrained range of thermal, physical and electronic properties has been shown by the CNT's. All the above discussed properties vary with the type of nanotubes that are not just limited to SWNT or MWNT, both these types are having large amount of variety based upon various parameters such as length of nanotubes, their aspect ratio, functional group attached or angle of twist, etc. In most of the cases, even steel and Kevlar have a lower tensile strength than the carbon nanotubes.

The structure of CNT is created by carbon atom's layer and in hexagonal mess, these carbon atoms are tightly bonded with each other. Graphene is made of carbon's layer having thickness of one carbon atom. A carbon nanotube can be formed by wrapping in the cylindrical shape and bonding together. A nanotube having a single outer wall of carbon is known as a single-walled carbon nanotube and nanotube having multiple walls (cylinders inside another carbon cylinder) is known as multi-walled cylinder carbon nanotube.

1.1 Types of CNT

1.1.1 Single Walled Carbon Nanotube (SWCNT)

By rolling a sheet of graphite along chiral axis, we can obtain single walled nanotube. SWNT carries very large density of current without heating because of its ballistic nature of conduction of electrons and photons. Carbon materials have excellent thermal conductivity, electrical conductivity, specific heat capacity. Its structure is 1-dimensional axial symmetry. SWCNT can be produced by placing a small amount of iron a dimple in a cathode and mixture of benzene and argon atmosphere is very necessary in this method. This strategy is called curve release technique. SWNT can likewise be delivered by vanishing of hot change metal containing carbon and took after by buildup cool finger. Single-walled carbon nanotubes can be made in various outline, for example, Chiral, Zigzag and Armchair. The CNT configuration relies upon the technique for wrapping graphene into a barrel. For instance, one outline can be framed by rolling the paper from its corner and other plan can be made by rolling the sheet of paper from its edge. The structure of single-walled nanotube is represented through a chiral vector (n, m). In the figure 1.2, the chiral vector is defined.

Nanotube's electrical properties can be specifically influenced by its outline. The nanotube will be called as metallic (highly conducting) when n - m is a numerous of three, in general the nanotube is a semiconductor. The Armchair configuration is constantly metallic whereas different plans can make the nanotube a semiconductor. SWNT can be sorted as-Armchair write, Zigzag compose and chiral compose. It has been talked about below –

(i) Armchair Type CNT

The type of CNT as shown in Figure 1.3 is an achiral nanotube and it has been decided on basis of “Symmetric classification”, achiral means the nanotube structure is symmetrical; When chiral vector becomes n = m, then chiral = (n, n). The value of chiral angle (θ) is 30°, we call it as armchair.

(ii) Zigzag Type CNT

When chiral vector becomes, m = 0, then chiral = (n, 0). The angle of chirality (θ) is 0°, we term it as Zigzag type of CNT, and it is shown in Figure 1.4.

(iii) chiral Type CNT

The nanotube is with a spiral symmetry is called as chiral and it does not give it a mirror image. A chiral nanotube has general n and m values, therefore chiral = (n, m). The angle of chirality (θ) lies in between 0 and 30, therefore $0° < \theta < 30°$, it is depicted in figure 1.5.

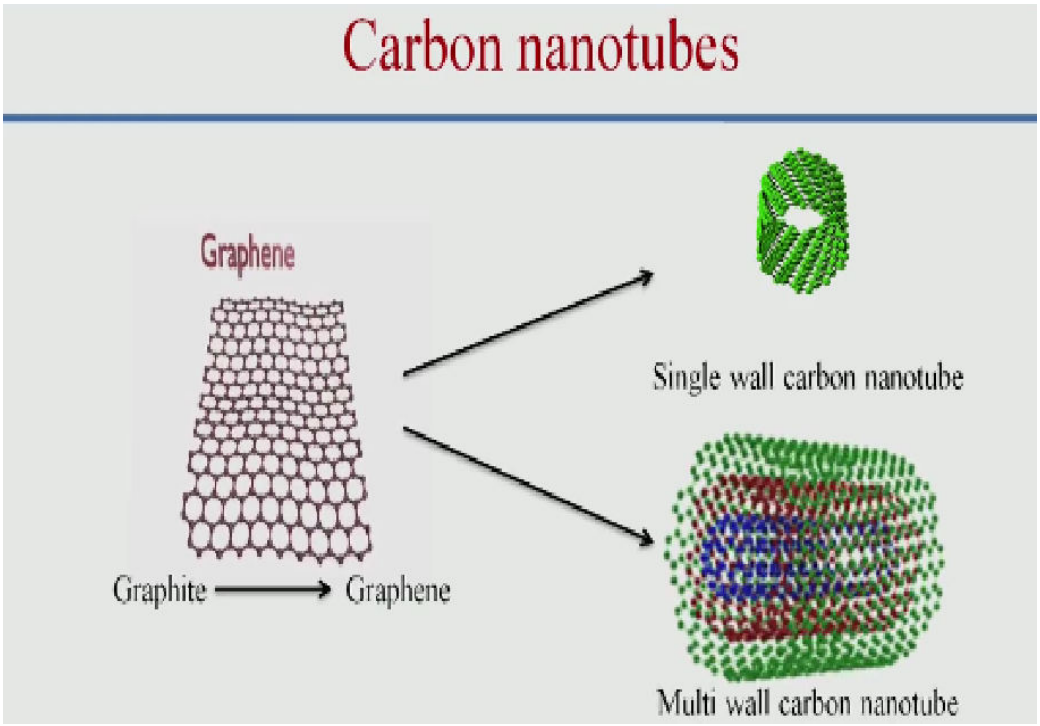

Figure 1.1 Types of CNT

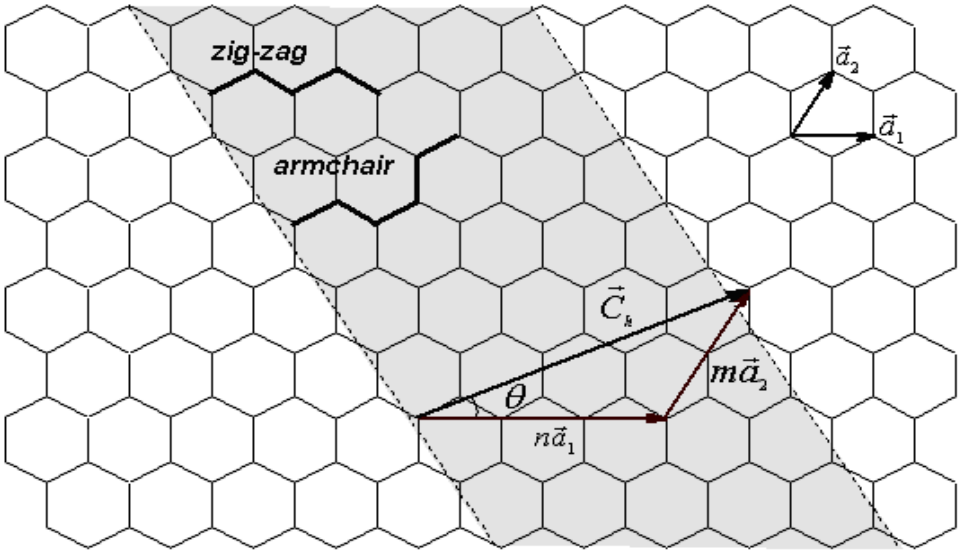

Figure 1.2 Schematic diagram showing how a hexagonal sheet of graphite is 'rolled' to form a carbon nanotube [3]

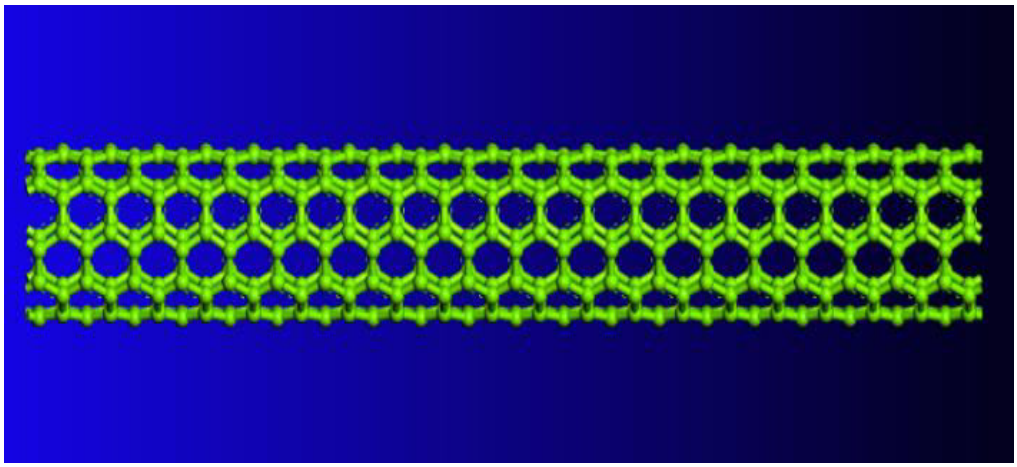

Figure 1.3 Armchair SWCNT

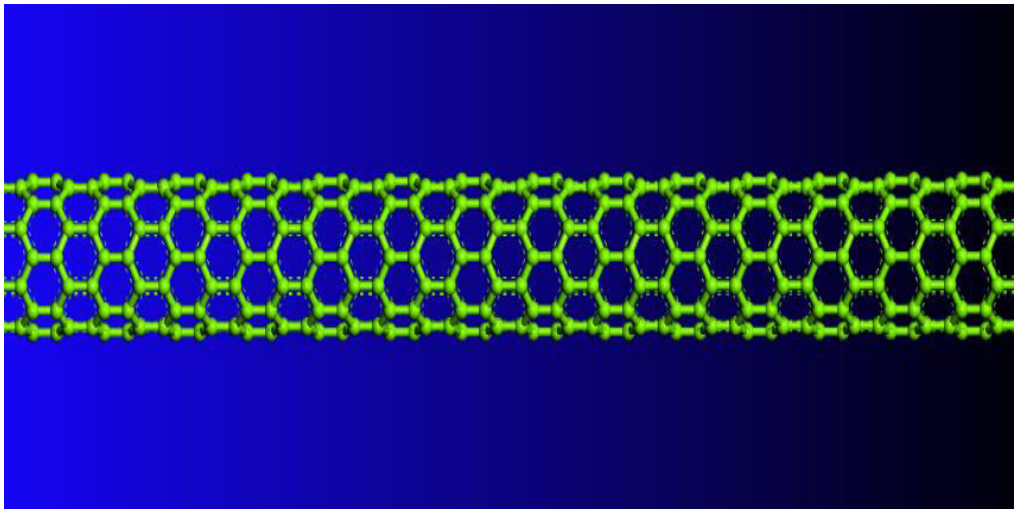

Figure 1.4 Zigzag SWNT

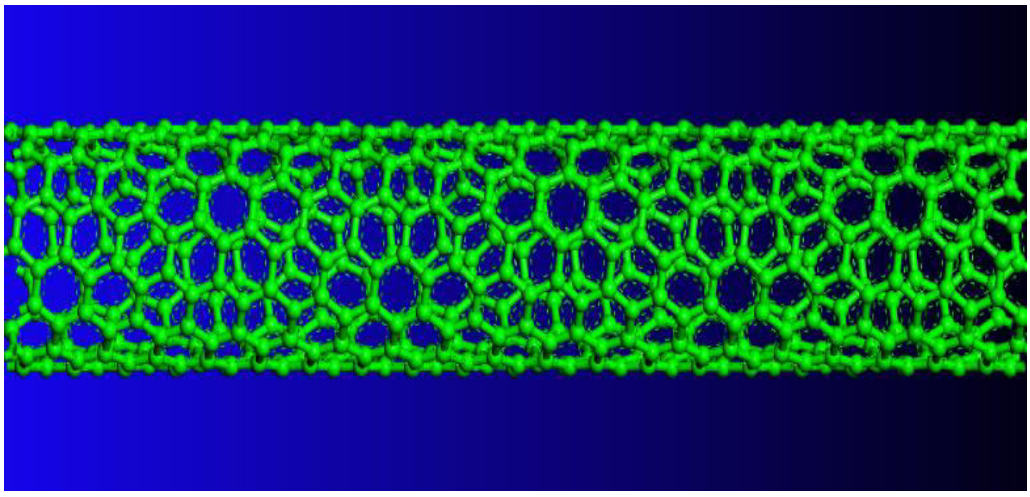

Figure 1.5 chiral CNT

1.1.2 Multi-Walled Carbon Nanotube (MWCNT) Structure

Multi-walled CNT can be produced by evaporation of carbon from anode and deposition at cathode. CVD grown carbon nanotube is impure in comparison to arc discharge carbon nanotube. It happens due to the presence of Nano catalyst particles.

MWNT structures grown by the CVD process are high defect densities prone and this is the major drawback of this CVD technique. MWNT is five times stronger than carbon fiber.

1.2 Properties of CNT

CNT has extraordinary mechanical, thermal and electrical properties and only carbon atoms rearrangement is responsible for this unique property. Some of the properties are as follows:

1.2.1 Electrical Conductivity

Metallic CNT is highly electrically conductive material. The conductivity of CNT can be determined by chirality. Depending upon a chiral axis, both the metallic as well as semiconducting properties can be exhibited by CNT. In the case of MWCNT, its electrical conductivity is very complex due to non-uniform distribution of current by inter-wall interaction over the individual tube. However, in the case of metallic SWCNT, it has been observed that current is uniformly distributed across different parts of metallic SWCNT.

1.2.2 Strength and Elasticity

CNT acts as an ultimate high strength fiber. SWCNT has a higher modulus of elasticity than steel and it makes it as a highly resistant fiber. Although CNT can bend on pressing on the tip and it retains its original state when forces will be removed. It has been reported that SWCNTs are having a Young's modulus of elasticity is about one TPa.

1.2.3 Thermal Conductivity and Expansion

In graphene, sheet-carbon atoms are strongly bonded with three carbon atoms and due to this strong in-plane bonding properties, CNT can show properties like superconductivity below 20K. CNT are having extraordinary strength and stiffness against axial strains only due to the strong C-C chemical bonding. Moreover, single wall carbon nanotube exhibit high flexibility against non-axial strains due to zero in-plane thermal expansion and the greater inter-plane.

1.2.4 Field Emission

The field emission phenomenon can be observed when from the metal tip to the vacuum tunneling of electrons occurs by the strong electric field. It results from the

small diameter of nanotubes and the high aspect ratio. The field emitters are best for flat-panel display application. Due to the emission of light and electrons the properties of field emission occurs in MWCNT.

1.2.5 Aspect Ratio

For CNTs, the high aspect ratio is unique and exciting properties, inferring that similar electrical conductivity of other conductive additives can be achieved by applying a lower load of the CNT. It has been observed that unique electrical conductivity has been possessed by the high aspect ratio of the CNT as compared to the conventional additive materials such as chopped carbon fiber, carbon black, or stainless steel fiber.

1.2.6 Absorbent

Due to the unique properties like superior electrical properties, extraordinary mechanical strength, larger flexibility and lightweight, CNT and its composites have been emerging as perspective absorbing materials. Therefore, for use in water, gas and air filtration, only CNT will be an ideal candidate.

1.3 Production of CNT

There are many methods available which is being used for producing carbon nanotube, some of them are discussed here:

1.3.1 Arc Discharge Method

Carbon arc discharge method is most commonly used method for producing CNT in easy way. By using this method, CNT can be separated from catalytic metals and soot by the help of produced complex components. CNT are produced by using Arc vaporization and in this method two carbon atoms will be placed in an enclosure from end to end and will be separated by 1 mm. Usually Inert gas is filled in the enclosure at low pressure. An immediate current of 50 to 100 A between two cathodes is connected for making a high temperature release. By the high temperature release carbon terminals surface vaporized and consequently a little anode (bar molded) gets shaped. In high return, the CNT generation is completely subject to plasma curve consistency. CNT can likewise be delivered with fluid nitrogen by method of arc discharge.

1.3.2 Laser Method

In 1996, for producing CNT a technique was used called as a dual-pulsed laser. This synthesizing technique was produced CNT with purity of 70 %. Nowadays, for producing CNT laser vaporization process is being used. In this process produced CNT are having diameter 10–20 nm more and 100 μm or more in length. Average diameter and size distribution for CNT depends on catalyst composition, growth temperature and other process parameters. For producing high quality CNT in small amount laser vaporization and arc discharge methods are used in recent years. These two methods are also having some drawbacks like:

(i) Evaporation by carbon source is being used by this method and for scaling the production with standards of industry level it follows very unclear approach.

(ii) The produced CNT is mixed with residues of carbon by the method of arc discharge. Therefore, purification, manipulation and assembling of CNT for making nanotube device architectures of practical applications are quite difficult.

1.3.3 Chemical Vapour Deposition

In this process, by catalytic CVD of acetylene CNT in large amount can be produced over cobalt and iron. Along with the MWNT, fullerenes and bundles of SWNT can be produced by the carbon/zeolite catalyst. At 1000 ° C, high yields of SWNT can be obtained by Catalytic decomposition of H_2/CH_4 mixture over nickel, iron and cobalt. In this method by using the decomposition of CH_4 over the newly formed nanoparticles, lower proportions of MWNT and higher proportions of SWNT can be achieved.

1.3.4 Ball Milling

Ball milling is one of the simple methods for producing the CNT followed by subsequent annealing. From boron nitride powder and carbon, CNT can be produced by thermal milling. In this method, in a stainless-steel container that consists of four hardened steel balls the graphite powder will be placed. At room temperature, for milling process argon is introduced for up to 150h and the steel container is purged using the milling process, under an inert gas flow at 1400ºC for 6h the graphite powder is annealed. More MWNT and few SWNT can be produced by this method.

1.3.5 Other Methods

Different Methods CNT can likewise be created utilizing fire blend, electrolysis, amalgamation from mass polymer, utilization of sun powered vitality and low-temperature strong pyrolysis. In electrolysis technique, an electric current is being in liquid ionic salt between graphite anodes for delivering CNT. As a cathode, high immaculateness carbon bar is utilized. By consuming the cathode at high softening point, a wide scope of CNT created. In the fire blend technique, for working the hydrocarbon reagents at a raised temperature a segment of the hydrocarbon gas.

1.4 Purification of CNT

After synthetization, by separating it from other entities purification of CNT is done, like carbon nanoparticles, residual catalyst, amorphous carbon and other unwanted species. For removing the unwanted impurities from CNT classic chemical methods has failed. Therefore, for purifying the undesirable impurities, intercalation, liquid phase and gas phase like basic methods are used. Generally, for removing the nanoparticles, a microfiltration operation is carried out using membrane filters. In this method, amorphous carbon and unwanted nanoparticles are removed without any chemical modification in the CNT. The different purification methods are as follows:

1.4.1 Gas Phase

It is a most successful technique. For nanotubes, significant enrichment can be produced by this method. The combination of repeated extraction with nitric acid and high-temperature oxidation and hydrochloric acid is being used by this method. In this method, nanotube's stability is considerably improved with a negligible reduction of impurities for instance residual catalyst and non-nanotube forms of carbon.

1.4.2 Liquid Phase

It is an effective purification method. All the essential steps of this method are as follow

Step 1: For removing large graphite, particle preliminary filtration is used.

Step 2: for removing catalyst particles and fullerenes, dissolution will be used.

Step 3: Microfiltration

Step 4: Centrifugal separation and

Step 5: Chromatography

In this process, CNT is subjected to the liquid phase oxidation step with hydrogen peroxide (H2O2) solution. Amorphous carbon can be removed by itself without any damaging of tube wall damage. Thus, CNT can be easily separated in the separation's last stage.

1.4.3 Intercalation

It is used for insertion of a molecule (or ion) into compounds having layered structures. Between adjacent layers, Vander Waals gap can be expanded by this technique, which requires energy. Between the dopants and the solid charge transfers and due to this energy will be supplied. It has some drawbacks also at oxidation stage some amount of nanotube may be lost. The final material may contaminate with intercalates residue.

1.5 Applications of CNT

The outstanding properties of CNTs make then very useful and thus expand its application area from thermal conductivity, field emission, energy storage, conductive properties, molecular electronics based on CNTs, conductive adhesive, structural applications, thermal materials, fibers & Fabrics, catalyst supports, biomedical applications, air & water filtration and some other applications. Due to unique atomic arrangements, CNT is having outstanding properties like mechanical strength, large current carrying capability, excellent thermal conductivity and long ballistic transport length. Due to having extraordinary properties, it is used in biological fields, microelectronics/Nano electronics, optics, spintronic, material science and mechanical fields. Especially, Graphene nanoribbons (GNRs) and CNT are being used in Nano electronics field such as devices that can store energy, the devices that can convert energy including photovoltaic and thermoelectric devices, a display for field emission and sources of radiation, NEMS, nanometer semiconductor transistors, ESD protection, passives and interconnects. The usage of CNT in various fields is discussed below.

1.5.1 Structural Applications

CNT is having unique properties and qualities that act as structural materials. There are following applications given below:

(i) Textiles

(ii) Body Armor

(iii) Concrete

(iv) Polyethylene
(v) Sports equipment
(vi) Bridges
(vii) Flywheels
(viii) Fire protection

1.5.2 Electromagnetic Applications

CNT can be fabricated as electrical insulators, conductors and semiconductors. Some of the applications are listed below:

(i) Bucky paper
(ii) Light bulb filament
(iii) Magnets
(iv) Solar cells
(v) Electromagnetic antenna

1.5.3 Electroacoustic Applications

In the field of electroacoustic CNT can be used in loudspeaker

1.5.4 Chemical Applications

CNT tremendous applications are listed below:

(i) Air pollution filter
(ii) Water filter
(iii) Chemical Nanowires
(iv) Sensors

1.5.5 Mechanical Applications

CNTs can be used in mechanical engineering. Some of the applications are listed below:

(i) Oscillator
(ii) Waterproof

1.6 Polymer

A polymer can be defined as a macromolecule, which is formed by the repeated units of several simple molecules called monomers through covalent bonds. Polyester, Polyethylene, Teflon, PVC, Bakelite, Nylon, are the examples of polymer. Polymerization has been defined as “the chemical reaction in which monomer is converted into polymer”. Monomer needs the initiator, but it cannot undergo

polymerization. In this study, Natural rubber has been taken as a polymer and has been created using Material Studio 2017. Repeat unit has been taken as 10 and it is of a single chain. “Diene” library has been used for creating Natural rubber in MD simulation.

1.6.1 Classification of Polymers

a) Based on their origin polymer:
   (i) Natural polymers: the polymers, which are acquired from natural sources like plants and animal, called Natural rubbers. Natura polymer include Starch, Protein, Cotton, Silk, Wool, Cellulose and Glycogen.
   (ii) Synthetic polymers: the polymers, which are synthesized from simple molecule, are called synthetic polymers. Polyethylene, polyester, Teflon, PVC and Nylon are the examples of synthetic polymers.

b) Based on their thermal behavior:
   (i) Thermoplastics polymer: The polymer that becomes soft on heating and hard on cooling are called Thermoplastics. Teflon, Polyethylene, PVC and Plexiglas are the thermoplastics polymer.
   (ii) Thermosetting polymer: The polymers that undergo chemical changes, cross likings on heating, and become permanently rigid, hard and infusible are known as thermosetting. Urea-formaldehyde resin, Phenol-formaldehyde resins and epoxy resin are the thermosetting polymers.

c) Based on their methods of polymerization:
   (i) Addition polymers: The polymers, which are formed by addition polymerization reaction in which self-addition of several olefin monomers to each other takes place without elimination of by products, are called addition polymers. PVC, Polystyrene, Teflon and polyethylene are the addition polymers.
   (ii) Condensation polymers: Condensation polymers are formed by intermolecular condensation reaction through functional groups of monomers with continuous elimination of byproducts. Nylons, polyesters and phenol-formaldehyde resins are condensation polymers.

1.7 Natural Rubber

It is an elastic substance, which is obtained from latex sap of trees, belongs to Ficus and general Hevea. In technical language, it is known as an elastomer. Natural

rubber is a kind of rubber that also includes vulcanized rubber and it is finished into various types of rubber products. It is also known by the name gum elastic. It has unique properties such as excellent green strength and tack, high resistance to tearing, chipping and cutting, with the improved fuel economy it has low rolling resistance. It also having drawbacks like those that it has moderate resistance to damage caused by environment like ozone, light and heat. It can be used as a spring material and it forms strong barrier to water.

1.8 Defects in CNTs

There are two kinds of manufacturing defect can be found in the carbon nanotubes. One is a vacancy and other is a stone-Wales defect..

1.8.1 Stone-Wales Defect

It is a defect, which takes place in crystal structure, and we can call it as a crystallographic defect or structural defects. In this defect, the connectivity of π- bonded carbon atoms change from its original position by an angle 90° rotation with respect to the midpoint of their bond. Due to this effect, naphthalene-like structure is converted into fulvalene like structure. This defect occurs in carbon nanotubes, graphene. Due to this effect, structure of carbon nanotube is changed. Due to rearrangement, the properties like electrical and mechanical properties are affected. The rearrangement is an example of pyracyclene arrangement. The defect is responsible for nanoscale plasticity. It can be determined by using vibrational spectroscopy techniques.

1.8.2 Vacancy Defect

When any atom removes from lattice, then that place will be vacant and it is called vacancy. It is also called a point defect or Schottky defect. We can also call it as a zero-dimension effect. This defect arises when lattice possesses imperfection. It is also called as a crystallographic defect.

1.9 Functionalized CNT Polymer Composites

Since many researchers have done a great job with respect to CNTs, there is a hidden zone and that is composites based on CNTs. Although numerous researches were done, in this case also with varying resins but much more can be done here. Researchers in the pursuit of better physical properties have tested and tried many composites like epoxy or polypropylene etc. Quite an untouched area is functionalization of CNTs, in which very less research has been done. Therefore, the

main focus of this study is functionalization of CNT based composites and the resin chosen is Natural rubber. This study is based on SWNT type of CNT, mixed with Natural rubber as reinforcement, and Functionalization of CNT based composites. Addition of additional functional groups to the surface of any material is called functionalization. In other words, it is the process of adding new features, functions, properties, or capabilities to a material by changing the surface properties of the material. It is a fundamental technique used throughout materials science, chemistry, and biological engineering, and nanotechnology. A pre-functionalized CNT is to be mixed with polymer matrix by any of the composite forming methods.

Types of Functionalization:

(i) Non-Covalent Functionalization

(ii) Pi-stacking

(iii) Defect Functionalization

(iv) Endohedral Functionalization

(v) Sidewall Functionalization

For this study, sidewall functionalization is chosen, as it is very advanced, and a proper care is taken to maintain the structural symmetry as well. Functional groups were added by attaching the atoms of different functional groups of ester ($-COOCH_3$) to the surface of SWCNT shown in figure 1.8.In this era of modern nanotechnology, method of microscopic analysis is required to generate functional materials and investigation of physical phenomena based on molecular level. There are different methods for investigating the physical phenomena like “Monte Carlo” also known as “Molecular simulation Methods” and “Molecular Dynamics Methods”. Both the above methods are useful to analyze properties in thermodynamic equilibrium. Monte Carlo is not suitable for investigating dynamic properties whereas Molecular Dynamics is used for investing the dynamic properties in both equilibrium and non-equilibrium states, but MD is more useful in a non-equilibrium situation. Apart from these above said two methods, there are some others method which is useful for finding the physical properties in a molecular level. These methods are as follows:-

(i) Brownian dynamics methods.

(ii) Dissipative particle dynamics.

1.10 Molecular Dynamics Method

The MD methods concept is very straightforward and logical. Newton's equation of motion is used for governing the motion of molecules. This method is based on computer simulation for microscopic analysis. Due to the number of molecules interaction in areal system are large so it is very difficult to analyze it mathematically the position of a particle at particular time but it can be evaluated easily in MD simulations by the different ways. These ways are as follows:-

(i) Vertex Method

(ii) Velocity Vertex Method

(iii) Leap Frog Method

1.11 Monte Carlo Method

In the approach of MD method, molecules motion is modeled according to the equation of motion therefore, it is applicable to thermodynamic and non-thermodynamics equilibrium. However, in Monte Carlo Method, the concept of explicit time and equation of motion is not used and thus it is used only as a simulation technique for thermodynamic equilibrium. Thus, it is not suitable for the properties, which are dependent on time.

1.12 Brownian Dynamics Method

When the dispersed fine particles are dispersed in a base liquid, then it is very difficult to be treated by simulations by MD method. This difficulty is due to the difference in motion time of the solvent particles and the dispersed particle. So MD is not used as simulation technique for particles dispersions. Now to overcome this complexity, the solvent molecules treated as a continuum medium rather than to consider motion of each solvent molecule.

1.13 Dissipative Particle Dynamics Method

In this method, the characteristic time of motion of the solvent particles clusters observed as virtual fluid particles, which is not so different from that of dispersed particles. These virtual fluid particles called "dissipative particles". The simulation of both the motion of dispersed and fluid particles carried simultaneously. The technique for conducting the simulation in dissipative particle dynamics methods is similar as that of Brownian dynamics method.

CNT based composites have the prospective to provide extremely tough and ultra-light new materials. However, huge challenges remain in the growth of such nanocomposites. Currently, fabrication of CNT based composites is still a challenging and expensive process. Many fundamental issues extending, for example, from characterizations, experimental techniques to simulation methods, have not been fully addressed for the development of CNT-based composites. It is very complicated to solve, test and expensive to conduct an experiment after establishing the analytical model at the nanoscale. Computational approach can play an important role in the development of the CNT-based composites through simulation results, which helps in understanding, design and analysis of such nanocomposites. On the other hand, Modeling and simulations of nanocomposites can be realized readily and cost effectively on a computer. Characterizing the interfacial and mechanical properties of CNT-based composites is just one of the important and urgent tasks that can be completed by simulations. In this study, the effective mechanical and thermal properties of CNT based composites have been evaluated using Molecular Dynamics (MD) simulation.

Chapter wise description of dissertation is briefly described below:

Chapter 1: Introduction

This chapter gives brief introduction about the CNTs and their properties. The different computational techniques that can be used for predicting mechanical and thermal properties of nanocomposites also be briefly discussed. It provides an outline of "Molecular Dynamics" (MD), "Monte-Carlo simulation", "Dissipative Particle Dynamics", "Brownian Dynamics" and "Lattice Boltzmann" methods.

Chapter 2: Literature review

An exhaustive review of research has been carried out for various modeling techniques. More specifically, we focus on classical atomistic simulation using Molecular Dynamics at the nanoscale. Finally, some important conclusions have been made.

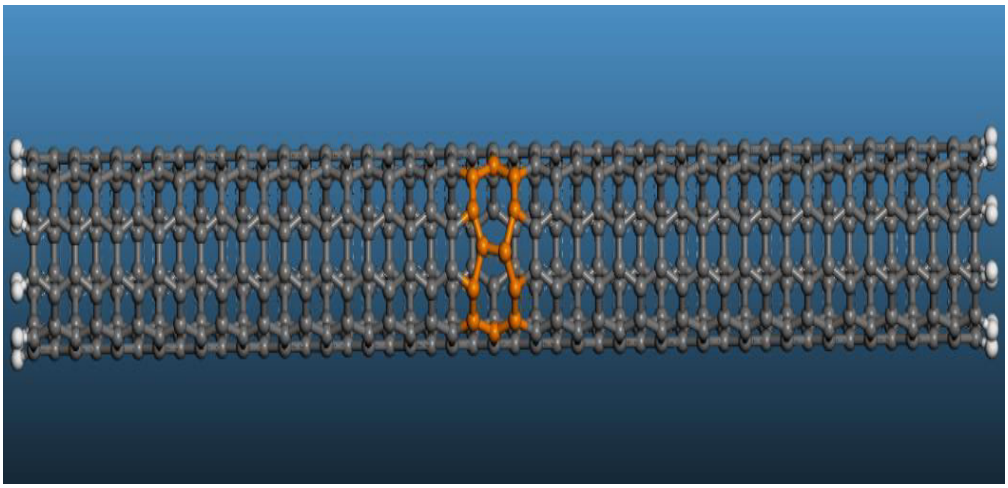

Figure 1.6 Stone-Wales Defect in armchair type (5, 5) SWCNT

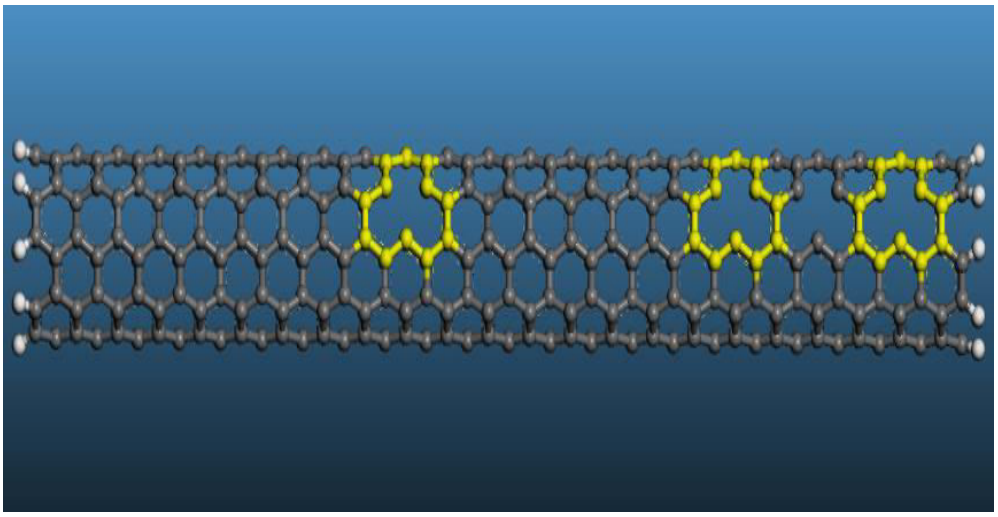

Figure 1.7 Vacancy Defect in armchair type SWCNT (5, 5)

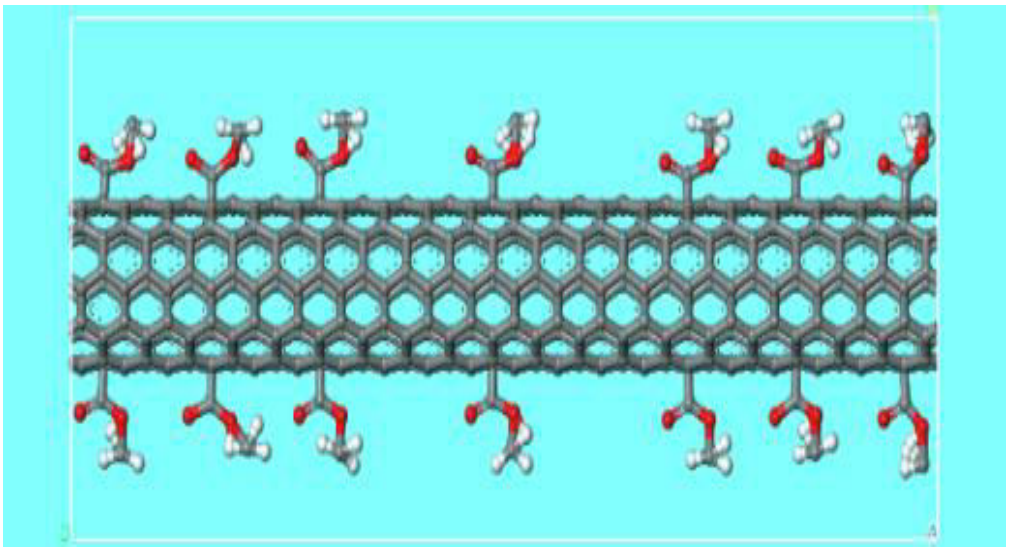

Figure 1.8 Functionalized SWCNT of $COOCH_3$

Chapter 3: Materials and methodology

The materials used in this study have been listed along with the MD methodology. The optimization and dynamics steps of simulation have also been explained in this chapter. In context to the molecular modeling, the force field parameters were explained which is required to describe the properties of the single walled carbon nanotubes reinforce with polymer composite.

Chapter 4: **To analyze the effect of chirality, nanotube length and diameter on the interfacial properties of CNT reinforced polymer composites**.

In this chapter, Simulations have been performed for studying the effect of Chirality of polymer/carbon nanotube (CNT) composites, composed of single wall (5,5) CNT have been performed with different length and diameter. The pullout simulations have been performed for finding the effect of length and diameter. The interfacial properties of the single walled armchair carbon nanotube reinforced with Natural rubber composite have been calculated. Pullout simulations have been performed for calculating the Interfacial shear stress and surface density of the using Molecular Dynamics with the help of Material Studio 2017.

Chapter 5: To predict the mechanical properties of CNT reinforced polymer composites with fiber volume fraction and fiber ratio using MD simulation.

In this Chapter, we predict the mechanical properties of different types of SWCNTs reinforced polymer composites using the MD simulation method. The longitudinal, transverse, longitudinal shear and transverse shear storage moduli of CNT reinforced polymer nanocomposites were also determined in this chapter. In addition to this, simulations have been performed for analyzing the effect of NR/SWCNT composites with different volume fraction (V_f) and aspect ratio (l/d).

Chapter 6: To evaluate the effect of Stone-Wales and vacancy defects on thermo-mechanical properties of CNT reinforced polymer nanocomposites.

Molecular Dynamics (MD) simulation has been used to study the effects of these defects on mechanical properties of single-walled carbon nanotubes (SWCNTs) reinforced Natural rubber composites. MD pullout simulation has also been done to analyze the effect of defective CNTs, for finding the interfacial properties of the SWCNT/NR composites. Different types of SWCNT/NR have been used in this study and the number of defects is varied from 1 to 10. The stone-wales defects and the

vacancy defects were introduced in the CNTs/NR composites for finding their effect on the mechanical properties of the carbon nanotube reinforced with Natural rubber polymer composites. The thermal conductivity of the single-walled carbon nanotubes (SWCNTs) reinforced Natural rubber composites with defects has been calculated using the Molecular Dynamics simulation. An armchair (5,5) have been used for finding the thermal conductivity of the SWCNT/NR with number of defects of 1 to 10.

Chapter 7: To study the effect of functionalization of CNTs on the modulus of CNT composites and predicted the thermal conductivity of the functionalized SWCNT/NR composite.

This chapter analyzes the effect of carboxylic (COOH), ester ($COOCH_3$), and alcohol (OH) groups attached on the surface of SWCNT on elastic properties of Natural rubber (NR) composites reinforced with functionalized SWCNTs along the axial direction of the CNTs by using MD approach. The results obtained showed variation in the Young's modulus of the CNTs with the increase in number of functional groups varied from 1 to 20%. Thermal conductivity of the single walled carbon nanotube reinforced Natural rubber composite has been calculated using the Molecular Dynamics simulations A armchair (5,5) SWCNT has been used in this study with the percentage introduction of functional groups as 1, 5, 10, 15, and 20, for study of variation with varying percentage.

Chapter 8: To predict the damping of CNTs reinforced polymer composites using MD simulation.

Molecular Dynamics simulations have been used for finding the damping of the single walled carbon nano tube reinforced polymer composites. In this chapter, we also find the damping loss factor (η) with fiber volume fraction and fiber ratio using MD simulation.

Chapter 9: Executive summary and scope of future work

Summary of the various aspects of the present work are presented in this chapter along with the scope of future work.

Chapter 2

Literature Review

2.1 Literature Review

CNTs are extremely small which one of his major characteristics. Due to this, the major problem arises in finding its material characterization. In nanoscale materials, the biggest hindrance is to investigate and measure the interfacial behaviors of the material. The experimental measurements of the interfacial properties of CNT reinforced polymer have been limited and it can be measure by using the modeling and computer simulation. In this chapter, different modeling and simulation methods are reviewed based on the time and scale which has been carried out by the various researcher. Exhaustive review of literature is presented which has been carried out using various different techniques in determining the effects of defects on the interfacial properties of CNT reinforced polymer. In addition to this, the literature based on the mechanical properties of CNT reinforce polymer determine by various researchers with different methods has been reviewed. The literature review based on the effect of functionalization on the CNTs using the Molecular Dynamics simulation is also discussed in this chapter. Various properties of CNTs been studied by the different researchers using different simulation techniques were also discussed. The literatures based on the properties of the CNTs have been discussed below-

Iijima, Sumio in 1991[1] used an arc-discharge evaporation method, a new structure of finite carbon was prepared which looks like a needle. With the help of electron microscopy, author examined the needled structure and showed that along the axis of needle a lattice structure that suggested a tubular and seamless structure. The author also suggested that each needle consists of an arrangement of coaxial graphitic tubes with the wall thickness ranges from 2 up to about 50 sheets and the diameter ranging from few to few ten nanometers.

2.1.1 Literature Review Based on Interfacial Shear Stress (ISS)

Frankland *et al.* in 2002 [2] carried out a pull-out of a functionalized CNT from the polymer using MD. The results showed an improvement of the interfacial shear stress and negligible change in modulus involving less than 1% of carbon atoms.

S.C. Choudhury and T. Okabe in (2010) [3] have studied the effects of the chemical cross-links in the interface, matrix density and geometrical defect in the CNT on the ISS of CNT reinforced polyethylene composites. In this study, Molecular Dynamics simulation has been performed for CNT pull-out from the polymer matrix. It has been reported that an energy based switching criterion has been proposed for cross-links traveling on the CNT. It has been concluded from Molecular Dynamics simulation result that ISS increase with the increase in matrix density. ISS of CNT–polymer composites increase with the presence of chemical cross-links in the interface. It has also been reported that ISS is affected by cross-link position. Pentagon–heptagon geometrical defect significantly reduces the ISS when crosslinks are present in the interface.

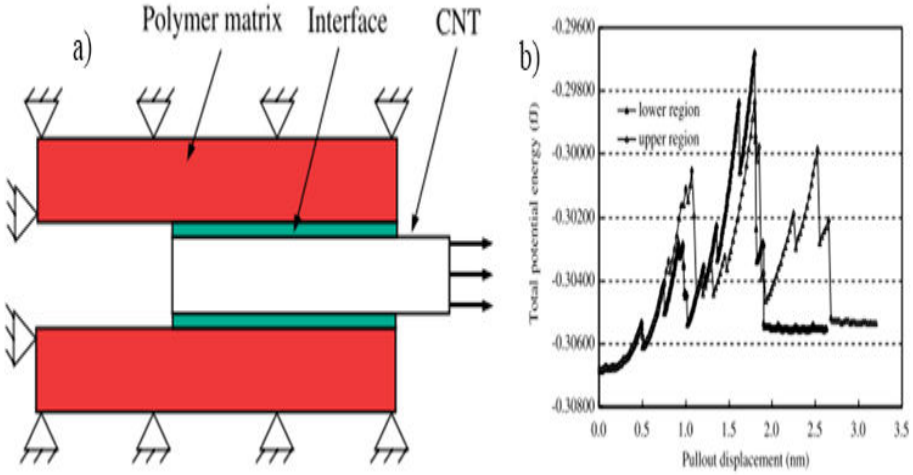

Figure 2.1 (a) Schematic of partially embedded CNT pull-out from polymer matrix (b) Energy variatition during the pullout of CNT [3]

M.N. Yuan *et al.* in 2012 [4] predicted the interfacial fracture toughness by developing an analytical model of fiber-reinforced matrix composites. Authors validate the analytical solution by making a finite element model. This analytical model explains the unusual phenomena in high-temperature push-out tests on SiC fiber-reinforced titanium matrix composites, in which the critical applied stress initially increases, and then decreases with increasing temperature.

J.M. Wernik *et al.* in 2012 [5] investigated the interfacial properties of carbon nanotube (CNT) reinforced polymer composites by simulating a nanotube pull-out experiment using the ABC multiscale modeling technique. In this technique, authors considered only Vander Wall interactions between the atoms in the CNT and the polymer implying a non-bonded system. The information collected from results that the ISS shows a linear dependence on the Vander walls interaction density and decays significantly with

increasing nanotube embedded length. Authors also found that increasing the diameter of the CNT, increase the peak pull-out force approximately linearly.

Fakhrabadi *et al.* in (2013) [6] was studied about pull-in phenomena for carbon nanotube which is defected with stone-wales defect. In this study Molecular Dynamics simulation has been performed for investigation pull-in charges for SW defected carbon nanotube. It has been reported that longer CNTs having smaller diameters shows less pull-in charges, whereas shorter CNTs possessing larger diameters. Furthermore, it has been observed that the pull-in charges shown by the doubly clamped CNTs are more than the cantilevered CNT's pull-in charges. It has been concluded that SW defects could reduce the pull in charges greatly and its position and the no. of defects affects pull-in charges.

2.1.2 Literature Review Based on Structure

Noriaki Sawada Hamada et. al. in 1992 [7] studied systematically the electronic band structure of graphitic microtubules and predicted micro hollow tubes of carbon exhibit variation of properties depending upon the structure of the tubule. The author also used the Tersoff's empirical relation for finding the geometry of the each microtubule and found the band structures, which gives a rich variety in energy band structure.

R. Saito et. al. in 1992 [8] observed that the chiral angle and the fibre diameter helps in identifying the electronic structure of the graphitic tubules which may be semiconductor or metallic, either no doping impurities are exist or no difference between the carbon atoms chemical bonding. After the calculations, authors found that one third of these tubules are stable and other two third are semiconductors but both are one-dimensional.

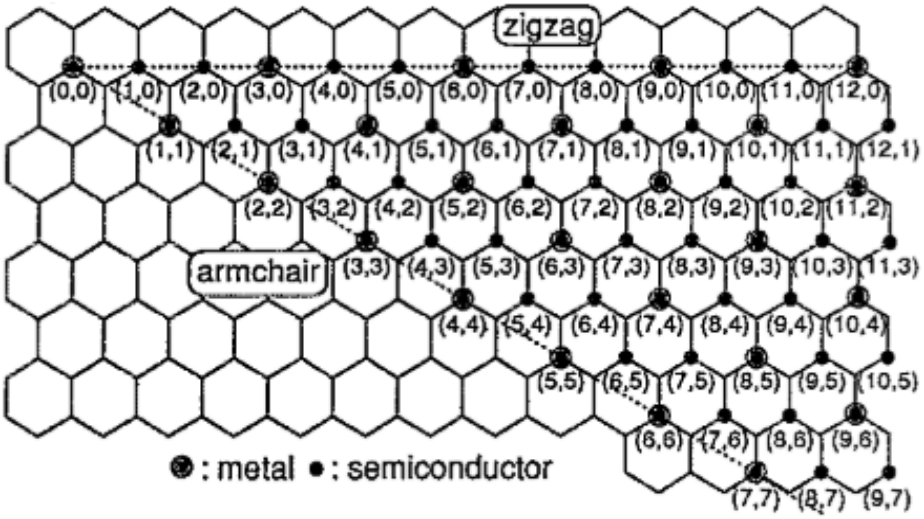

Figure 2.2 Possible vectors for chiral fibers [8]

J. W. Mintmire and C. T. White in 1995 [9] studied the electronic structure of the nanotube based on the helical symmetry and observed resulting trends by using empirical and first-principles techniques. Authors also examined the elastic properties and change in energies of small-diameter graphitic nanotubes.

2.1.3 Literature Review Based on Elastic Properties

J. T. Seitz in 1993 [10] developed the method for estimating the mechanical properties of polymeric materials. Based on the molecular structure of the repeat unit, only basic molecular properties of the polymer can be calculated which is helpful in design the new polymeric materials.

Kazuyoshi Tanaka et. al in 1993 [11] was the first to examine the electronic property of the purified multi cylinder structured carbon nanotube based on the electron spin resonance (ESR) spectroscopy and found that only one peak is similar to that of graphite by the Raman scattering measurement technique. This also showed that the purified multi cylinder structured carbon nanotube examined is a semiconductor without impurity and inactive doping.

C. F. Cornwell and L. T. Wille in 1997 [12] investigated the elastic properties of single wall carbon nanotubes.The author also investigated the axial compression response of the single wall carbon nanotube.The calculated data is also used to determine the Young's modulus of the tubes.

Krishnan *et al.* in 1998 [13] observed the single-walled carbon nanotubes stiffness with the help of a transmission electron microscope.Vibration amplitude and the nanotube dimensions are also measured using the help of electron micrographs.

E. Hernandez *et al.* in 1999 [14] performed a extensive study of the structural, energetic, and mechanical properties of single-wall nanotubes of different chemical composition. The results shows that carbon nanotubes having smaller Young's modulus, due to which swcnt are expected to be stiffer than any of the composite nanotubes having good agreement with the experimental model.

M. B. Nardelli *et al.* in (2000) [15] was studied about mechanical and elastic behavior of carbon nanotubes. In this study quantum mechanics, simulation has been carried out. In this study it has been reported by the author that high defects affect more the transport properties of individual nanotube while in case of armchair nanotube having small diameter maintain its electrical properties even on larger deformation with no any missing atoms or SW defect. It has been concluded that defect density reduces the

conductance at the Fermi energy and carbon nanotube's electrical response is highly affected by large geometrical deformations.

Yao *et al.* in 2001 [16] computed and simulated the mechanical properties of single-walled carbon nanotubes (SWCNTs) by using MD. Brenner potential function has been used to describe the bonding structure and properties of CNTs.

Li and Chou in 2003 [17] carried out a study of the elastic behavior of multi-walled carbon nanotubes (MWCNTs) and predicted the Young's and shear moduli of MWCNTs. The effect of tube diameter, chirality and number of tube layers on elastic properties of MWCNTs has also been predicted. Comparison of elastic behavior of SWCNT and MWCNTs in light of the effect of van der Waals forces has also been made.

Yu Wang, Xiu-xi Wang *et al.* in 2005 [18] used the technique Tersoff–Brenner potential for describing the main mechanical response features i.e interactions of atoms in CNT. Molecular Dynamics simulation were performed on compression deformation of single-walled carbon nanotubes (SWCNTs) and results shows the decrease of the young`s modulus with the increase of the CNTs radius. Authors also found that the Young`s modulus of armchair CNT is lower than that of zigzag CNT.

Ahmed Al-Ostaz *et al.* in 2008 [19] calculated the transverse and elastic properties of nanoparticle consists of a (SWCNT) inserted in polyethylene matrix and their constituents by using the Molecular Dynamics simulations. The results obtained from different types of loadings applied to SWCNT shows those SWCNTs having very poor transverse properties as compared to SWCNT/Polymer. Authors also observed that the elastic constants are same under various loadings for SWCNT. Authors concluded that the SWCNT acts as a linear elastic material.

Libo Deng *et al.* in (2011) [20] used the Raman spectroscopy method for finding the effect of young`s modulus of the reinforced SWCNT-Polymer. After preparing the nanocomposite fiber by electro-spinning and then compared the behavior with same composition of then nanocomposite films. Author also developed a "self-consistent method" for facilitating the efficiency of reinforcement by nanotubes.

Sumit Sharma *et al.* in (2013) [21] determined the elastic properties of single walled carbon nanotubes (SWCNTs) and evaluated the mechanical properties of three types of SWCNTs viz., armchair, zigzag, and chiral nanotubes by using the Molecular Dynamics (MD) simulation. From the results, it can be concluded that the with the increase in

radius of SWCNTs the young's moduli of SWCNT decreases but with the increase in the aspect ratio and volume fractions of CNTs the young`s moduli of CNT increases.

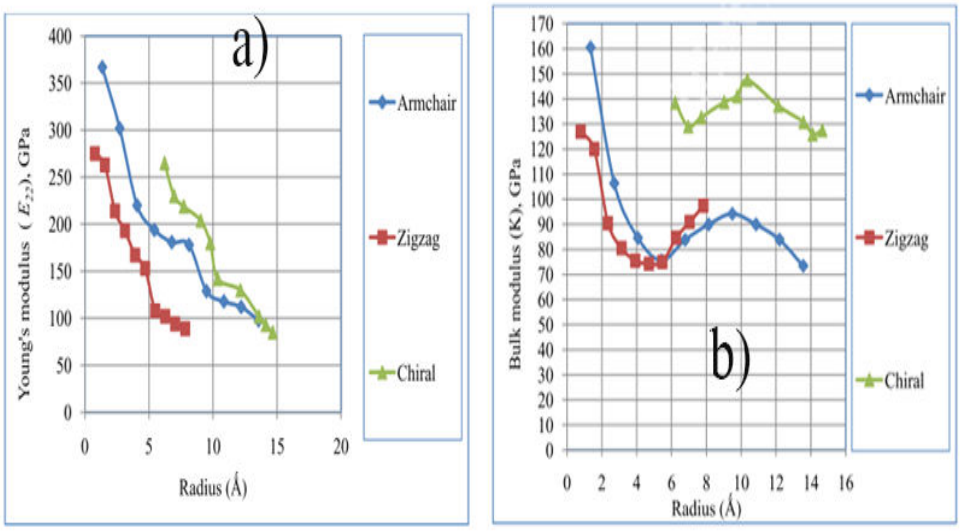

Figure 2.3 Variation of Young's modulus and Bulk modulus with radius for different types of SWCNTs [21]

Behrouz Arash and Quan Wang in (2014) [22] used the Molecular Dynamics (MD) simulations with a carbon nanotube-based nanopore system for investigating the molecular separation feasibility with carbon nanotubes. Author examined that complete separation of lead nanoparticles and water molecules is possible by applying the impact load, which can be realized by the propagation of impulse waves.

Nayebi *et al.* in (2015) [23] studied about the mechanical properties like stress, strain and elasticity modulus and Molecular Dynamics simulation has been used for computing these properties. In this study effect of graphene loading to the polymer, the orientation of tension, nanocomposite's temperature and graphene's defect on these properties has been investigated. It is analysed that along the zigzag orientation, mechanical characters of tension are higher than other directions. It has been observed that in composite graphene's weight concentration is directly proportional to Young's modulus and breaking strain. It has been concluded that Young's modulus has been decreased after increasing the temperature. By applying graphene structure defect, it has been reported that one atom is missing from the structure and this lowers the Young's modulus and modulus of elasticity gradually decreases when concentration defect increases.

Sumit Sharma *et al.* in (2015) [24] focused on modelling of carbon nanofibers (CNFs) and evaluated the effect of their reinforcement in poly propylene (PP) matrix. By using the Molecular Dynamics (MD) simulation, authors studied the effect of volume fraction

and aspect ratio of carbon nanofibre on mechanical properties of CNF–PP composites. From the results obtained it was concluded that with only 2% volume fraction of CNF in PP, 748% increase in E_{11} which was comparively high as compared to E_{22}.

Sumit Sharma *et al.* in (2015) [25] examined the mechanical properties of multi-walled carbon nanotubes–polycarbonate composites (MWCNT–PC), through a Molecular Dynamics (MD) simulation. By using the material studio 5.5, authors modeled the multiwall carbon nanotubes (MWCNTs) compositions in polycarbonate (PC) by varying the weight from 0.5% to 10% and by volume from 2% to 16%. For finding the mechanical properties Material studio 5.5, Forcite module was used and it was found that there was increase in the mechanical properties.

Norihiko Taniguchi *et al.* in (2016) [26] experimentally investigated the tensile strength of unidirectional carbon fiber reinforced plastics under a high strain rate by using tension-type split Hopkinson bar technique. The experimental result showed that tensile modulus and strength in the longitudinal direction are independent of the strain rate and observed that the strain-rate dependence of the shear strength is much stronger than that of the transverse strength.

2.1.4 Literature Review Based on Defects

T. W. Ebbesen and T. Takada in 1995 [27] discussed about the importance and existance of defects in carbon nanotubes. The author observed that the defects might affect strongly on the properties of nanotube such as band gap and their conductivity.

H. Jiang *et al.* in (2004) [28] was studied about stone-wales transformation in single walled carbon nanotubes. Defect nucleation in carbon nanotubes has been analysed under tension and torsion. In this study, continuum mechanics model has been introduced for studying the stone-wales transformation. It has been concluded that for SW Transformation critical strain has been analysed as 4.95% and the critical shear strain has been observed as 12%. The author has observed that this study shows better agreement between Molecular Dynamics studies and hybrid atomistic model studies.

N. Chandra *et al.* in (2004) [29] studied at atomic scales three different stresses had been measured and also strain had been introduced The introduced strain has been measured as conjugate quantities. These measurements have been validated for non-defected carbon nanotube by the author and it has been used in single wall tubes for finding topological defects. The author has analysed that in defected region load

carrying capacity has been decreased and in a change in kinematics and kinetics in the defected vicinity, this measure could be attributed.

Q. Lu and B. Bhattacharya in (2004) [30] were studied about the effect of randomly occurring stone-wales defect. Molecular Dynamics simulation performed for analysing the mechanical properties of single walled carbon nanotube, which is defected with stone-wales defect occurring randomly. In this simulation armchair and zigzag type carbon nanotube has been simulated and ultimate tensile strength and strength has been analysed. It observed that in case of single walled carbon nanotube having a single vacancy crack starts at random places. The author has observed that for the tube, mean value of strength, stiffness and ultimate strain reduced as the average number of defects amplified. It has been analysed that the zigzag tube was more brittle and exhibits more uncertainty in its mechanical properties than the armchair.

S. L. Mielke *et al.* in (2004) [31] has studied the effect of vacancy by using quantum mechanics calculation using DFT theory and semi empirical methods. In this study under uniaxial tension, the role of vacancy defects has been analysed using molecular mechanics calculation and fracture of carbon nanotubes has been analysed. After calculation author observed that one and two vacancy defects decreases the failure stress by 26%, but vacancy with no, three or more greatly reduces the mechanical properties and observed that in comparison to the stone-wales defect vacancy affects more on the strength of defected carbon nanotubes. Thus, concluded that vacancy may be the strength limiting for CNTs having high qualities.

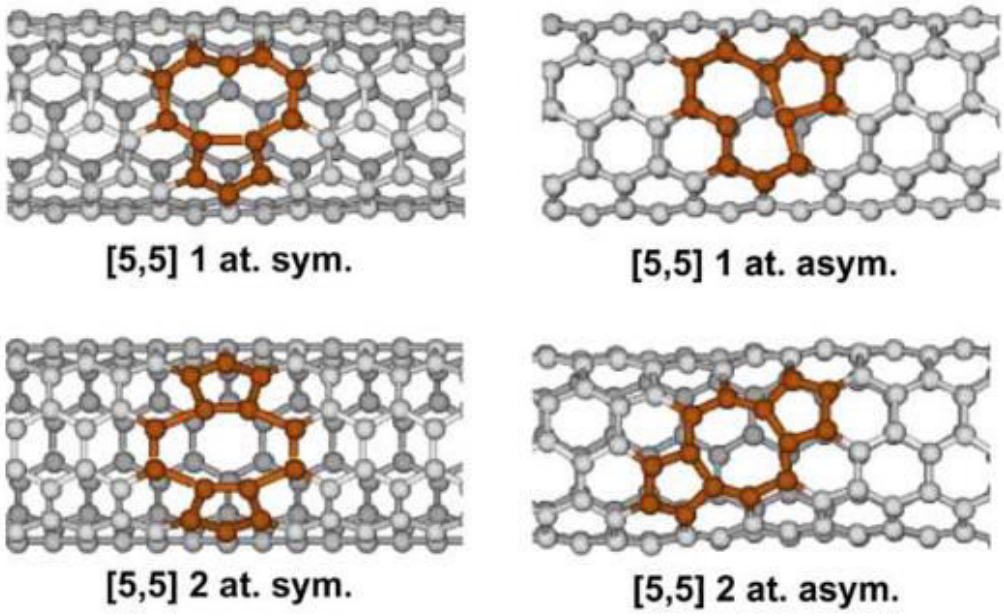

Figure 2.4 The reconstructions of the one- and two-atom vacancy defects considered [31]

Y. R. Jeng *et al.* in (2004) [32] author have carried out a Molecular Dynamics simulation for analysing the effect of temperature and vacancy defects on single-walled carbon nanotubes. In this study under tensile loading mechanical properties of zigzag, armchair and chiral single walled carbon nanotubes has been analysed. It has been concluded that under tensile loading armchair single walled carbon nanotube has the highest tensile strength as well as toughness. It has been concluded that mechanical properties get decreases with increasing of temperature and in case of vacancy defects, mechanical properties also decreased on increasing vacancy defects.

S. Zhang *et al.* in (2005) [33] analysed the fracture of defective carbon nanotube. In this study molecular mechanics and coupled molecular mechanics has been employed for the calculation and both the results were compared. It has been analysed by the MM Calculation that one- and two-atom vacancy defects reduces the strength of CNTs by 20%–33%, whereas from QM calculations it has been observed that CNTs strength gets reduced by 14%–27% due to these defects. The author observed that fracture strength is size dependent for a range of tube diameters with a variation of few GPA in DWCNTs with two-atom vacancy defects.

Brodka *et al.* in (2006) [34] was studied about the carbon nanotube's structure. In this study, defected carbon nanotube used as material and Molecular Dynamics simulation had been done analyzing it. Powder diffraction pattern has been calculated from carbon configuration, which is resulted from Molecular Dynamics simulation. The MD simulation results obtained for 0.87% of the defects in CNT were compared with experimental data and observed that simulated result were quite matched with the previously suggested concentration of the Stone-Wales defects.

H. Fan *et al.* in (2006) [35] analysed thermal conductivity of single-walled carbon nanotube by using material Studio software. In these study two kinds of Molecular Dynamics simulation equilibrium MD simulation and non-equilibrium MD simulation has been used. They have analysed the thermal conductivity of SWCNT which is affected by different kinds of defect and for defect free SWCNT also. Both the results were compared and it was found that defective SWCNT has very less thermal conductivity than a non-defective single-walled carbon nanotube. It has been observed that due to C-C bonding configuration stone-wales defects have less impact on thermal conductivity of carbon nanotube in comparison to vacancy defects.

Wang *et al.* in 2007 [36] studied the fracture of a chiral carbon nanotubes (CNTs) with one atomic vacancy and also observed Non uniform variation of the fracture strain using

molecular mechanics simulations. Author investigated the dependence of hardening or softening domains on the length and diameter of the CNTs and observed that the rupture progress of defected carbon nanotubes with the vacancy at different locations with molecular mechanic's simulations.

W. Hou1 and S. Xiao in (2007) [37] in this study author considered armchair and zigzag nanotube for investigations and effect of vacancy defect (which is randomly distributed) on mechanical behavior on single wall carbon nanotube has been investigated.Author has analysed by the Molecular Dynamics simulation that nanotube strength has decreased due to vacancy defects and nanotube can't be used as torsion springs as vacancy defects prevent.

Tserpes, K. I., & Papanikos, P. in (2007) [38] has analysed the effect of the stone-wales defect on the fracture and tensile behavior of the armchair, chiral and zigzag single-walled carbon nanotube. The author using atomistic based fracture model has performed this study. In chiral SWCNT the effect of defect lies in between armchair and zigzag SWCNT and it depends on the chiral angle. Author has analysed that there were no any defects present in stiffness of carbon nanotube. It has been analysed that tensile behavior of carbon nanotube affected by nanotube size is very small and larger decrease in stress failure has been observed.

R. W. Haskins *et al.* in (2007) [39] was studied about role of defects by analysing elastic moduli and failure for single walled nanotube. For this study Molecular Dynamics simulation has been performed and effect of defects has been analysed based on bond rupture. In this study Young's modulus for both the defective and non-defective single walled carbon nanotube has been analysed and found that Young's modulus for defective single walled carbon nanotube is reduced by 160 GPa and critical strain is reduced by 13%. In addition, it has been observed that in case of pair adjacent vacancy Young's modulus is lowered by 100 GPa and rupture strain is reduced by 10%.

Xin Hao *et al.* in (2008) [40] has compared the buckling load of both single walled and multi-walled carbon which is defective, with buckling of non-defective carbon nanotube. In this study Molecular Dynamics has been carried out and observed that load carrying capacity of the defective carbon nanotube is reduced due to vacancy defect. It has been analysed that defect intensity is related to the carbon nanotube buckling properties.

Jianhui Yuan and K.M. Liew in (2009) [41] examined the vacancy defect reconstruction and elastic properties of the typical armchair single-walled carbon nanotubes

(SWCNTs) with different defect ratio using the Molecular Dynamics method and discovered different reconstructions in the single vacancies and di-vacancies in SWCNTs at different temperatures, through optimizing. Authors found the Young's moduli of armchair SWCNTs with vacancy defects. Authors observed that due to vacancy defects, Young's modulus will be decreased, but their reconstruction helps in stabilizing the modulus.

S. N. H. Rubaiyat in (2009) [42] has studied the mechanical properties of defected CNT by using Molecular Dynamics simulation under both the tensile and compressive load. Vacancy defected, stone-wales defected and non-defected CNT has been simulated by this Molecular Dynamics simulation. Author has concluded modulus of elasticity is very less affected and tensile strength and compressive strength is insignificantly affected.

Mehrdad Arjmand *et al.* in 2010 [43] studied the effect of length on Young's modulus of zigzag carbon nanotubes (CNTs) by implementing new theoretical model and predicted that the elastic modulus of a CNT decreases with vacancies. The Young's modulus of an intact CNT unit cell of length equal to 0.639 nm was calculated about 940 GPa. As the length of unit cell increases to 0.781 nm causes a decrease in the modulus and it becomes 887 GPa, The result shows that all the defective CNTs have the moduli less than an intact one, but by increasing the length, effect of defects reduces and modulus of a defective CNT approaches that of an intact one.

S.C. Chowdhury and S.N.H. Rubaiyat in (2010) [44] has analysed the effect of defective carbon nanotube and non-defective carbon nanotube on mechanical behavior using Molecular Dynamics simulation. Results were compared and it was found that defected carbon nanotube has very less effect on elasticity modulus of the single-walled carbon nanotube. Author has also concluded that strain and stress failure is significantly affected.

Dinadayalane *et al.* in (2010) [45] studied about reactivities of sites on armchair single walled carbon nanotube and compared for both defective and defect free single walled carbon nanotube. For this study computer simulation has been carried out. It has been concluded that the presence of vacancy defects increases the energy gap. It has been analysed that through local ionization energy and pyramidalization angle most and least reactive sites can be observed. It has been concluded that the most reactive sites have lowest local ionization energy and largest pyramidalization angle whereas the least reactive sites have highest local ionization energy and lowest pyramidalization angle.

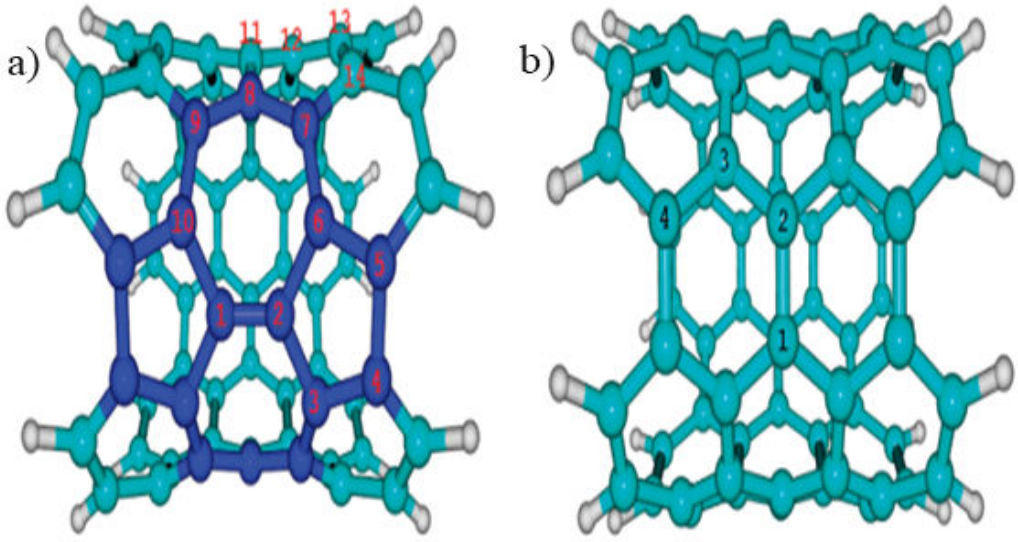

Figure 2.5 Stone-Wales defect (a) and defect-free (b) armchair (5,5) SWCNTs, C70H20. Atom numberings are indicated. The carbon atoms of the Stone-Wales defect region of 1 are shown in blue for clarity [45]

M.R. Davoudabadi and S.D. Farahani in (2010) [46] were investigated the effect of different vacancy defects on the Young's modulus of zigzag and armchair carbon nanotube reinforcement polymer composite in the axial. In this study, structural model is used in ANSYS software for the investigation. Molecular structural mechanics (MSM)/finite element (FE) Multiscale modelling has been used for investigating the effect of vacancy on CNT polymer nanocomposites. It has been concluded that in shorter length young's is greatly reduced while in longer tube vacancy impact is negligible. This method shows the good agreement with MD simulation. This method can be used for investigation of buckling behaviour of carbon nanotube.

Vali Parvaneh and Mahmoud Shariati in (2010) [47] were studied the effect of stone-wales and vacancy defects on Young's modulus of single walled carbon nanotube. For investigating Young's modulus, a structural mechanics model has been developed. It has been reported that best method for calculating Young's modulus of carbon nanotube is tension test. It has been observed that sufficiently large carbon nanotube has negligible effect of defects.

K. Talukdar and A. K. Mitra in (2011) [48] were studied the fracture behavior and mechanical properties of single-walled carbon nanotube by using Molecular Dynamics simulation. The author has introduced four stone-wales defects in three different single walled carbon nanotube and it has been found that single-walled carbon nanotube has significantly affected. The maximum strain has been affected due to the inclusion of stone-wales defect and the zigzag tube has not seen any such changes. In the case of

chiral and armchair sharp breaking has been seen and in the case of the zigzag tube, there is no such sharp breaking is observed.

H. Zeng *et al.* in (2011) [49] were studied about effect of Stone-wales and doping on electronic transport properties of graphene nanoribbons. In this study zigzag nanoribbon's electronic transport properties have been studied using the density functional theory which is combined with the non-equilibrium green's function. It has been analysed that defects affects more on centre rather than edge as for graphene nanoribbon energy are more at centre. It has been suggested that doping may not be sufficient for zigzag graphene nanoribbon's electronic transport properties modification.

K. Sharma *et al.* in (2012) [50] were studied about the defect of vacancy and multiple stone-wales using Molecular Dynamics simulation. In this paper, Molecular Dynamics simulation has been performed for both the defective as well as a pristine single-walled carbon nanotube. The stress-strain relationship has been established based on Molecular Dynamics simulation result. Results were compared and it was found that mechanical properties like the strength of defective SWCNT were gradually decreased on increasing of diameter. It has been also found that on increasing of a number of defects in Armchair CNT, failure of tube starts easily as it creates voids or holes. On the increment of defect density strain failure increases. For the same defect, density Vacancy affects the strength of nanotubes more in comparison with stone-wales defects.

K. K. Saxena and A. Lal in (2012) [51] studied the material properties of pristine carbon nanotube and defective carbon nanotube by using molecular simulation method. Author has analysed that tensile strength and strain of carbon nanotube, which is detected by vacancy defect, is more reduced in comparison to stone-wales defected carbon nanotube. It has also been analysed that stone-wales defected carbon nanotube needs more energy than a non-defected carbon nanotube to stabilize the structure. The author has also studied that Young's modulus of defected carbon nanotube is having less value than the pristine structure that is reduced by 9.3%.

K. Talukdar and A. K. Mitra in (2012) [52] have studied the fracture behavior and elastic properties of single-walled carbon nanotube by using Molecular Dynamics simulation. It has been analysed that single-walled carbon nanotube elastic properties has significantly affected by the presence of stone-wales and vacancy defects, also observed that defects play major role in breaking of single-walled carbon nanotube. For higher strain values, the energy difference fluctuations in case of zig zag tube is more as compared to other tubes for the same defect alignment and hence zigzag tube is less

stable with defects. It has been observed that defects will depend upon chirality of the single walled carbon nanotube as well as on its length.

S. Yang *et al.* (2012) [53] has analysed defect of thrower stone-wales on CNT composites. It has been identified that CNT is degrading and interfacial adhesion is improved between polypropylene and defected carbon nanotube having different thrower stone-wales defect. By mixing carbon nanotube with polypropylene, by using MD simulation method author has found the effect of TSW defect on polypropylene composite's elastic stiffness. The author has concluded using molecular software that non- adhesive bond energy between non-defective CNT and polypropylene chain is lesser than that between pp and defective CNT chain.

Jing Jie Yeo *et al.* in (2012) [54] were studied about the effect of double vacancy and Thrower-Stone Wales defects on graphene nanoribbon's thermal conductivity. In this study Molecular Dynamics simulation has been performed and force field has been chosen as LAMMPS. The author was reported that randomly dispersed Stone-Wales and vacancy defect causes large decreases in thermal conductivity. Performance also depends on chirality and types of defect.

Feng Dai-Li *et al.* in (2013) [55] has applied non-linear Molecular Dynamics method for investigating thermal conductivity of single-walled CNT with a stone-wales defect, doping, and non-defective SWCNT. After comparing the results author concluded that thermal conductivity of SWCNT with doping is nearly similar to non-defective SWCNT while SWCNT having vacancy defect and the stone-wales defect is lesser. The Author has analysed that armchair tube is greatly affected by stone-wales and doping while zigzag is more affected by vacancy defect. It has been concluded that stone-wales tube is having shorter thermal conductivity convergence than non-defected or vacancy defected single-walled carbon nanotube.

Monon *et al.* in (2013) [56] studied the effects of stone-wales defect on the mechanical behavior of single-wall carbon nanotube has been simulated by the atomistic finite element analysis and Molecular Dynamics simulation. The Author has analysed that elasticity modulus of SWCNT is depends on a number of the stone-wales defects, tube structure, and diameter of the nanotube. The author has compared both the results and concluded that molecular simulation shows good agreement for defect free SWCNT whereas FE simulation rejects for the defective CNT have a diameter less than 9.5 angstroms.

Xiao *et al.* in (2014) [57] were developed an atomistic based finite bond element model and effect of stone wales defect on mechanical properties of carbon nanotubes and graphene sheets has been analysed. For prediction of the stress-strain relationship and Young's modulus of pristine and defective carbon nanotube and graphene sheets modified Morse potential has been used. It has been analysed that vacancy and stone-wales defects depend upon chirality and diameter of carbon nanotubes and graphene sheets. It has less impact on longer carbon nanotube and higher density.

Sharma *et al.* in (2014) [58] studied about the defects of CNT and its effects on mechanical properties. In this study both non-defected and defected SWCNT has been analysed using Molecular Dynamics simulation method and properties for both the defected and non-defected CNT has been compared. It has been found that with the increase in number of defects the CNT moduli of SW defective CNT decreases rapidly in comparison with the decrease in the moduli of the vacancy defective CNT. With the increase in the volume fraction of CNT, the moduli of vacancy defective CNT is greater as comparison to the SW defective CNT. It has been observed that with an increase in diameter elastic moduli is gradually degraded.

Xia *et al.* in (2014) [59] studied about the effects of vacancy and stone-wales defect on atomic-scale friction for graphite. For this vacancy defects study computer simulation has been carried out. In this study force field has been chosen for this Molecular Dynamics simulation as LAMMPS. It has been concluded by the author that vacancy defects have more influence on graphite in comparison to Stone-Wales defect. It has been observed that the defect location/position and number has more impact on the frictional force for graphite. This occurs due c-c bond configuration in Stone-wales defect and vacancy defects.

Marino Brcic *et al.* in (2014) [60] studied about the influence of waviness and vacancy defects in carbon nanotubes properties in this study. In this study finite element method has been used for calculation of mechanical properties of CNT which is defected with vacancy. In this study after the theoretical calculation author has concluded that properties of CNTs are dramatically reduced by vacancy and waviness. As the waviness ratio increases the longitudinal elastic modulus of the straight carbon nanotube also decreases. It has been reported that position and number of vacancies have more impact on the properties of CNTs.

R. Rafiee and M. Mahdavi in (2015) [61] has analysed the effect of vacancy defect on mechanical properties of carbon nanotube by Molecular Dynamics simulation. The

author has analysed Young's modulus of both non-defected carbon nanotube and defected carbon nanotube and then the results were compared. It was found that non-defected carbon nanotube has less Young's modulus in defected carbon nanotube than a non-defected carbon nanotube. It has been analysed that vacancy defect plays a vital role in the decrease in Young's modulus. It has been analysed that six vacancy defects have ability to reduce the Young's modulus of CNT up to 10%.

Aghadavoudi *et al.* in (2016) [62] analysed the effect of elastic behavior on mechanical properties for both non-defected and defected carbon nanotube materials by using Molecular Dynamics software. Results were compared and it was concluded that the defected carbon nanotube is having very less Young's modulus. The author has analysed that the CNT affects modulus of elasticity greatly in the transverse direction. It has been also analysed that number of defects also affect the mechanical properties of the material. It has been analysed that Stiffness of nanocomposite reduces by increasing the number of defects in the CNT. It has been reported by the author that mechanical behavior of nanocomposites is greatly affected by non-constructed vacancy defects. The author has concluded the behavior of cross-linked epoxy based nanocomposites by the above molecular modelling.

X. Peng and S. A. Meguid (2017) [63] studied about the buckling behavior of single walled carbon nanotube. Molecular Dynamics simulation has been carried out for the simulation of stone-wales defect and vacancy defected carbon nanotube. In this simulation, force field has been chosen as LAMMPS for Molecular Dynamics simulation. It has been observed that Vacancy and SW defect reduces the buckling resistance. The author has analysed that buckling load of defect free SWCNTs have more than defected SWCNTs. It has been analysed that the buckling load of free standing SWCNTs gets decreases as no. of missing atom increases.

2.1.5 Literature Review Based on Functionalization

E. T. Mickelson *et al.* in (1999) [64] formed "fluorotubes" by fluorinating the pristine SWNT. Fluorotubes were then solvated in liquor solvents utilizing "ultrasonication". Nuclear power microscopies (AFM) utilized for the examination. Natural examination and number of microscopy and spectroscopies utilized for precise outcomes. SWNTs can be fluorinated or functionalized with fluorine and sonicated in liquor to give exceptionally stable fluorotubes. This solvation technique allows us to manipulate functionalized SWNTs in numerous ways. Important point is that alcohol solvent was

used in this research which itself help in further functionalization, and stability of Fluro tubes.

Ya-Ping Sun *et al.* in (2002) [65] attempted to identify and analyze properties as well as applications of functionalized CNTs. It was observed that CNTs could be functionalized through esterification and amidation of the nanotube-bound carboxylic acids. The dissolvability of the functionalized CNTs makes it conceivable to describe and contemplate the properties of carbon nanotubes utilizing arrangement-based strategies. Agent comes about concerning the solvency, de-functionalization, scattering, and optical properties of the functionalized carbon nanotubes were displayed. Functionality and solubility of functionalized CNTs were found to be up to the mark.

Haiqing Peng *et al.* in (2003) [66] reacted SWNTs with glutaric acid acyl peroxides with o-dichlorobenzene at a temperature of around 80-90 degree centigrade, to get three carboxy-propyl groups on the side walls of SWNT. FTR, Raman spectroscopy, and transmission electron microscopy (TEM) was done for better results. In examination with the perfect or pure SWNTs, the functionalized SWNTs were found to be demonstrating an enhanced dissolvability in polar solvents, for instance, alcohols and water, which empowers their preparing for joining into polymer composite structures and additionally for an assortment of biomedical applications.

Bumsu Kim *et al.* in (2004) [67] oxidized MWNTs using nitric and sulfuric acid (in in ratio of 1:3) that is ultrasonication of MWNTs. Complex development of charged gold nanoparticles and negative MWNTs was accomplished of and without polyelectrolyte coatings by electrostatic collaboration. The perplexing arrangement was described by high-determination transmission electron microscopy and dispersive X-ray spectroscopy. This technique is more of a fault detection than a composite formation.

M.C. Paiva *et al.* in (2004) [68] functionalized CNTs with vinyl group were reinforced into PVA matrix and mechanical as well as morphological properties were observed. Both Pristine as well as functionalized SWNTs were tested under tension, it was observed that functionalized SWNT is superior to pristine SWNT in every aspect of mechanical properties. CNTs were wetted well by PVA matrix, in case of functionalized SWNT, as per SEM results.

N.O.V. Plank *et al.* in (2004) [69] functionalized SWNTs using traditional Reactive Ion Etching to get fluorinated SWNTs when reacted with CF_4 and SF_6. The functionalized SWNTs were then examined with X-ray photoelectron spectroscopy. Microscopic plasma parameters including ion current density and fluorine pressure

within the plasma were also studied using a Langmuir probe and optical emission spectroscopy. This process of making functionalized SWNT is found to be reliable as fluorine was attached to SWNT for a longer period.

L.Liu *et al.* in (2005) [70] observed mechanical properties of nanocomposites of functionalized SWNTs -polyvinyl alcohol. With the help of absorption spectroscopy, sidewall functionalization was obtained via chemisorption. Author observed that functionalized CNTs produce comparatively better Young's modulus than pristine CNTs for the composite case with PVA matrix. Hydroxyl groups helped to increase interfacial properties to a significant extent.

Ramanathan *et al.* in (2005) [71] Single-walled carbon nanotubes (SWCNT) functionalized with amino groups were readied through chemical adjustment of carboxyl groups presented on the carbon nanotube surface. Two varying methodologies (amide and amine-moieties) were utilized to create the amino-functionalized nanotubes. The amino-end permits promote science of the functionalized SWCNTs and makes conceivable covalent bonding to polymers and natural frameworks, for example, DNA and sugars. The functionalization of the SWCNTs was also portrayed in detail utilizing FTIR and XPS.

Jie Liu *et al.* in (2006) [72] used free radical addition using aryl to do sidewall functionalization of SWNTs. They reported another SWNT functionalization technique using 4-methoxyphenyl free radical expansion. The 4-methoxyphenyl radicals were produced via air oxidation of 4-methoxyphenylhydrazine hydrochloride. Raman spectroscopy demonstrates the covalent idea of the bond among the functional groups and the nanotubes. The TGA and XPS information outfit quantitative data on the level of functionalization.

Rahul Jain *et al.* , in 2006 [73] investigated the effect of carbon nanofibers (CNFs) after mixing with phenolic matrix on composite microstructure and inter-laminar shear strength (ILSS) of the as-cured and carbonized composite specimen. Authors found that surfactant treatment of the C-fabric adversely affected the interfacial properties, at both as-cured and carbonized stages. At the as- cured stage, the non-surfactant treated specimens, for 0% CNF loading, showed 12% and 631% higher ILSS values than the 12.5% and 50% surfactant treated specimens respectively. The surfactant treatment of the carbon fibers weakens the interface due to reduced cross-linking of the matrix in the resulting composite.

Prabhjeet singh *et al.* in (2009) [74] did Esterification and fluorination at different conditions to obtain functional groups as ester and fluorine on the surface of CNT, Organic functionalization process were used for this research and results obtained says that process-ability and capability is more in the case of functionalized CNTs.

Robert Menzel *et al.* in (2010) [75] used a solvent-free, versatile methodology to functionalize CNTs. The conveyance of the functionalized destinations was researched at the infinitesimal scale utilizing labelling responses. The joined items have been described by electron microscopy, thermal analysis (TGA), inverse gas chromatography (IGC), and Raman spectroscopy.

Ailin Liu *et al.* in (2011) [76] observed the impact of functionalization SWNTs on the damping attributes of SWNT-based epoxy composites by means of multiscale analysis. Carboxylic (-COOH) group was used to functionalize the SWNT, and epoxy was used as matrix. Results were obtained using molecular simulations. It was observed that as the number of functional groups increases, the interfacial shear strength also increases. However, the damping properties did not follow any general trend, unpredictability was observed in case of damping properties.

Hailong Chen *et al.* in (2012) [77] used Methoxy Polyethylene Glycol Amine as functional group ,also used micro RNA analysis for functionalizing SWNTs. This type of approach to do functionalization finds its application in the field of biology, as it makes drug delivery easy.

Valentini Lara *et al.* in (2014) [78] used radial deformation method to functionalize CNT with carboxylic groups. In this research, the reliance of the basic and the electronic properties of functionalized (5, 5) SWNTs were examined through ab initio thickness utilitarian simulations when the carboxyl gathering is fortified on the bended or flatter areas. Radial deformations result in measurement diminishing of up to 20 for each penny of the first size of diameter, which was the breaking point decrease that keeps up the SWNT functionalized structure. Changes on the electronic structure were seen because of the symmetry break of the SWNT caused by both the carboxyl group and the C–C bond twists came about by the radial deformation. It was concluded that the functionalization procedure is uncommonly supported by the sp_3 hybridization actuated on the more bended district of the twisted SWNT.

Zahra Mohammadi *et al.* in (2015) [79] did a relative report on non-covalent functionalization of CNTs by chitosan, as functional element, and its subsidiaries for conveyance of doxorubicin. This type of approach to do functionalization finds its

application in the field of biology, as it makes drug delivery easy. It was observed that applying Carboxymethyl Chitosan rather chitosan for functionalization prompted 10% expansion in stacking productivity.

E.V. Basiuk *et al.* in (2015) [80] used amines to do solvent free functionalization of CNTs. In this study filtration of the MWCNTs-ox scatterings created uniform perfect BP mats, promptly expelled from their fundamental help membranes. The tangle thickness as measured by SEM and HeIM differed in the scope of 35-50μm. The maximum amine content, as examined from TGA curves, was found for BP-ODA, and the minimum one was found for BP-DAN. However, it is accurate, but expensive approach for functionalization.

Kong N. *et al.* in (2015) [81] used a different approach for functionalization of CNTs. In outline, author proposed a successful strategy to conjugate carbohydrate structures to perfect SWNTs utilizing microwave-helped response of perfluoro phenylazides. This was the first case of applying microwave radiation to PFPA actuation, speaking to another approach to integrate carbon nanotube-based glycol nanoparticles. This strategy utilized pristine SWCNT rather than oxidized SWCNT, maintaining a strategic distance from broad modification to the cross section and the inherent properties of SWCNT. The subsequent materials were less packaged and very much scattered in water contrasted with pristine SWCNT.

Vinay Deep Punetha *et al.* in (2016) [82] did a comparative analysis between CNT and graphene based on the nanocomposites formed by functionalization of CNTs. Mechanical, electrical, and thermal properties was compared, and it was found that CNT as well as graphene both shows remarkable properties. It was reported that the only different arises with their compatible polymer matrix.

Ge Tian *et al.* in (2016) [83] observed substituent impacts in p-stacking of histidine on graphene and functionalized-SWNT. Molecular simulation was run for SWNT zigzag (10, 0), three varying groups –COOH, –OH and $–NH_2$, were attached directly on the sidewalls of the SWNT structure. The results show that the pi-stacking for functionalized-SWNT is weakened.

Sumit Sharma *et al.* in (2016) [84] used Molecular Dynamics simulations to analyze functionalized SWNT-polymer nanocomposites; In this research both dynamics as well as mechanical properties of SWNT with varying functional groups were observed. Armchair (4, 4) SWNT was chosen and molecular simulation was done with proper consideration of practical environment conditions. Aspect ratio was fixed to 10. It was

reported that functionalization reduces the Young's modulus of SWNT, the largest reduction was observed in case of carboxylic (-COOH) functional group. Research Gaps

2.2 Research Gaps

Based on the above reviewed literature and the knowledge gap for the MD method, the following conclusions can be drawn:-

Mostly the work carried out by the researchers based on the molecular level on CNTs, the area of interfacial properties of the carbon nanotube reinforced polymer composites need to be explored fully.

(i) After reviewing the literature, we come to know that the lots of work carried out for finding out the mechanical properties of the defective CNTs, but the effect of the Stone-wales and vacancy defects on the interfacial properties of the CNT reinforced polymer composites not much explored.

(ii) Not enough data/work is carried out on finding the interfacial properties of the CNT reinforced polymer composites based on the effect of the functionalization. No data is available on the effect of aspect ratio and the interfacial properties of the CNT reinforce Natural rubber composites.

2.3 Objectives

Objectives of the present work have been derived based on comprehensive literature review. Scope of the work includes:

(i) To study the effect of chirality, length and diameter of Carbon nanotube on the interfacial properties of CNT/polymer composites.

(ii) To predict the mechanical properties of CNT reinforced polymer composites with fiber volume fraction and fiber ratio using MD simulation

(iii) To predict longitudinal, transverse, longitudinal shear and transverse shear moduli of CNT reinforced polymer nanocomposites using MD simulation

(iv) To study the effect of Stone-Wales and vacancy defects on thermal and mechanical properties of CNT reinforced polymer nanocomposites

(v) To study the effect of functionalization of CNTs on the young`s modulus of CNTs composites

(vi) To predict the damping and thermal conductivity of the CNTs reinforced polymer using Molecular Dynamics simulation

Chapter 3

Materials and Methodology

3.1 Materials

3.1.1 Single Walled Carbon Nanotube (SWCNT)

In this study, Single Walled Carbon Nanotube (SWCNT) has been developed using commercial software "Material Studio". Single walled carbon nanotube is having unique properties such as high thermo-mechanical and excellent electrical properties. In this study, armchair (5, 5) type SWCNT has been used. The diameter has been taken as 0.678nm and length has been taken as 5.58 nm.

3.1.2 Natural Rubber (NR)

Natural rubber consists of polymers of the natural compound called isoprene, with a few polluting influences of other natural mixes, in addition to some water. Directly, elastic is collected as the latex that is obtained from the elastic tree. It is an elastic substance, which is obtained from latex sap of trees, belongs to Ficus and genera Hevea. In technical language, it is known as an elastomer. Elastomers are the types of poly-isoprene that are utilized as normal elastic. Normal elastic is utilized as a part of numerous applications, either in mix with different materials or might be distant from everyone else. In its helpful structures, it has a high strength and is exceptionally waterproof in nature. The soonest utilization of normal elastic was by the human evolution of Mesopotamia. Characteristic Rubber shows one of a kind compound and physical properties. Regular rubber's stress–strain conduct demonstrates the Payne and the biscuits impact and is frequently considered as hyper-flexible. The nearness of a twofold bond in each rehashing monomer unit makes regular elastic defenseless to ozone splitting and vulcanization. The two noteworthy solvents for elastic are turpentine and naphtha. As elastic does not break up effectively, the material is partitioned finely by destroying before its inundation. Mostly, smelling salts are utilized to keep the coagulation of crude latex. Normal Rubber begins to soften at around 180°C or 356°F. The model of characteristic elastic is shown in Figure 3.1

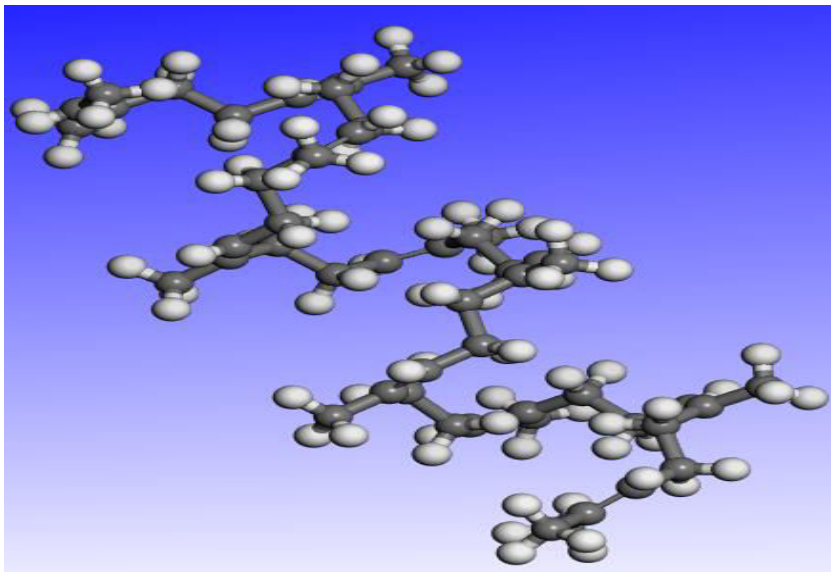

Figure 3.1 Molecular model of 10 repeat units of one NR chain consisting of 132 atoms

3.1.3 Properties of Natural Rubber

The bulk mechanical and thermal properties for continuum scale analysis are highly dependent on experimental study. Molecular simulations give a tremendous opportunity to study the influence of nanoparticles on the structure and dynamics of polymers. Detailed information on the properties near a nanoparticle surface is difficult to obtain experimentally. Natural rubber possesses the excellent abrasion resistance, tear resistance and resilience properties. It has unique properties such as excellent green strength and tack, high resistance to tearing, chipping and cutting, with the enhanced fuel economy. It also has drawbacks like it has moderate resistance to damage caused by ozone environment, light and heat. It can be used as a spring material and it forms a strong barrier to water.

3.2 Molecular Dynamics (MD)

In Molecular Dynamics, a molecule is expressed as a series of charged points linked by springs. The methods available for carrying out computations are molecular mechanics, Molecular Dynamics (MD), Monte Carlo (MC), Free energy and solvation methods, structure/activity relationship and many other established procedures. It is the only method available for solving complex body problems. Hamiltonian is not known to us until we calculate the quantum many-body problem. It requires many approximations, so it is not possible in most of the cases for solving complex many-body systems. However, any complex system can be analyzed using MD simulation. Experiments are expensive and limited in many cases. Experiments can be

complemented by the simulations. Even at a single molecule level, microscopic understanding can be provided by the molecular dynamic simulation.

3.3 Methodology

This section presents the methodology involved in the MD simulations in general. Starting from the geometry optimization to dynamics and force filed calculation methods are presented.

3.3.1 Geometry Optimization

In Molecular Dynamics simulation, it is essential to minimize the potential energy of the system to create a stable system and is frequently used. During sketching the molecules, the state of molecules would be at high energy configuration and when the simulation performed on such high energized molecules with un-optimized structure can give inaccurate results. In the Material Studio, optimization techniques such as conjugate gradient method, smart algorithm method and steepest descent method are available. In the conjugate gradient and smart algorithm method, an algorithm refines the direction in each successive step towards the minimum energy so as to produce a completely basic set of conjugate directions. If these conjugate directions truly extend the space of the energy surface, then minimization along each direction in turn must be a minimum.

A set of direction has been constructed and followed by the conjugate gradient algorithm. N^2 independent data points are essential to solve a harmonic function with N variables numerically. To converge the gradient-based minimizer in N steps, the gradient must be a vector with N variable. To exploit the second derivative information optimization might converge in one-step, due to each second derivative is the $N \times N$ matrix. Newton-Raphson is the commonly used, the reason behind the variable metric optimization algorithms used is the principle of the $N \times N$ matrix. Another way of looking at Newton-Raphson is that, in addition to using the gradient to identify a search direction, the second derivative (the curvature of the function) is also used to predict where the function passes through a minimum along that direction. The curvature in each gradient direction can be defined through the complete second-derivative matrix whereas a vector that translates directly to the nearest minimum can be obtained by multiplying the inverse of the second-derivative matrix with the gradient. In the steepest descent's method, the line search direction is defined along the direction of the local downhill gradient. Each line search generates a new direction that is perpendicular to

the previous gradient; however, the directions oscillate along the way to the minimum. This inefficient behavior is characteristic of steepest descents, especially on energy surfaces having narrow valleys. Convergence is slow near the minimum because the gradient approaches zero, but the method is extremely robust, even for systems that are far from being harmonic. This method is most likely to generate the true low-energy structure, regardless of what the function is or where the process begins. When the gradients are large and the configurations are far from the minimum then the steepest descents method is often used. This is commonly the case for initial relaxation of poorly refined crystallographic data or for graphically built models. The steepest descent method converges slowly near the minimum because each segment of the path tends to reverse progress made in an earlier iteration. It would be preferable to prevent the next direction vector from undoing earlier progress. In this study, we have used the smart algorithm, which is a cascade of the above stated methods.

3.3.2 Dynamics

In this step, a dynamics simulation can be run, once an energy expression and, if required, optimized structures have been defined for the system of interest. This simulation is based on the classical equation, which is modified to deal with the effects of temperature and pressure on the system, where appropriate. The models constructed, are then put into an ensemble with the constant number of atoms, volume and temperature (NVT) simulation with a temperature of 300° K for 5 ps with a simulation time step of 1 fs. Through this approach, the structure has been thermally stabilized. The Andersen thermostat is applied to simulate and maintain the temperature at 300 K. MD simulation was performing approximately 5000 steps when the temperature attained a constant value. The main product of a dynamics run is a trajectory file that records the atomic velocities, atomic configuration and other information at a sequence of time steps, which can be analyzed subsequently.

3.3.3 Force Field

In the context of molecular modeling, force field refers to the form and parameters of mathematical functions used to describe the potential energy of a system of particles (typically molecules and atoms). Force field functions and parameter sets are derived from both high-level quantum mechanical calculations and experimental work. "All-atom" force fields provide parameters for every type of atom in a system, including hydrogen, while "united atom "force fields treat the carbon and hydrogen

atoms in ethylene and methyl groups as a single interaction center. “Coarse-grained" force fields provide even more crude representations for increased computational efficiency, which are frequently used in long-time simulations of proteins, the usage of the term "Force field" in chemistry and computational biology differs from the standard usage in physics. In chemistry, it is a system of potential energy functions rather than the gradient of a scalar potential, as defined in physics. The basic functional form of a Force field encapsulates both bonded terms relating to atoms that are linked by covalent bonds, and non-bonded (also called "non -covalent") terms describing the long-range electrostatic and van der Waals forces. The specific decomposition of the terms depends on the force field, but a general form for the total energy in an additive force field can be written as:

$$E_{total} = E_{bonded} + E_{non-bonded} \quad (1)$$

Where, the components of the covalent and non-covalent contributions are given by the following summations:

$$E_{bonded} = E_{bond} + E_{angle} + E_{dihedral} \quad (2)$$

$$E_{non-bonded} = E_{electrostatic} + E_{wandewalls} \quad (3)$$

Generally, the terms in any force field that describes the total potential energy are following:

$$E_{total} = E_{valence} + E_{cross-term} + E_{non-bond} \quad (4)$$

The sum of the valence, cross-term, and non-bond interaction energies of a system of interacting particles can be expressed as the total potential energy of a system.

$$E_{valence} = E_{bond} + E_{angle} + E_{torsion} + E_{loop} + E_{UB} \quad (5)$$

The valence energy consists of a bond stretching term, E_{bond} a two-bond angle term, E_{angle} a dihedral bond-torsion term, $E_{torsion}$ an inversion term, E_{loop} and a Urey-Bradlay term, E_{UB}

$$E_{cross-term} = E_{bond-bond} + E_{angle-angle} + E_{bond-angle} + E_{end-bond-torsion} + E_{middle-bond-torsion} + E_{angle-angle-torsion} \quad (6)$$

$E_{cross\text{-}term}$, the cross-term interacting energy generally includes: $E_{bond\text{-}bond}$ describes the stretch-stretch interactions between two adjacent bonds, the term $E_{angle\text{-}angle,}$ describes the bend-bend interactions between two valence angles which is associated with a common vertex atom, $E_{bond\text{-}angle}$, indicates the stretch-bend interactions between a two-bond angle and one of its bonds, stretch-torsion interactions between a dihedral angle

and one of its end bonds given by term, $E_{end\text{-}bond\text{-}torsion}$, $E_{middle\text{-}bond\text{-}torsion}$ which is stretch-torsion interactions between a dihedral angle and its middle bond, $E_{angle\text{-}torsion}$ the term defines bend-torsion interactions between a dihedral angle and one of its valence angles and the term $E_{angle\text{-}angle\text{-}torsion}$ represents the end-bend-torsion interactions between a dihedral angle and its two valence angles.

$$E_{non-bond} = E_{vdW} + E_{Coulomb} + E_{H-bond} \quad (7)$$

The non-bonded interaction term, $E_{non\text{-}bond}$, describes the interactions between non-bonded atoms and includes the van der Waals energy, E_{vdW}, the Coulomb electrostatic energy, $E_{Coulomb}$, and the hydrogen bond energy, which is, $E_{H\text{-}bond}$. The COMPASS force field includes the following terms for the total potential energy [86, 87]:

$$E_{valence} = \sum_b [K_2(b-b_0)^2 + K_3(b-b_0)^3 + K_4(b-b_0)^4] + \sum_\theta [H_2(\theta-\theta_0)^2 + H_3(\theta-\theta_0)^3 + H_4(\theta-\theta_0)^4] + \sum_\emptyset [V_1[1-\cos(\emptyset-\emptyset_1^0)] + V_2[1-\cos(2\emptyset-\emptyset_2^0)] + V_3[1-\cos(3\emptyset-\emptyset_3^0)]] + \sum_\chi K_x\chi^2 + E_{UB} \quad (8)$$

$$E_{cross-term} = \sum_b \sum_{b'} F_{bb'}\ (b-b_0)(b'-b_0') + \sum_\theta \sum_{\theta'} F_{\theta\theta'}\ (\theta-\theta_0)(\theta'-\theta_0') + \sum_b \sum_\theta F_{b\theta}\ (b-b_0)(\theta-\theta_0) + \sum_b \sum_\theta F_{b\theta}\ (b-b_0) \times [V_1 cos\emptyset + V_2 cos2\emptyset + V_3 cos3\emptyset] + \sum_{b'} \sum_\theta F_{b'\theta}\ (b'-b_0')(b'-b_0') \times [F_1\, cos\emptyset + F_2\, cos2\emptyset + F_3 cos3\emptyset] + \sum_\theta \times \sum_\emptyset F_{\theta\emptyset}\ (\theta-\theta_0) \times [V_1 cos\emptyset + V_2 cos2\emptyset + V_3 cos3\emptyset] + \sum_\emptyset \sum_\theta \sum_{\theta'} K_{\emptyset\theta\theta'}\, cos\emptyset \times (\theta-\theta_0) \times (\theta'-\theta_0') \quad (9)$$

$$E_{non-bond} = \sum_{i>j} \left[\frac{A_{ij}}{r_{ij}^9} - \frac{B_{ij}}{r_{ij}^6}\right] + \sum_{i>j} \frac{q_i q_j}{\varepsilon r_{ij}} + E_{H-bond} \quad (10)$$

Where q defines the atomic charge, ε is the dielectric constant, and r_{ij} is the i-j atomic separation distance. The lengths of two adjacent bonds are given by b and b′, θ is the two bond-angle, ∅ is the dihedral torsion angle, χ and is the out-of-plane angle. b_0, $k_i(i=2-4)$, θ_0 , $H_i\ (i=2-4)$,

$\emptyset_i^0(i=1-3)$, $V_i(i=1-3)$,

$F_{bb'}$ b_0', $F_{\theta\theta'}$, θ_0', $F_{b\theta}, F_{b\emptyset}, F_{b'\theta}, F_i(i=1-3)$,

$F_{\theta\emptyset}, K_{\emptyset\theta\theta'}, A_{ij}$ and B_{ij} are the parameters which depend on the system.

3.4 Simulation Strategies

In this study we have performed simulations for finding the mechanical properties of the SWCNT reinforced polymer, effect of defects on thermo-mechanical properties of SWCNT reinforced polymer, effect of functionalized SWCNT reinforced polymer. For studying the molecular structure, we have used "Material Studio 2017"

software. The flow chart of the steps involved in simulation is shown in Figure 3.2 and the details of the steps adapted in Molecular Dynamics simulation in this study are highlighted below.

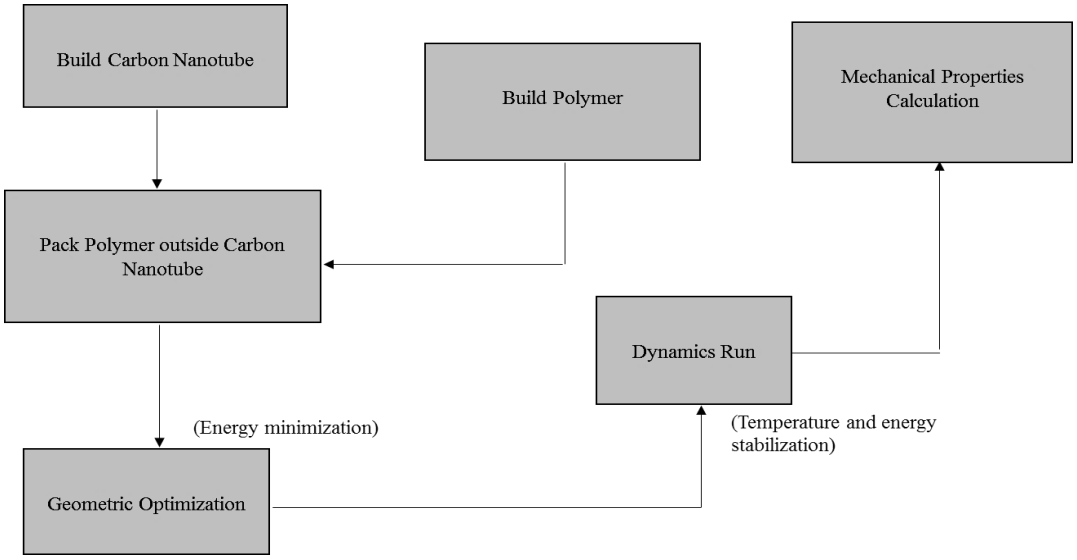

Figure 3.2 Flow chart containing the steps adapted in simulation

Step 1: Create molecule like nanostructure, polymer etc. To build a SWCNT Using "Build nanostructure" tool from the Build drop down menu. SWCNT was chosen, and the n and m values were set according to the configuration of CNT i.e. chiral (n, m), armchair (n, n) and Zigzag (n, 0). Hydrogen atoms were terminated from both the ends. So, finally a SWCNT was obtained. Then the length of the SWCNT could be increased by using the "Build Symmetry" option under the "Build" tool by entering the numerical value. Natural rubber as a polymer, Using "Build monomer" tool in Build drop down menu to make a polymer. A library of diene was chosen, and repeat unit was set to Natural rubber with the number of repeating units set to 10.

Step 2: Packing of a composite system using "amorphous cell module". After the modeling of the polymer and SWCNT, around the SWCNT packing has been done by the polymer using the "Amorphous cell" module. In the amorphous cell module, the following data shown in Table 3.1 was used.

Table 3.1 Packing parameters for SWCNT/NR composite

Parameter	Value
Task	Packing
Quality	Fine
Density	0.98 g/cm^3
Composition	Natural rubber

Step 3: Geometry optimization was performed using Forcite tools. This step is crucial because configurations in the beginning is in the higher state of energy and thus needs to be minimized. Many optimization methods are available in material studio and steepest descent method was particularly chosen for this study. The parameter and the desired value required to run the optimization is shown below in Table 3.2.

Table 3.2 Geometry optimization parameters for SWCNT/NR composite

Parameter	Value
Algorithm	Steepest Descent
Quality Tolerance	Fine
Energy Tolerance	10^{-4} kcal/mol
Force Tolerance	0.005 kcal/mol/ A^0
Displacement Tolerance	5 X 10^{-5} A^0
Maximum Iterations	90000

Step 4: After the geometric optimization step, the dynamics run step followed. This step also comes under “Forcite Module”. However, in the Dynamics using Forcite module, some the parameter needs to specify like NPT (Constant pressure, constant temperature), “Nose” as a thermostat and “Berenderson” as a Barostat.

Once an energy articulation and, if required, an improved structure have been defined for the arrangement of intrigue, elements dynamics can be run. The premise of this reproduction is the traditional conditions and equations of motion which were modified, where fitting, to manage the effects of temperature and weight on the system. After the dynamics run is completed, we can check whether the system is stabilized or not by viewing the energy plot and the temperature plot. The parameter used which is required to run the dynamics under the Forcite module is mentioned in the Table 3.3.

Table 3.3 Dynamics run (NPT) parameters for SWCNT/NR composites

Parameter	Value
Ensemble	NPT
Initial Velocity	Random
Temperature	298K
Time Step	1 fs
Total Simulation time	60 ps
Number of steps	60,000
Frame output	5,000
Energy deviation	50,000 kcal/mol
Thermostat	Nose
Barostat	Berendsen

Step 5: Geometry optimization uses Forcite tools, for minimizing the energy and stabilization of the structure. Same procedure with the same values used in step 3, and Table 3.2 are to be repeated.

Step 6: In Dynamics using Forcite tools, this tool consists of NVT (Constant volume, constant temperature), "Anderson" as a thermostat. Dynamics as need could be done again after energy optimization, and this time using NVT ensemble. In addition, some different parameters and values were taken as described in Table 3.4.

Table 3.4 Dynamics run (NVT) parameters for SWCNT/NR composites

Parameter	Value
Ensemble	NVT
Initial Velocity	Random
Temperature	298K
Time Step	1 fs
Total Simulation time	40 ps
Number of steps	40,000
Frame output	5,000
Energy deviation	50,000 kcal/mol
Thermostat	Andersen

Step 7: Geometry optimization using Forcite tools, for stabilization of the structure. Energy optimization for the final time, for stabilization of the structure, needs to be done before the mechanical properties analysis. Values the same as given in Table 3.2 were to be used.

This step depends on the results of geometric optimization. After successful completion of this step, mechanical properties for the equilibrated system will be analyzed. At the end of this step, we will obtain a stiffness matrix and the values of Young's moduli. Following data mentioned in Table 3.5 was used for the mechanical characterization of the SWCNT/NR composite.

Table 3.5 Mechanical properties simulation parameters for SWCNT/NR composites

Parameter	Value
Number of strains	6
Maximum strain	0.003
Pre-optimize structure	Yes
Algorithm	Steepest Descent
Maximum iterations	90000
Force field	COMPASS

Step 8: This is the final step, which involves “Mechanical property” calculation. In this step also, the output of the seventh step will be the input for this final step. In this step mechanical properties have been calculated using “Forcite” tools and method for calculating mechanical property has been selected as the “constant strain method”. This step depends on the results of geometric optimization. After successful completion of this step, mechanical properties for the equilibrated system would be analyzed. At the end of this step, we would obtain a stiffness matrix and the values of Young’s moduli. The data mentioned in Table 3.5 was used for the mechanical characterization of the single walled carbon nanotube reinforce Natural rubber composite.

Chapter 4

Effect of Chirality, Length and Diameter of Nanotube on the Interfacial Properties of CNT Reinforced Polymer Composites

In this chapter, we evaluated the interfacial properties of the SWCNT reinforced polymer composites. For finding the interfacial properties of the SWCNT reinforced polymer, a single wall arm chair composites (5, 5) packed with the Natural Rubber polymer has been used. The pull out of the three (5, 5) single walled carbon nanotube from the matrix with different length of same diameter has been performed to study the effect of the length. Similarly the pull out with different diameters of the single wall carbon nanotube composed of Natural rubber of same length has been performed to study the effect of the diameters on CNT/Nr composities. Also the Interfacial Shear Stress (ISS) and the Surface Density (γ) were predicted. The obtained results have been compared with the results of the other studies available in the literature i.e., Li et.al [88], Haghighatpanah and Bolton [89] and Chawla and Sharma [90]. Al-Ostaz et.al [39] to verify the present study.

4.1 Introduction

In 1991, the discovery of carbon nanotubes (CNTs) by Iijima was a great development that resulted in the user of CNT`s in many applications, such as for chemical and biological separation, purification, catalysis, for energy storage and in composites for coating, filling, and structural materials and also used in transistors and field emission devices for X-ray instruments. In order to understand the structure and properties of CNTs, the knowledge of the structure and properties of carbon atoms must be known. The carbon nanotube discovery opens a new and active research field in theoretical and experimental condensed matter physics and materials science. CNTs exhibit exceptional electronic, mechanical, thermal, and transport properties. For CNTs, the determination of the Young`s modulus has been the subject of considerable interest. Despite the different types of theoretical studies conducted on the macroscopic elastic behavior of CNTs, complex issues regarding the effect of geometric structure of CNTs on elastic moduli still exist. The Molecular Dynamics (MD) simulation helps us to re-

examine the elastic behavior of CNTs in detail. With the help of MD, we could also determine the elastic properties as well as the mechanical properties of Singled-walled Carbon Nanotubes (SWCNT) [2]. Due to the exceptional properties of SWCNT, researchers tried to use these in polymer composites to increase the toughness and strength of the composites. The interfacial strength and toughness in macroscopic composites could be improved by studying the pull out of CNT from the composites using the mechanism of fiber bridging on the crack opening [91]. Thostenson et. al [92] experimentally found that the presence of the CNT at the fiber/matrix interface significantly improved the interfacial shear stress.

The present study reveals the interfacial properties of the SWCNT-NR nanocomposites using a series of pullout simulations with the help of Molecular Dynamics. Material Studio 2017, a commercial software, has been used to estimate the Interfacial Shear Stresses (ISS) during pullout out of CNTs from Natural Rubber (NR) polymer . The variations in the potential energy and the pull-out force for the SWCNT-NR nanocomposites were determined. Further, the effect of length and diameter of CNT on pullout were studied. In addition, the ISS and the Surface energy density were predicted.

4.2 Materials and Methodology

Single-walled carbon nanotube structures are classified into three categories, i.e., armchair, chiral and zigzag. To study the interfacial properties, a (5,5) armchair SWCNT of diameter .678 nm and length of 5.58 nm was built. To avoid the effects of unsaturated boundary conditions, both the ends of the CNT were terminated by 20 Hydrogen atoms. After adding the hydrogen atoms, the final structure consists of 460 atoms. A single chain of Natural rubber consists of 10 repeated units has been used as input for packing the molecules in simulation cell. The most common Force Field technique, i.e., Condensed Phase Optimized Molecular Potential for Atomistic Simulation Studies (COMPASS) has been used for describing the Intra and Intermolecular atomic interactions [86]. The size of the simulation cell was 2.12 nm X 2.12 nm X 5.58 nm which provided the volume fraction (Vf) of ~ 8% shown in Figure 4.1. The SWCNT-NR nanocomposite that was obtained after the equilibration had been shown in Figure.4.2.

4.2.1 Molecular Dynamics (MD) Simulation of Natural Rubber (NR)

In this study, an elastomer polymer Natural Rubber (NR) has been used as a matrix. NR is soft and sticky solid with low tensile strength and low elasticity. NR is also categorized as a crosslinking type of polymer as it contains a double bond in its basic cis [93] structure. The homopolymer NR was created using the "Build" tool in the Material Studio 2017.

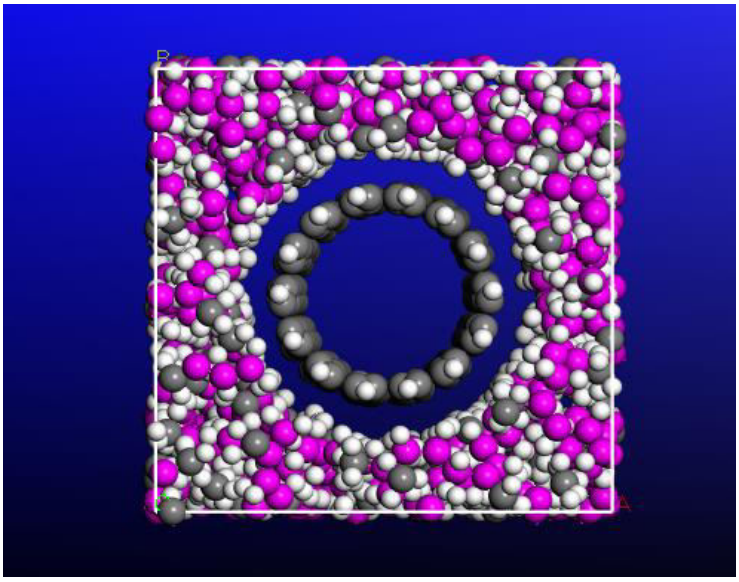

Figure 4.1 Molecular Unit Cell with NR matrix with a size of 2.12 nm X 2.12 nm X 5.58 nm reinforced with a (5, 5) CNT with a length of 5.58 nm

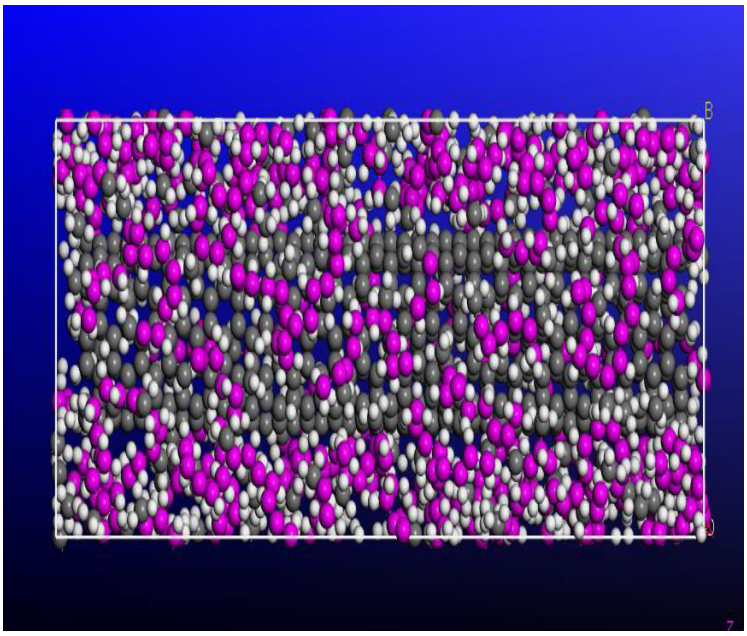

Figure 4.2 Molecular Unit cell with NR as Matrix reinforced with CNT after equilibration

Then one chain of NR containing the 10 repeat units was generated and packed around the SWNCT using the "Amorphous Cell" module with an initial density of 0.98g/cm^3.

The number of atoms in the monomer of NR of 10 repeat units was 132 as shown in Figure 4.3 After the equilibration, the final density found to be 1.084 g/cm^3 which made a good agreement with the model presented by Sabu et al.,[94]. In a unit cell of NR matrix, 5036 atoms were present as shown in Figure 4.4. There are the two main steps, which are to be followed for the equilibration process and the calculation of the interfacial properties of the system:

(i) In the study of the MD simulation, the first step is to optimize the structure of unit cell containing the NR as matrix and CNT as reinforcement. In this process, the energy of the system is minimized so that the structure becomes stable. "Smart Algorithm" of the Material Studio 2017 which uses steepest descent [95], conjugate gradient [96] and Newton-Rapson [97] method to minimize the energy. During the geometric optimization, a minimum of 5000 iterations were performed so that the system takes minimum time for computation. The other parameter used for the optimization of the structures is convergence tolerance. Under the convergence tolerance, the energy tolerance of 1×10^{-4} kcal/mol, force tolerance of 0.05 kcal/mol/ nm and displacement tolerance of 5×10^{-7} nm were used. Whenever the unit cell system is satisfied with the convergence criteria, the unit cell system considered to be optimized.

(ii) The output of the first step (optimized unit cell structure) is used as an input for the second step. The second step is of dynamics simulation run, which is used to compress the system, to obtain proper density with low residual stresses. In the dynamics run, the main product was a trajectory file, which records the atomic configuration, atomic velocities and the other information in a sequence of time steps, which could be analyzed subsequently. The constant-temperature, constant-pressure (NPT) ensemble allows control over both the temperature and pressure was used to perform the dynamics at 300K temperature with the pressure of 1 atm. The total time provided for the simulation was 60 ps with the time step of 1 fs [89, 98]. After this, dynamic run repeated the step 1 using the output of step 2 as input. The output came was further used as an input for the NVT ensemble (constant number of atoms, volume, and temperature) at 40 ps which provide the equilibrated system and proper structure with low residual stresses. The Figure 4.4 shows the complete equilibrated NR system.

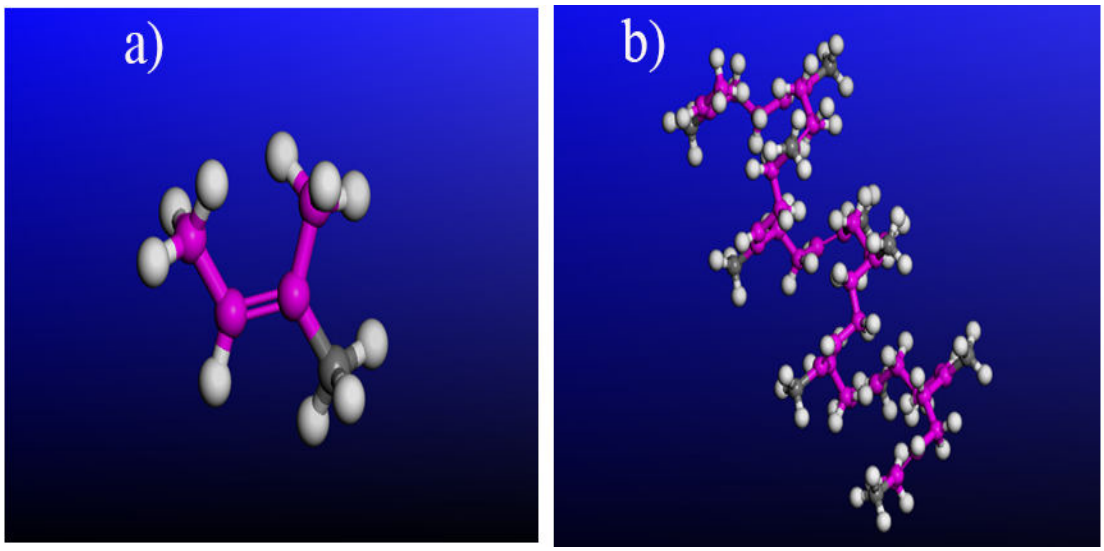

Figure 4.3 (a) A monomer of NR (b) Molecular model of 10 repeat units of 1 NR chain consisting of 132 atoms.

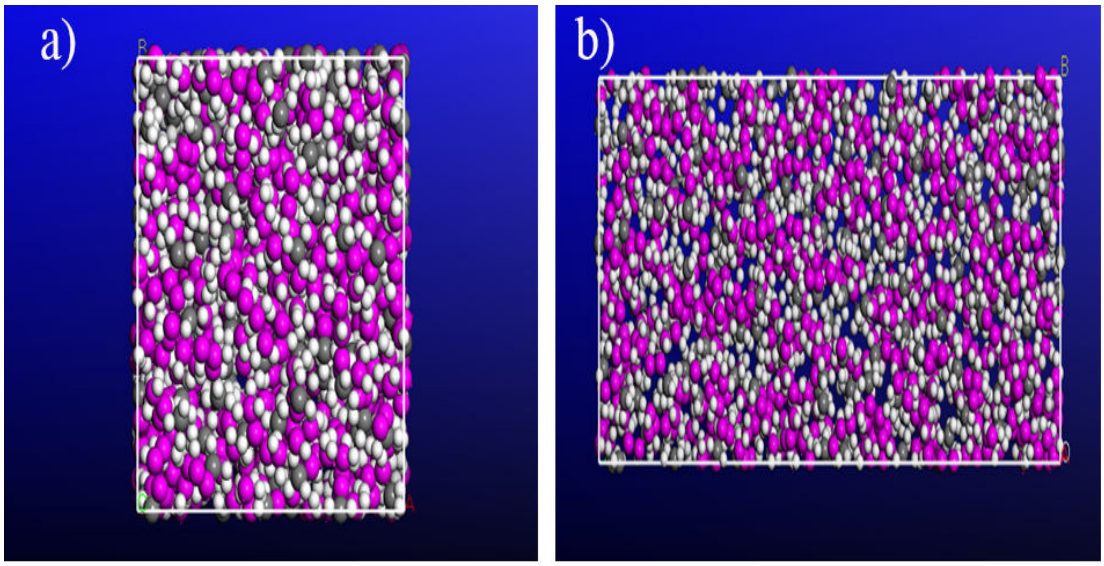

Figure 4.4 RVE of NR matrix consisting 5036 atoms (a) cross section view (b) side view

4.2.2 MD Simulation of SWCNT-NR Composites

Five SWCNT-NR composite systems were generated using the "Amorphous Cell" module of Material Studio 2017. The process that has been already discussed in the previous section 4.2.1 for geometry optimization and dynamics calculation were used. Figure 4.1 shows the equilibrated SWNCT-NR system with 5584 atoms.

4.3 Results and Discussions

4.3.1 Potential Energy

The pull out of the CNT from the NR polymer matrices has been done and the work done by the pull-out force was equal to the energy increment at each pull-out step

and energy change, which is helpful for analyzing the corresponding pull out force and Interfacial shear stress (ISS) of the CNT-NR nanocomposite system. The results showed that the Potential Energy (E) increases gradually as (5, 5) armchair SWNCT was pulled out from the NR matrix. The variations obtained which had been identical with all the previous results of the CNT reinforced polymer composites [39, 98-100]. The calculated energy increment ΔE with respect to SWNCT (5, 5) displacement from the NR polymer matrix has been given in Figure 4.5. The incremental energy increased sharply to a peak value at a specified displacement in the first stage and then in the stage second the incremental energy remained steady between specified peak values as described in Figure 4.5 and then decreased quickly in stage three until the complete pull-out. After the complete pull out the energy became stable and the binding energy nearly approaches to zero. The binding energy helps to study the adhesive strength between the CNT and matrix material. It has been observed that the trend followed is coincident with MWNCTs which is observed experimentally from the literature [101].

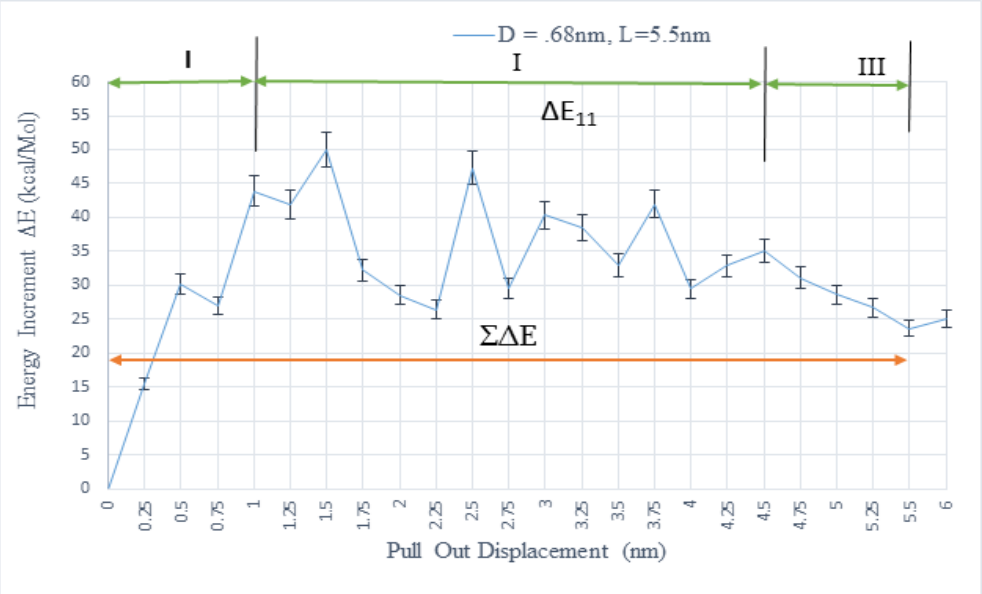

Figure 4.5 Variation of energy increment during the pullout of SWNCT (5, 5)

4.4 Effect of Carbon Nanotube Dimensions

4.4.1 Effect of Length of Nanotube

Three (5,5) armchair single-walled carbon nanotube of different lengths was pulled out from the NR matrix by a series of 5 nm displacements. The graph is plotted between the energy increment and the pullout displacement shown in Figure 4.6. As

stated above three pull-out stages has been obtained to observe the effect of nanotube length on the variations of energy and one can conclude by the graph that maximum energy increment obtained for length (l=7.0nm).

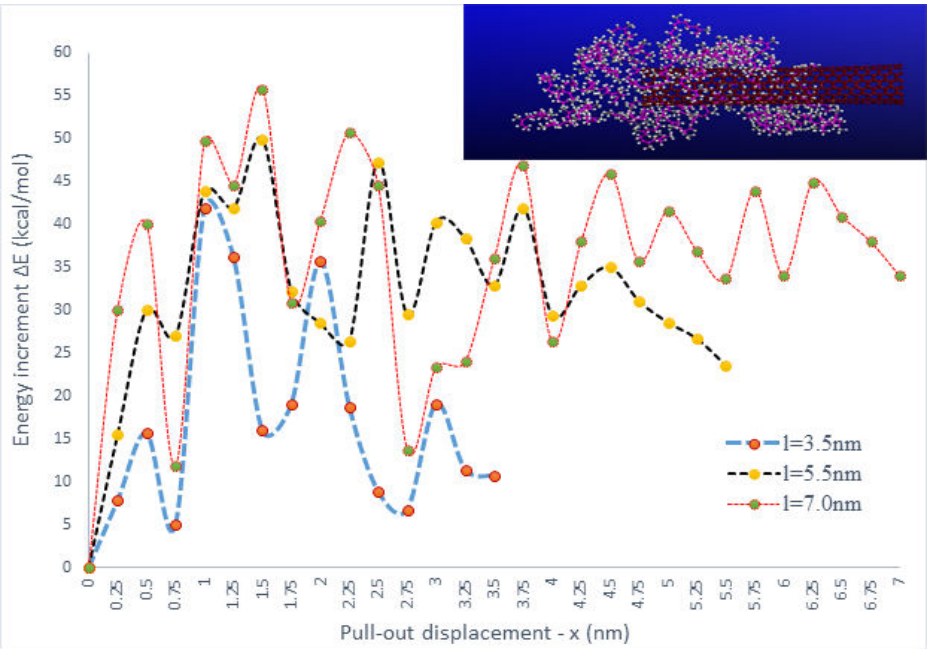

Figure 4.6 Effect of nanotube length on energy increment of SWNCT (5, 5)

The energy increment in stage *II* ΔE_{II} that was the relatively long stage among all the three curves showed that there was no change in the magnitude in the stage second. This average indicates that the energy increment in stage second ΔE_{11} is independent of nanotube length [14, 18].

4.4.2 Effect of Diameter of Nanotube

To study the effect of diameter of a CNT of nanocomposites, the pullout test for different diameters is being carried out for the same length. The diameters used for the different CNTs are the 0.678 nm, 0.989 nm and 1.085 nm with a length of 5.580 nm. The energy increments ΔE Vs the pullout displacement of the CNTs of nanocomposites with different diameters is shown in Figure 4.7.

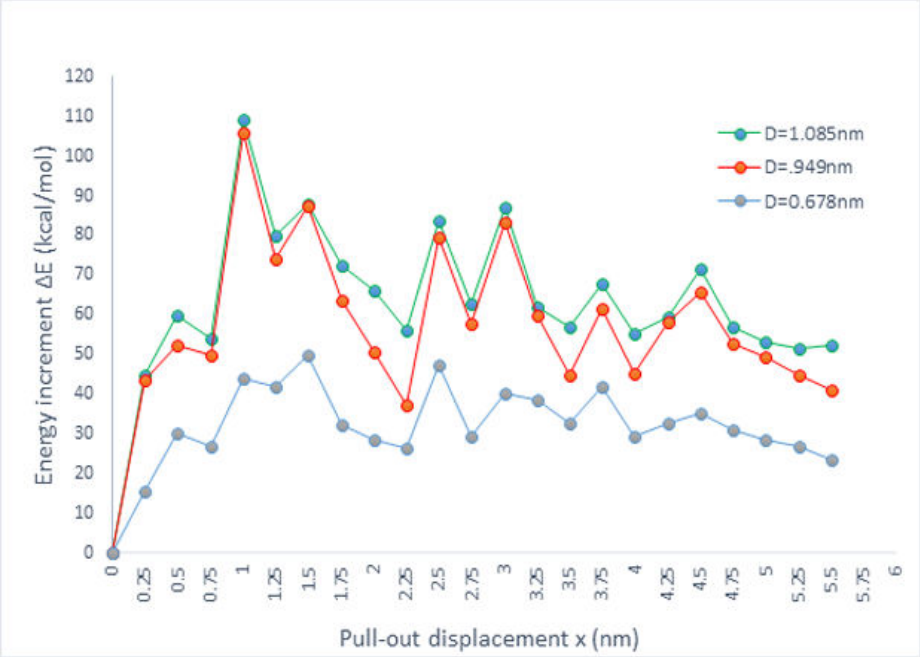

Figure 4.7 Variation of energy increment with nanotube diameter

The results show that both the average energy increment in stage II and the pull-out energy ΣΔE increases linearly with increase in nanotube diameter D [102].

4.4.3 Pull out Force and Interfacial Shear stress

Despite some of the work progress but still, it is very difficult to find out the CNT polymer adhesion. Therefore, to quantify the adhesion between the CNT and surrounding matrices, a method of molecular modeling of SWCNT/polymer was constructed and simulation is being used to find out the CNT pull out force. Snapshots of the pullout simulation have been shown in Figure 4.8. The interfacial bonding energy and interfacial shear stress of the SWNCT-NR system were calculated using the pullout simulations. The real pull-out force could find out with the help of factors like vdw interactions between CNT and NR matrix, no chemical bonding between the CNT/polymer, nano mechanical interlocking resulted by the local non-uniformity of the nanocomposites and the mismatch in the coefficient of thermal expansion (CTEs) [103, 104].

The pullout force can be achieved from the energy increment ΔE_{II} and pullout displacement increment of $\Delta x = 0.5$nm which was calculated through simulation using the Material Studio software. The pull-out forces could be calculated from Eq. (4.1) [88, 89]:

$$F_{II} = \frac{\Delta E_{II}}{\Delta x} \qquad (4.1)$$

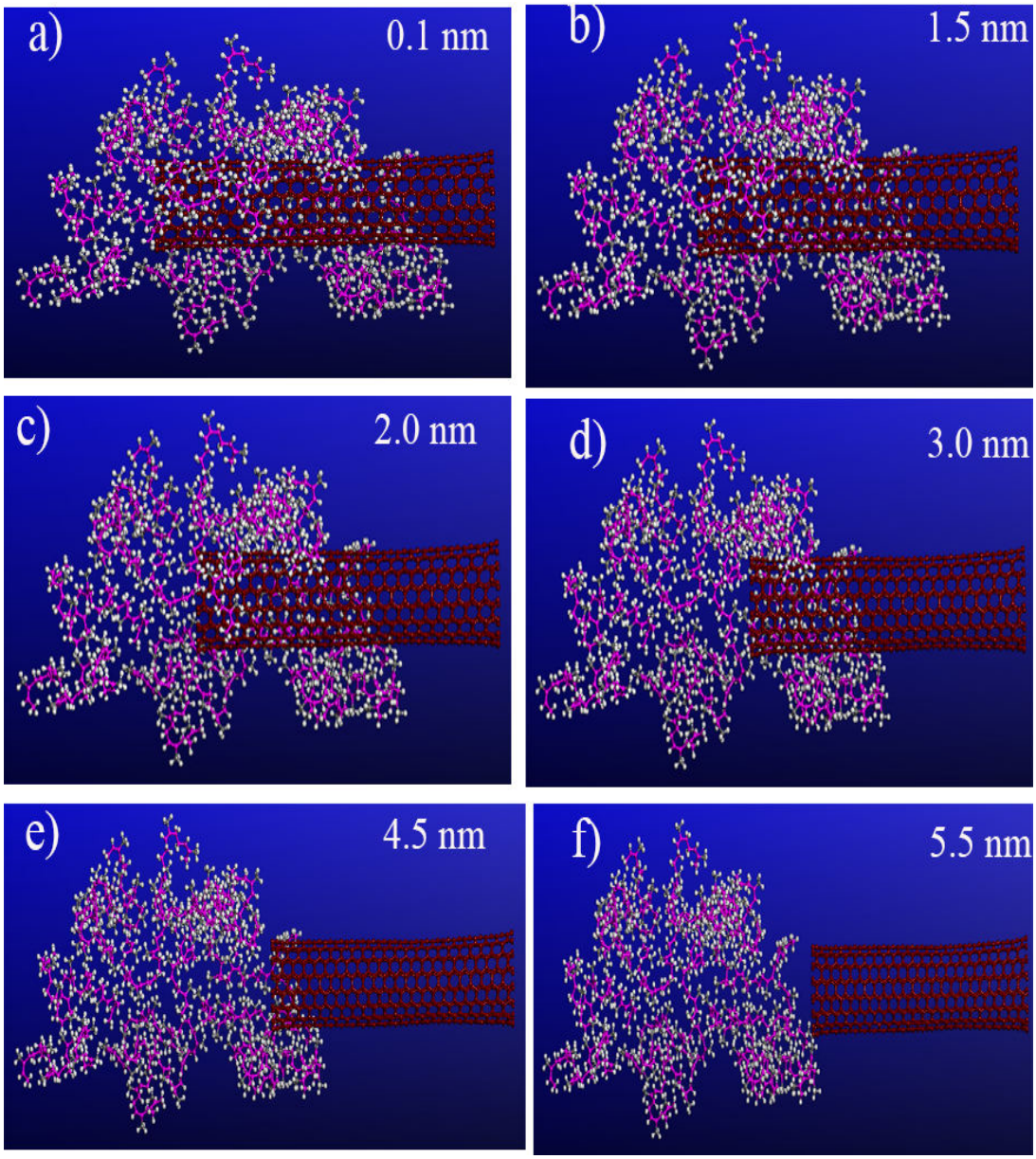

Figure 4.8 Snap shots of SWCNT pull out through the NR matrix. (a) 0.1 nm displacement, (b) 1.5 nm displacement, (c) 2.0 nm displacement, (d) 3.0 nm displacement, (e) 4.5 nm displacement, (f) 5.5 nm displacement.

The summation of the average energy increments $\Sigma\Delta E_{II}$ is coming out to be 483 kcal/mol and the average energy increment ΔE_{II} was obtained as 37.2 kcal/mol at ~8% volume fraction for the Armchair (5,5) SWCNT-NR nanocomposite system. The result obtained in the previous studies by the Haghighatpanah and Bolton [89] at ~7% volume fraction obtained the $\Sigma\Delta E_{II}$ = 419 kcal/mol. and the average energy increment ΔE_{II} was obtained as 17.4 kcal/mol for the SWCNT-PE nanocomposite system. Also the research conducted by the Chawla and Sharma [90] with the same system at ~8%.

volume fractions shows the $\Sigma\Delta E_{II}$ = 400 kcal/mol and the average energy increment ΔE_{II} was obtained as 17.4 kcal/mol and Lie et.al [88] observed that the value of $\Sigma\Delta E_{II}$ = 385 kcal/mol and the average energy increment ΔE_{II} was obtained as 17.4 kcal/mol for the SWCNT-PE nanocomposite system.

The pullout force F_{II} which was calculated by using the above equation came out to be 124 kcal/ (mol nm), while comparing with the other researchers works on the PE matrix, the value obtained by Chawla and Sharma [90] was 87 kcal/(mol nm) , the values obtained by Haghighatpanah and Bolton [89] was 87 kcal/(mol nm) and Li et. al [88] was 87 kcal/(mol nm). The results obtained in this study follow the similar trend from the other studies as compared above. During the SWCNT pullout throughout the polymer matrix, the stress was generated and the generated stress is called as the ISS, which was induced by the pullout forces. As the results of simulation shown in the Figure 4.5 gives us the clear idea that the energy increment ΔE_{11} fluctuates and does not have a constant value during the pullout. The fluctuation in the energy is due to the non-uniformity of the polymer matrix (NR) chains and was sues to the position sensitivity along the SWCNT walls. Due to the fluctuation in the energy increment ΔE_{11}, several researchers assume that constant ISS with a uniform distribution over the embedded length of SWCNT. So as per the previous studies, it can be concluded that the ISS was mainly distributed at each end of embedded CNT within the range of a=1.0 nm as a pullout displacement, where the energy increments are large. Using the assumptions, the ISS (τ) was calculated as per Eq.(4.2) [88, 89].

$$\tau = \frac{F_{II}}{2\pi D a} \tag{4.2}$$

where, D = Diameter of SWCNT (0.67 nm), a = 0.1nm (as per the assumption)

The results which can be obtained from the simulation and presented above can also be used to calculate the surface density γ, also known as the interfacial bonding energy, using Eq.(4.3) [88, 89].

$$\gamma = \frac{\Delta E}{2\pi D \Delta x} = \frac{F_{II}}{2\pi D} \tag{4.3}$$

The obtained values of the τ and γ for SWCNT-NR are 202.1 ± 2.87 MPa and 0.20 ± .002 N/m, respectively which is 1.42% more than that of SWCNT-PE obtained by the Li et.al [88], Haghighatpanah and Bolton [89] and Chawla and Sharma [90]. Al-Ostaz et.al [39] discussed in his studies that after pullout in the presence of boundary

conditions with same parameters, the energy remains unaffected. With the help of above-derived equations, The ISS, the pullout energy ΣΔE and the average pull out force F_{11} can be calculated for the SWCNT-NR nanocomposites. Yuan Li et.al [88] found that the calculated ISS and surface energy density decreases initially with nanotube diameter and saturated at some value for SWCNT-PE nanocomposites and similar trend follows for the SWCNT-NR nanocomposites as shown in Figure 4.9 and Figure 4.10. The ISS and surface energy density converged at 113.5 MPa and 0.1 N/m.

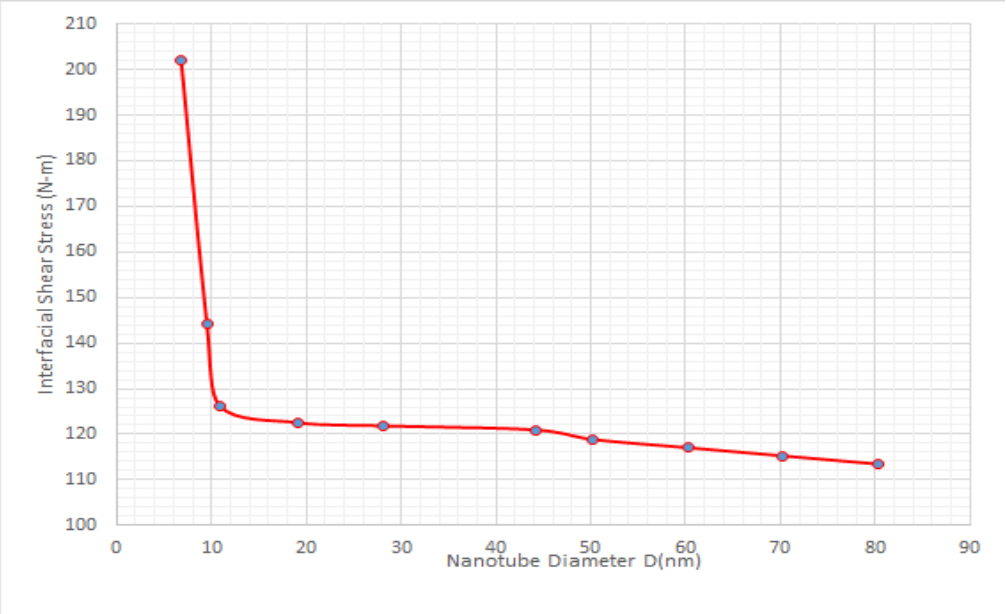

Figure 4.9 Dependence of interfacial shear stress on nanotube diameter

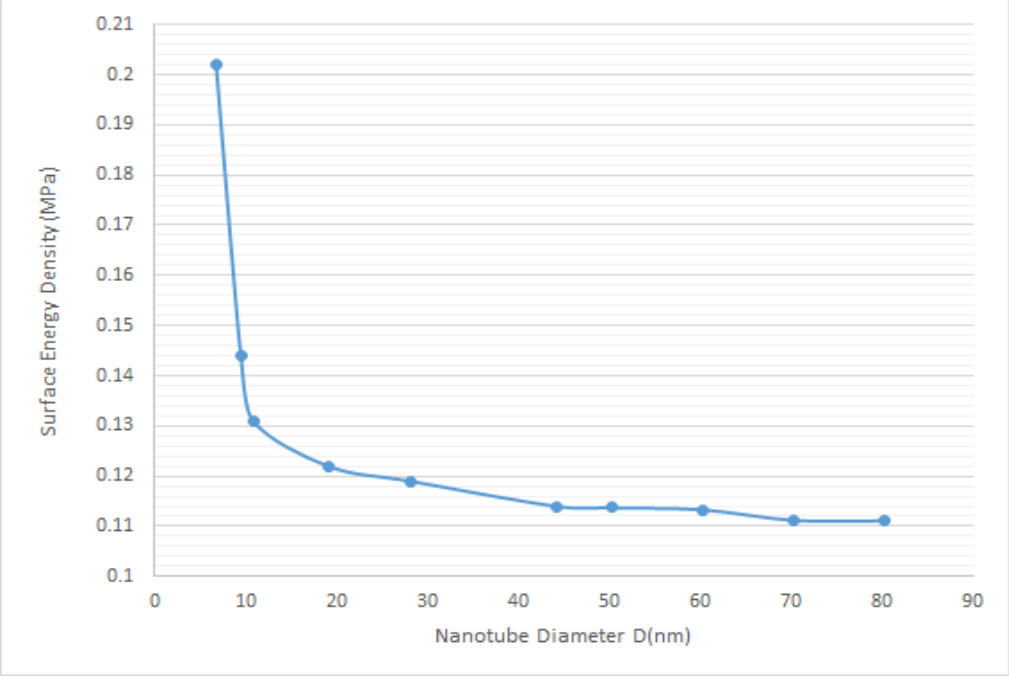

Figure 4.10 Dependence of surface energy density on nanotube diameter

4.5 Conclusions

A series of SWCNT pull out simulations from the NR matrix were performed using the MD simulation .The effect of CNT length and diameter on energy increment (ΔE) was studied. ISS and surface energy density (γ) are the main outputs of this study. Following conclusions could be drawn from the simulated results:

1. This is the first study highlighting the effect of CNT pullout on NR. There is no other study using the same matrix.
2. The incremental energy increased sharply to a peak value at a specified displacement in the first stage and then in the stage second there the increment energy remains steady between specified peak values.
3. The average energy increment in the second stage (ΔE_{11}) was independent of the nanotube length.
4. ΔE_{11} and the pullout energy $\Sigma\Delta E$ increased linearly with an increase in the nanotube diameter (D).
5. ISS and surface energy density (γ) decreased with an increasing SWCNT diameter and converged at some value.
6. The ISS and surface energy density converged at 113.5 MPa and 0.1 N/m.

Chapter 5

Effect of Volume Fraction and Aspect Ratio on Mechanical Properties of CNT Reinforced Polymer Composites

In this chapter, we have determined the mechanical properties of single walled carbon nanotubes reinforced Natural rubber with different volume fraction. In addition to this, we determined the mechanical properties of the Natural rubber polymer. Simulations have been performed for studying the mechanical properties as per the different aspect ratio of all the three types of CNTs/NR composites. The results obtained for present study have been compared with Mori-Tanaka`s approach.

5.1 Introduction

In the field of carbon nanotube, great research inspiration has been observed among the researchers since the Sumio Iijima [2] discovered the carbon nanotubes. The geometric structure of carbon nanotube is thought of a graphite sheet, which can be rolled into a cylinder. The shape of the CNT is like allotropes of carbon having hexagonal pattern. The CNTs are used now days due to their remarkable properties i.e. mechanical, electrical and thermal properties, which made CNT most promising materials for a wide range of applications. One of most expected application of a CNT is Ultra-strong reinforcement due to the excellent mechanical properties for high performance composites [105, 106]. The reinforcement of the fibers in a polymer matrix helps us to make a composite with high strength, low weight due to combination of low density with high aspect ratio along the axial direction. The exact knowledge of mechanical properties are required if carbon nanotubes are essential for the realization of the properties. Some of the experimental work has been done for finding the mechanical properties of the CNT reinforced polymer composite. During mixing process of CNT with polymer, the uniform alignment and proper interfacial bonding between matrix and CNT is required, but some variation occurred while mixing. So using MD simulations will provide the alternative method for finding the mechanical properties of CNTs reinforced polymer in which eliminates the variation occurred during mixing. It helps in understanding the experimental results. The literature show

that the geometric structure having some effect on the elastic moduli and cannot be used directly for design purposes in continuum framework. Therefore, the objective of this study is to find the mechanical properties of CNTs/NR composites using the MD simulation.

5.1.1 Stiffness of SWCNT/NR composites

The stiffness of the SWCNT/NR composites having different chirality has been evaluated using the Material Studio 2017 software. Calculation for the different types of the CNT reinforced Natural rubber composites with different aspect ratio and volume fraction have been explained in following sections.

5.2 Modelling of the SWCNT/NR Composites

Step 1: The first step is to model the SWCNT has been created using "Build Nano structure" tool of different chirality (n, m) used to construct the SWCNT. Three types of SWCNT i.e. arm chair (n,n), chiral(n, m) and zigzag (n,0) have been Built. The overall size of the nanotube is controlled by integer `n`. The minimum value of `n` is 1. The chiral angle and twist of the graphite sheet depends upon the value of the integer `m`. The value of `m` is 0 which is it`s minimum value. After that a polymer has been created using the "Build Polymer "tool. We selected the 'Natural rubber' as a polymer. This homo polymer structure is created using 'Dienes" library and repeat units has been taken as Natural rubber and it is a single chain structure having chain length 10.

Step 2: In this step, a simulation cell of different sizes according to the aspect ratio has been created and SWCNT has been adjusted on it at the centre. The aspect ratio taken is shown in Table 5.1. After that Connolly surface has been created for SWCNT using "Atoms volumes and surfaces" tools. Then iso-surface has been created by using "creating segregations". For packing of NR around SWCNT "Amorphous cell' module has been used and force field has been selected as a COMPASS. It is a most common force field for calculating the intra and intermolecular interaction forces. Density of NR has been taken as 0.98 g/cc and has been packed in the iso-surface. The fine quality of the polymer has been chosen and cumulative method has been used for electrostatic as "EWALD" and for Vander wall forces as "Atom Based "After that total number of the atoms has been observed.

Table 5.1 Cell parameters for different SWCNT/NR Composites with varying aspect ratio (l/d)

Aspect ratio (*l/d*)	Cell parameters for Armchair (5,5) SWCNT/NR	Cell parameters for chiral (4,6) SWCNT/NR	Cell parameters for Zigzag (8,0) SWCNT/NR
5	2.13X2.13X 3.44 nm^3	2.13X 2.13 X 3.71 nm^3	1.96X1.96 3.40 nm^3
10	2.13X2.13X6.88 nm^3	2.13X 2.13 X 7.42 nm^3	1.9X1.96X6.39 nm^3
15	2.13X2.13X10.33 nm^3	2.13X2.13X11.14 nm^3	1.96X1.96X9.37 nm^3
20	2.13X2.13X13.52 nm^3	2.13X2.13X12.99 nm^3	1.96X1.96X12.78 nm^3
25	2.13X2.13X16.97 nm^3	2.13X2.13X16.71 nm^3	1.96X1.96X15.76 nm^3

Step 3: The next step is the geometric optimization, which involves the stabilization of the system for optimizing the energy. The tool used for optimization is “Forcite tool”. The input for this step is the output of the step 2. For the optimization process, the steepest descent method is used. The algorithm used is the “Smart Algorithm”. The total number of iterations has been taken as 85000 and “Compass” force field has been selected for this process. The motion groups have been considered as rigid for optimization.

Step 4: In this step Dynamics has been performed using “Forcite” tools for SWCNT-Polymer composite system and this step helps in reducing the residual stress and obtaining the proper density by compressing the system. For this step to be done, the output of the first step has been considered as the input of this step. In this step, dynamics have been carried out by using NPT ensemble. NPT stands for constant temperature, constant pressure, and constant no. of atoms. In this step, total simulation time has been taken as 60ps and time step has been taken as 1fs. For this process, temperature has been considered as 298K. The thermostat has been chosen as “Nose” and Barostat has been selected as “Berenderson”.

Step 5: again, this step consists of geometry optimization process, optimization has been performed using “Forcite tools”, and no. of iteration steps has been taken as 85000. Input for this step has been taken as the output of the previous step.

Step 6: Again, this steps consists of dynamic process and this dynamics has been performed using “Forcite” tools. In this step, dynamics has been performed using NVT i.e., (no. of atoms, volumes, and temperature are constant) ensemble at 298K. The

thermostat has been selected as "Anderson", total simulation time for this step has been reduced to 100 ps, and time step has been taken as 1 fs. This step reduces the stress and gives proper structure. Input for this step has been taken as the output of the previous step.

Step 7: this step consists of geometry optimization process, optimization has been performed using "Forcite" tools, and no. of iteration steps has been taken as 85000. Input for this step has been taken as the output of the previous step.

Step 8: This is the final step, which involves "Mechanical properties" calculation. The output of the seventh step will be the input for this final step. For calculating the mechanical properties, "Forcite" tools have been used. In this method for calculating mechanical properties, "constant strain method" has been selected under. The value of constant strain has been provided for calculating the properties are 0.003. Fine quality has been chosen from the available options. After successful completion of this step, mechanical properties for the equilibrated system will be analysed.

5.3 Results and Discussions

In this segment, the elastic moduli of the single wall carbon nanotube reinforced Natural rubber polymer composites have been explained. The results obtained for the SWCNT/NR composites have been discussed in detail. Several model of SWCNT/NR composites of armchair, chiral and zigzag have been constructed at different aspect ratio (l/d) and also with different volume fractions (V_f).

5.3.1 Effect of Aspect Ratio on Elastic Moduli of Different SWCNT/NR composites

The different types of SWCNT/NR have been constructed. The simulation cell for an armchair (5, 5) have been shown in Figure 5.1 with volume fraction (V_f =0.08) and aspect ratio l/d=5. The number of the atoms in the cell is 6290 and the size of the cell has been taken as 2.13 nm X 2.13 nm X 13.57 nm. We have evaluated the dynamic properties of armchair (5, 5) single wall carbon nanotube reinforce Natural rubber composite. Calculations have been made for CNT aspect ratio (l/d) in between 05-25. The same procedure has been adopted as discussed in the previous section.

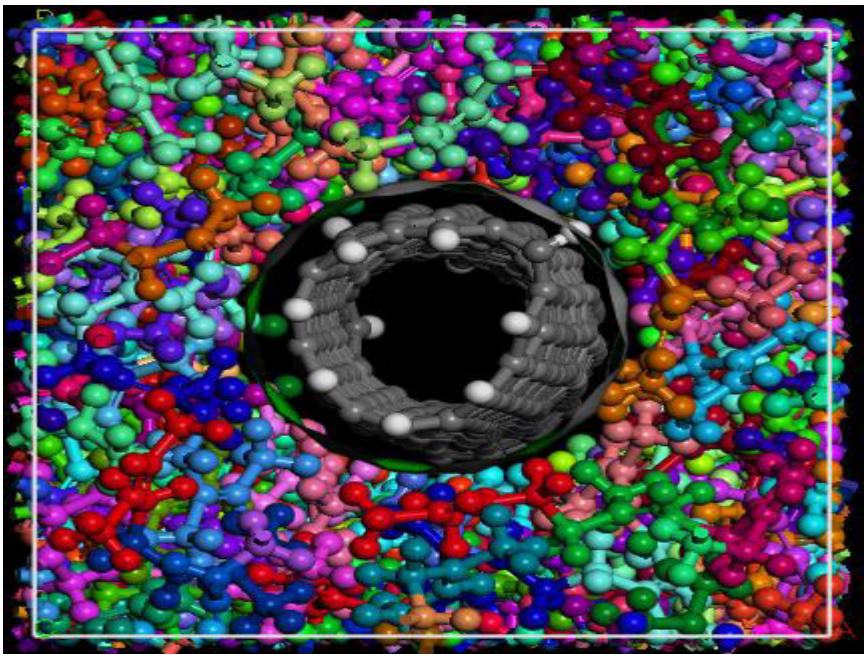

Figure 5.1 Simulation cell for an armchair (5, 5)

Figure 5.2 demonstrates the variation in the young`s modulus with $V_f$ = 0.08 for an armchair (5, 5) single wall carbon nanotube reinforced Natural rubber composites at an aspect ratio of 05-25. The results shows that the Young`s modulus E_{11} is increased as the aspect ratio is increased.

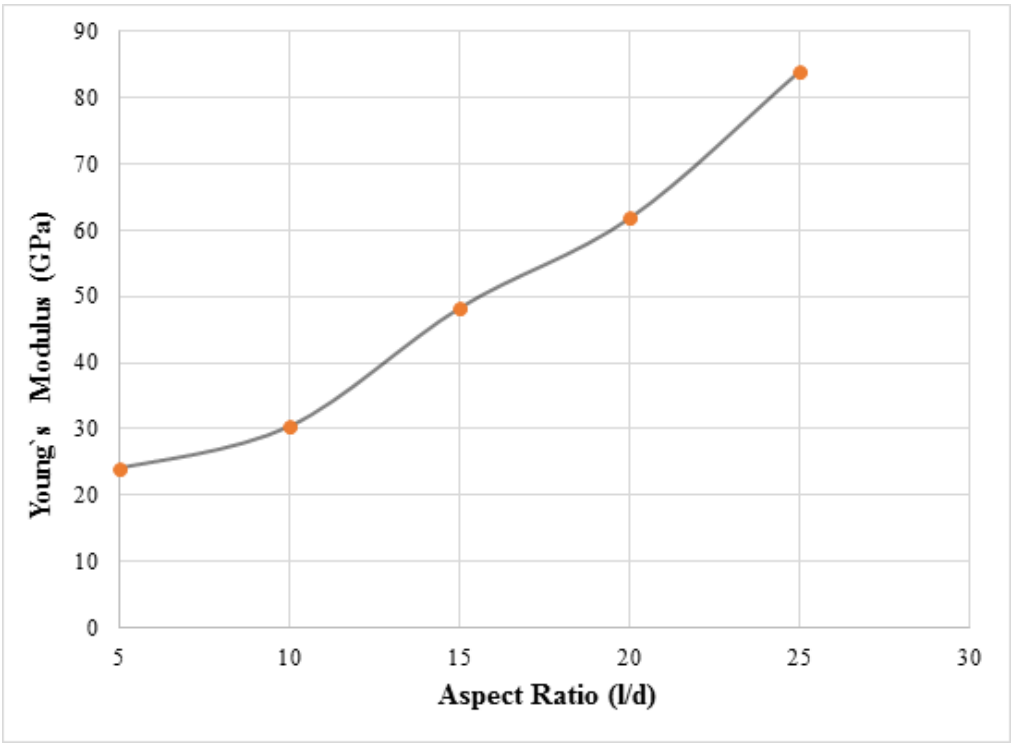

Figure 5.2 Variation in Young`s modulus (E_{11}) with Aspect ratio for armchair (5,5) with varying l/d

The value of the Young`s modulus is increased from 24.1 GPa to 84.03 GPa as the aspect ratio increased from 05-25.As the length of the CNTs is increases the load transfer efficiency is increases intensely. The reason for the increase in the young`s modulus due to the shear stress concentration is present at the ends of CNT in a composite and if we further increase the l/d >25 then the moduli increases slowly. Figure 5.3 shows the variation in the shear modulus, transverse modulus and bulk modulus of an armchair (5,5) SWCNT/NR composites. The shear modulus, bulk modulus and transverse modulus is increased as the aspect ratio increased. The reason for the increase in the shear modulus is that at lower aspect ratio, number of fibers will be more in the composites for same volume fraction. The stress concentration is the major factor for increase in shear moduli because more the discontinuous fibers at the end more will be stress concentration and due to this stress concentration, there will be increase in the shear moduli. This values having a good agreement with the rules of mixtures. After the calculation of the armchair SWCNT/NR the same process is repeated for finding the Young`s Modulus of chiral (4, 6) type SWCNT/NR composites.

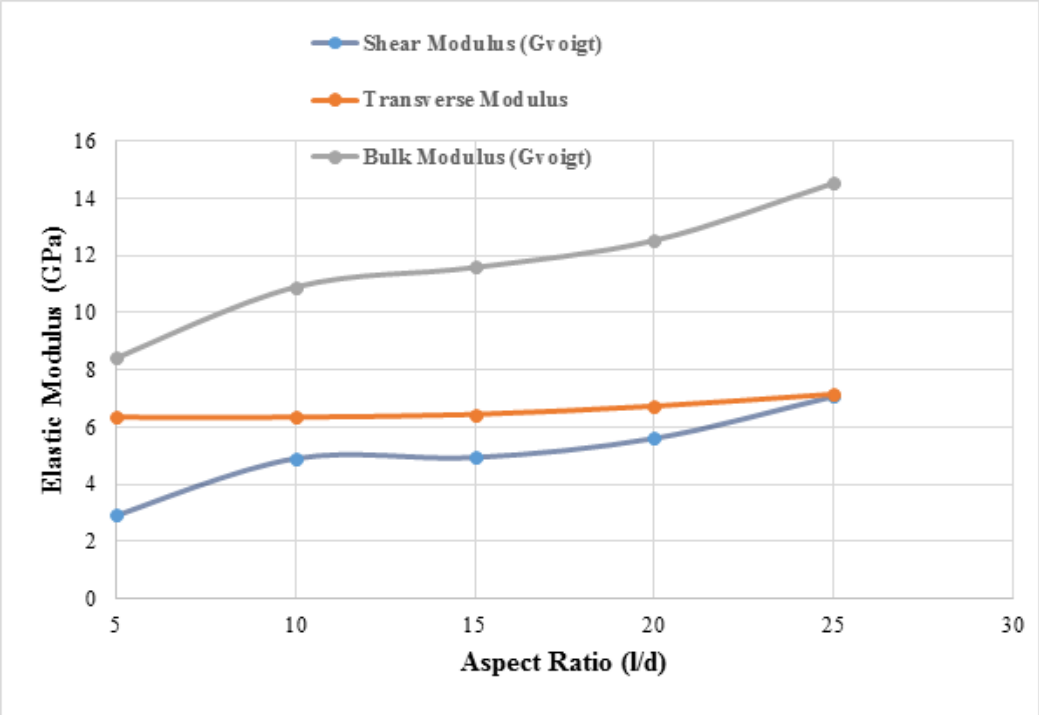

Figure 5.3 Variation in Shear modulus, Transverse modulus and Bulk modulus of Armchair (5,5) SWCNT/NR composites with varying l/d at $V_f = 0.08$.

Figure 5.4 shows the variation in young`s modulus with $V_f = 0.08$ for chiral (4,6) single wall carbon nanotube reinforced Natural rubber composites at an aspect ratio of 5-25. The results explains that the Young`s modulus E_{11} is increased as the aspect ratio

is increased. The value of the Young`s modulus is increased from 22.68 GPa to 44.40 GPa.The value of young`s modulus obtained for chiral (4, 6) is lower than that of the armchair (5, 5).

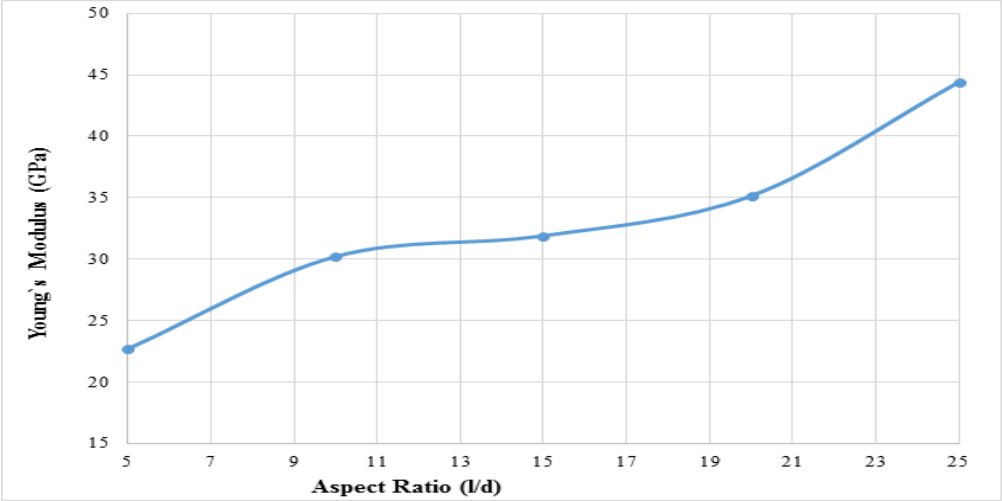

Figure 5.4 Variation in Young`s modulus with Aspect ratio for chiral (4,6) with varying l/d

In addition to young`s modulus Figure 5.5 shows the variation in the shear modulus, transverse modulus and bulk modulus of chiral (4, 6) SWCNT/NR composites. The bulk modulus decreased sharply with the increase in the aspect ratio (l/d) from 5-25 as the shear modulus and transverse modulus also decreased but to a smaller extend as compared to Bulk modulus.

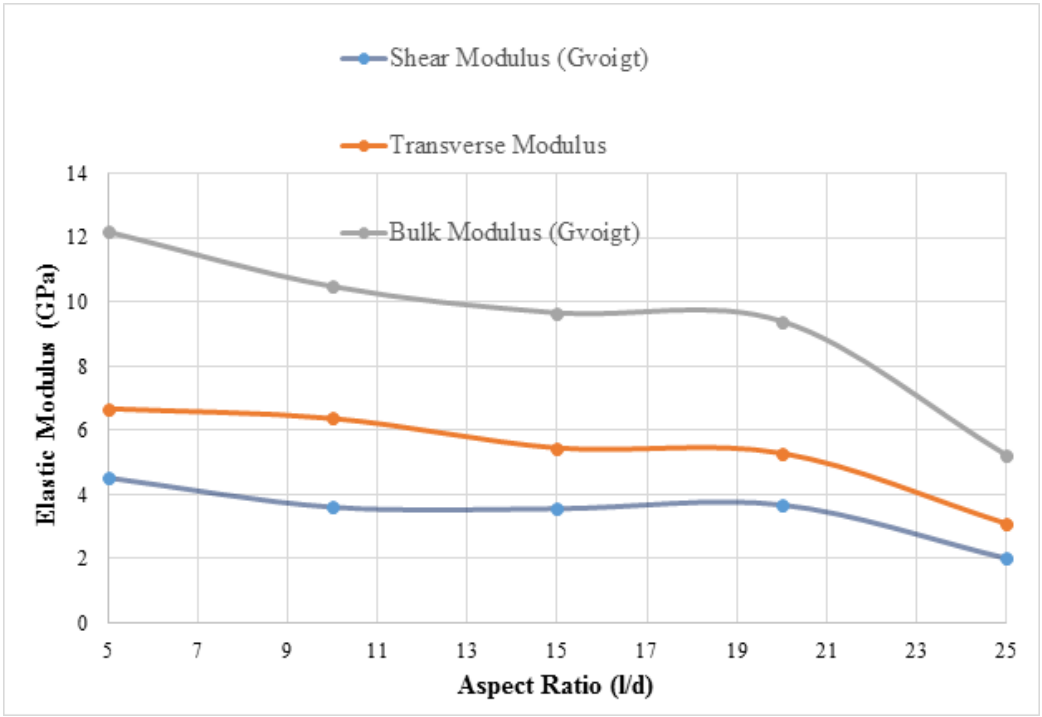

Figure 5.5 Variation in the shear modulus, transverse modulus and bulk modulus of chiral (4, 6) SWCNT/NR composites with varying l/d at $V_f = 0.08$

Figure 5.6 shows the variation in young`s modulus with $V_f$ =0.08 for zigzag (8,0) single wall carbon nanotube reinforced Natural rubber composites at an aspect ratio of 5-25. The process followed for calculating the elastic properties is same as we discussed earlier. The results shows that the Young`s modulus E_{11} is increased as the aspect ratio is increased. The value of the young`s modulus is ranges from 22.07 GPa to 53.94 GPa which is slightly better than that of chiral, but as compared with the armchair model the zigzag model have lower young`s modulus. Similarly the shear modulus, bulk modulus and transverse modulus have been calculated and observed that all elastic constant is decreases up to the aspect ratio of 10 and with further increases in the aspect ratio up to 25 all elastic constant increases.

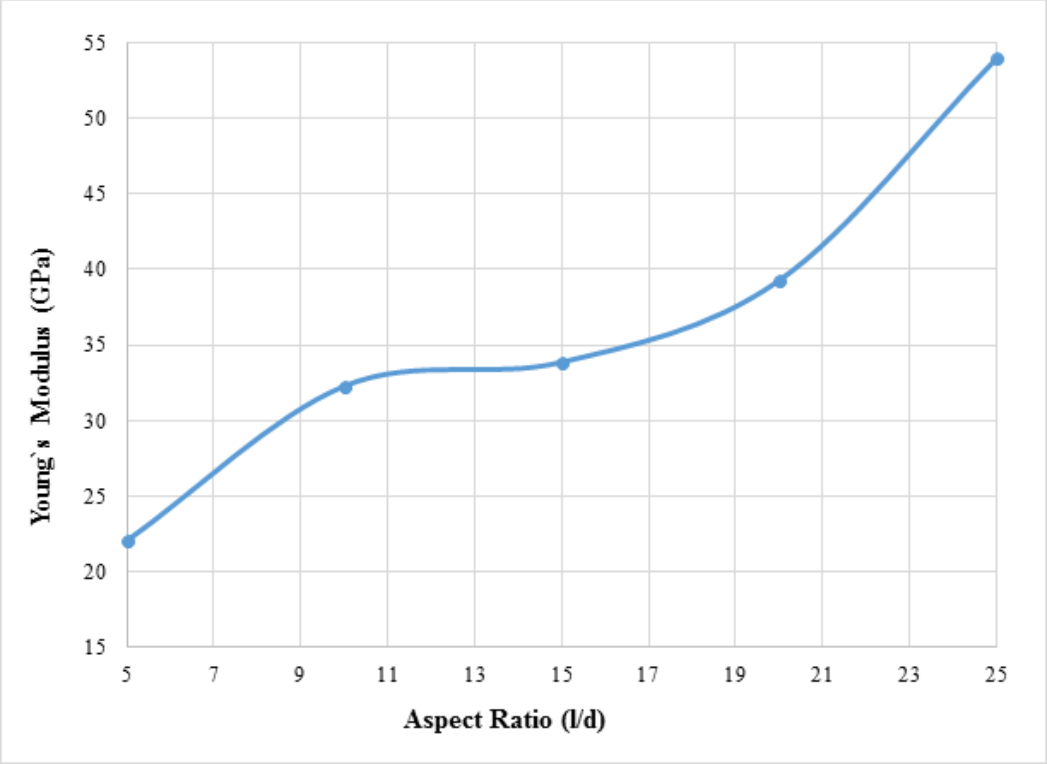

Figure 5.6 Variation in Young`s modulus for zigzag (8,0) with varying l/d.

The Figure 5.7 shows the variation in the shear modulus, transverse modulus and bulk modulus of Zigzag (8, 0) SWCNT/NR composites. The Figure 5.8 shows the comparison of the young`s modulus between the different types of the CNT reinforced Natural rubber composites. After comparing the young`s modulus between all the three different types of SWCNT/NR composites we find that the armchair has a higher young`s modulus as compared to the chiral and zigzag.

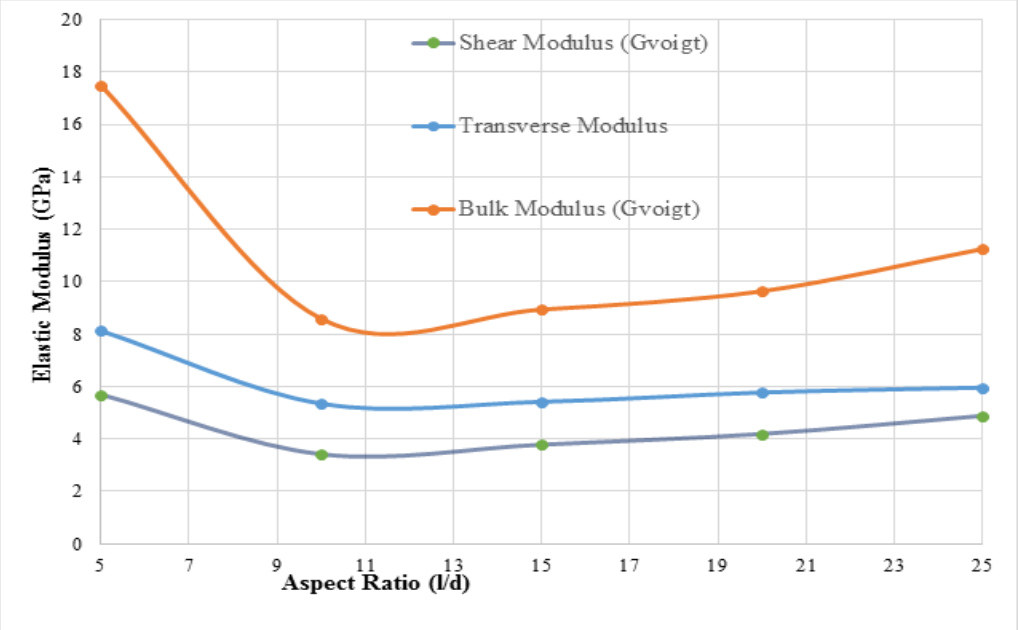

Figure 5.7 Variation in the shear modulus, transverse modulus and bulk modulus of Zigzag (8, 0) SWCNT/NR composites with varying l/d at $V_f = 0.08$.

As the aspect ratio crossed the 10 the value of young`s modulus for armchair increases sharply than that of others. Therefore, the armchair SWCNT/NR composites are preferred as compared to chiral and zigzag. The reason for having higher young`s modulus in case of armchair is due to the geometrical orientation of C-C bonds relative to nanotube axis as compared to zigzag. But in case of chiral SWCNT/NR composites which exhibits lower young`s modulus due to their curved nature of all the C-C sp-2 bonds.

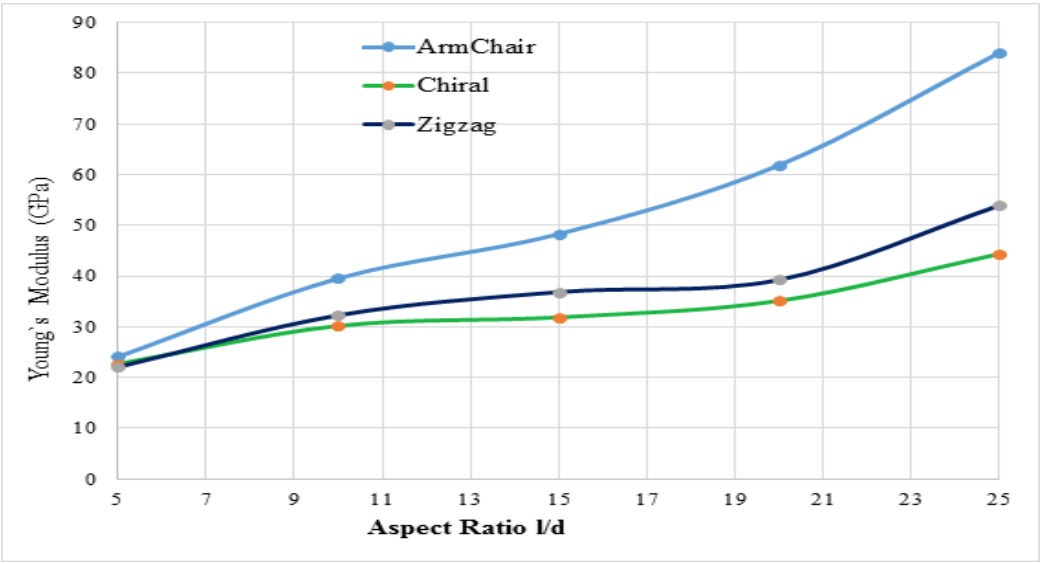

Figure 5.8 Comparison of Young`s modulus for different types of SWCNT/NR composites with varying l/d at $V_f = 0.08$.

5.3.2 Comparison of Results with Mori-Tanaka`s Approach

Results obtained from the MD Simulations have been compared with the Mori-Tanaka`s approach. The results shows that the Young`s modulus (E_{11}) for SWCNT/NR composites having a good agreement with the Mori-Tanaka. In this approach, the Mori-Tanaka [107] proposed to correlate the average stress and average strain with in matrix and fiber in a composite. This method is also named as Mori-Tanaka tensor because the tensor having dependency on the Eshelby`s Tensor [108]. This approach is very popular for finding the elastic properties of the composites, as lot of researchers like Tandon and Weng [109] used this approach for finding the mechanical properties. Eshelby's Mori-Tanaka`s method satisfies the symmetric conditions only for multiphase composites having same shape and same orientation as predicted by Benveniste [110]. Mori-Tanaka approach having high efficiency due to its explicit and stored from solution. The Mori-Tanaka`s basic equation is as follows:-

$$A^{MT}=A^{\text{Eshelby}}\,[(1\text{-}V_f)\,\mathrm{I}+V_f\,A^{\text{Eshelby}}]^{-1}1 \tag{5.1}$$

which is also used for find out the stiffness and damping of component's. The derived equations for the elastic constants for the Mori-Tanaka`s are as follows:-

$$C = C^m + V^f(C^t - C^m)A^{Eshbely} \tag{5.2}$$

V_f = Fiber Volume Fraction

C^m = Stiffness matrix of Polymer

C^t = Stiffness matrix of SWCNT

$A^{eshbely}$ = Stress concentration Factor

$$E_{11} = \frac{E_m}{1 + \dfrac{V_f\,(\mathrm{A}_1 + 2V_m\,\mathrm{A}_2)}{\mathrm{A}}} \tag{5.3}$$

$$E_{22} = \frac{E_m}{1 + V_f[(1 - V_m)\mathrm{A}_4 - 2V_m\,\mathrm{A}_3 + (1 + V_m)\mathrm{A}_5\mathrm{A}]/2\mathrm{A}} \tag{5.4}$$

$$G_{12} = \frac{G_m\,(1 + V_f\,)}{2(1 - V_f)\mathrm{S}_{1212} + \dfrac{G_m}{G_f - G_m}} \tag{5.5}$$

$$G_{23} = \frac{G_m(1 + V_f)}{2(1 - V_f)\mathrm{S}_{2323} + \frac{G_m}{G_f - G_m}} \quad (5.6)$$

$$v_{12} = \frac{\nu\mathrm{mA} - V_f(\mathrm{A}_3 - V_m\mathrm{A}_4)}{\mathrm{A} + V_f(\mathrm{A}_1 + 2V_m\mathrm{A}_2)} \quad (5.7)$$

$$v_{23} = \frac{E_{22}}{2G_{23}} - 1 \quad (5.8)$$

The equation for v_{12} shown here was derived by Tucker and Liang and provides a non-iterative formula to the iterative equation of v_{12} presented by Tandon and Weng. The constants are found using Eq. (5.9).

$$\mathrm{A}_1 = \mathrm{D}_1(\mathrm{B}_4 + \mathrm{B}_5) - 2\mathrm{B}_2$$

$$\mathrm{A}_2 = (1 + \mathrm{D}_1)\mathrm{B}_2 - (\mathrm{B}_4 + \mathrm{B}_5)$$

$$\mathrm{A}_3 = \mathrm{B}_1 - \mathrm{D}_1\mathrm{B}_3 \quad (5.9)$$

$$\mathrm{A}_4 = (1 + \mathrm{D}_1)\mathrm{B}_1 - 2\mathrm{B}_3$$

$$\mathrm{A}_5 = (1 - \mathrm{D}_1)/(\mathrm{B}_4 - \mathrm{B}_5)$$

$$\mathrm{A} = 2\mathrm{B}_2\mathrm{B}_3 - \mathrm{B}_1(\mathrm{B}_4 + \mathrm{B}_5)$$

The constants $\mathrm{B_i}$ and $\mathrm{D_j}$ are found from the following;

$$\mathrm{B}_1 = V_f\,\mathrm{D}_1 + \mathrm{D}_2 + (1 - V_f)(\mathrm{D}_1\mathrm{S}_{1111} + 2\mathrm{S}_{2211}) \quad (5.10)$$

$$\mathrm{B}_2 = V_f + \mathrm{D}_3 + (1 - V_f)(\mathrm{D}_1\mathrm{S}_{1122} + \mathrm{S}_{2222} + \mathrm{S}_{2233}) \quad (5.11)$$

$$\mathrm{B}_3 = V_f + \mathrm{D}_3 + (1 - V_f)(\mathrm{S}_{1111} + (1 + \mathrm{D}_1)\mathrm{S}_{2211}) \quad (5.12)$$

$$\mathrm{B}_4 = V_f\,\mathrm{D}_1 + \mathrm{D}_2 + (1 - V_f)(\mathrm{S}_{1122} + \mathrm{D}_1\mathrm{S}_{2222} + \mathrm{S}_{2233}) \quad (5.13)$$

$$\mathrm{B}_5 = V_f + \mathrm{D}_3 + (1 - V_f)(\mathrm{S}_{1122} + \mathrm{S}_{2222} + \mathrm{D}_1\mathrm{S}_{2233}) \quad 5.14)$$

$$\mathrm{D}_1 = 1 + 2\,(\mu\mathrm{f} - \mu_m)/(\lambda_f - \lambda_m) \quad (5.15)$$

$$\mathrm{D}_2 = (\,\lambda_m + 2\mu_m\,)/(\lambda_f - \lambda_m) \quad (5.16)$$

Where, μ_m, μ_f, λ_m and λ_f are Lame's constants for the matrix and fiber materials. Lame's constants are related to the Young's modulus E and Poisson's ratio ν by;

$$\lambda = E\nu/(1+\nu)(1-2\nu) \tag{5.17}$$

$$\mu = E/2(1+\nu) \tag{5.18}$$

The S_{ijkl} in Eqs. (3.70) to (3.74) are the Eshelby tensor components for a spheriodal inclusion defined as;

$$S_{1111} = \frac{1}{2(1-v_m)}\left\{(1-2v_m) + \frac{3\alpha_2 - 1}{\alpha_2 - 1} - \left[1 - 2v_m + \frac{3\alpha_2}{\alpha_2 - 1}\right]g\right\} \tag{5.19}$$

$$S_{2222} = S_{3333} = \frac{3}{8(1-v_m)}\frac{\alpha_2}{\alpha_2 - 1} + \frac{1}{4(1-v_m)}\left[1 - 2v_m - \frac{9}{4(\alpha_2 - 1)}\right]g \tag{5.20}$$

$$S_{2233} = S_{3322} = \frac{1}{4(1-v_m)}\left\{\frac{\alpha_2}{2(\alpha_2 - 1)} - \left[1 - 2v_m + \frac{3}{4(\alpha_2 - 1)}\right]g\right\} \tag{5.21}$$

$$S_{2211} = S_{3311} = -\frac{1}{2(1-v_m)}\frac{\alpha_2}{\alpha_2 - 1} + \frac{1}{4(1-v_m)}\left\{\frac{3\alpha_2}{\alpha_2 - 1} - (1-2v_m)\right\}g \tag{5.22}$$

$$S_{1122} = S_{1133} = -\frac{1}{2(1-v_m)}\left[1 - 2v_m + \frac{1}{\alpha_2 - 1}\right] + \frac{1}{2(1-v_m)}\left[1 - 2v_m + \frac{3}{2(\alpha_2 - 1)}\right]g \tag{5.23}$$

$$S_{2323} = S_{3232} = \frac{1}{4(1-v_m)}\left\{\frac{\alpha_2}{2(\alpha_2 - 1)} + \left[1 - 2v_m - \frac{3}{4(\alpha_2 - 1)}\right]g\right\} \tag{5.24}$$

$$S_{1212} = S_{1313} = \frac{1}{4(1-v_m)}\left\{(1-2v_m) - \frac{\alpha_2 + 1}{\alpha_2 - 1} - \frac{1}{2}\left[1 - 2v_m - \frac{3(\alpha_2+1)}{\alpha_2 - 1}\right]g\right\} \tag{5.25}$$

where α is the aspect ratio of the fiber and g is a parameter defined as;

$$g = \frac{\alpha}{(\alpha_2 - 1)3/2}\left\{\alpha\left(\sqrt{\alpha_2 - 1} - \cosh^{-1}(\alpha)\right\}\right. \tag{5.26}$$

These above equations are solved mathematically by using the Matlab software. We can solve the equations after writing a program in Matlab and then compared the results of the young`s modulus of armchair obtained by using the MD and Mori-Tanaka`s approach. Table 5.2 shows the increase of young`s modulus with the increase in aspect ratio (l/d) for fixed volume fraction (V_f = 0.08). This shows that the longitudinal Modulus (E_{11}) increases with the increase in aspect ratio. The results

obtained by the MD simulation have good agreement with Mori-Tanaka`s approach. The results is almost follows the similar trend and the difference between them up to the l/d=10 is zero. However, as we increases the aspect ratio from 10-25 there is a maximum difference of 32% at the l/d=25. The table 5.2 shows the percentage difference between Mori-Tanaka`s Approach using Matlab and MD simulation using Material Studio software.

5.3.3 Effect of Volume Fraction on Elastic Moduli of Different SWCNT/NR composites

The different types of SWCNT/NR have been constructed with the different volume fractions. The simulation cell dimensions of different sizes of the SWCNT/NR composites varying with V_f shown in table 5.3. The simulation cell for an armchair (5, 5) have been shown in figure 5.9 with volume fraction V_f =0.04. The number of the atoms in the cell is 5720 and the size of the cell has been taken as 3.00 nm X 3.00 nm X 5.58 nm. We have evaluated the dynamic properties of armchair (5, 5) single wall carbon nanotube reinforced Natural rubber composite. Calculation has been made for CNT with different volume fractions. The same procedure has been adopted as discussed in the previous section.

Table 5.2 Comparison of Molecular Dynamics Results of Young`s Modulus ($E_{11}$) for different aspect ratio with Mori-Tanaka`s approach.

Aspect ratio (*l/d*)	MD (E_{11}) (GPa)	Mori-Tanaka`s (E_{11}) (GPa)	Percentage difference between Mori-Tanaka model and MD model (%)
5	24.1	24.1	0
10	39.55	39.69	0.14
15	48.30	60	11.70
20	61.86	85.79	23.93
25	84.03	116.41	32.37

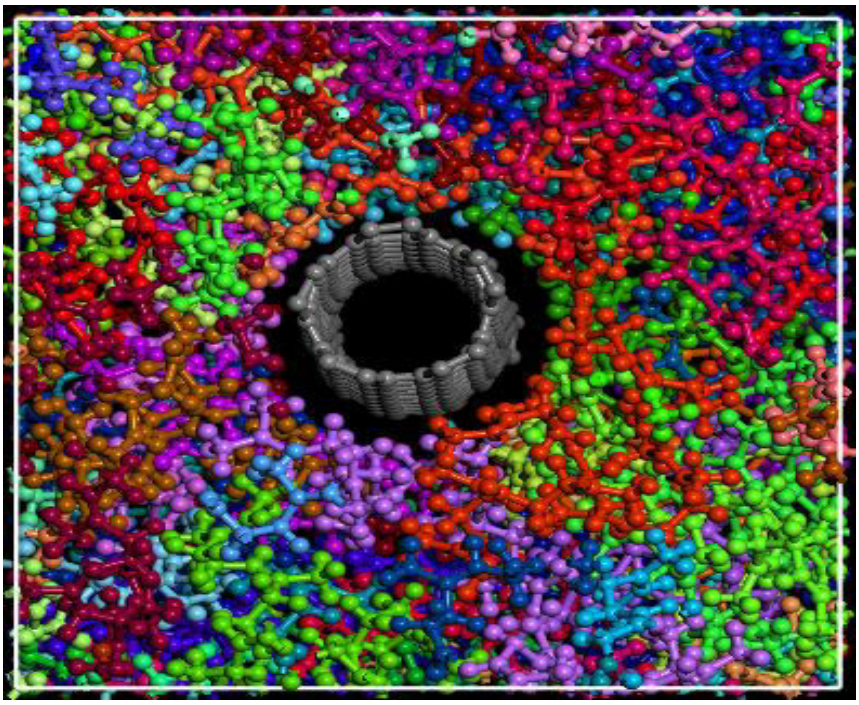

Figure 5.9 Simulation cell for an armchair (5, 5) with V_f =0.04

Table 5.3 Cell parameters for different SWCNT/NR Composites with varying Volume Fraction (V_f)

Volume Fraction (V_f) %age	Cell parameters for Armchair (5,5) SWCNT/NR	Cell parameters for chiral (4,6) SWCNT/NR	Cell parameters for Zigzag (8,0) SWCNT/NR
2	4.24X4.24X5.58 nm^3	4.27X4.27X5.57 nm^3	1.96X1.96X5.53 nm^3
4	3.00X3.00X5.58 nm^3	3.02X3.02X5.57 nm^3	2.77X2.73X5.53 nm^3
6	2.45X2.45X5.58 nm^3	2.47X2.47X5.57 nm^3	2.26X2.26X5.53 nm^3
8	2.13X2.13X5.58 nm^3	2.12X 2.13X5.57nm^3	1.96X1.96X5.53 nm^3
10	1.89X1.89X5.58 nm^3	1.91X1.91X5.57 nm^3	1.75X1.75X5.53 nm^3
12	1.73X1.73X5.58 nm^3	1.74X1.74X5.57 nm^3	1.60 X1.60X5.53 nm^3
14	1.60X1.60X5.58 nm^3	1.61X1.61X5.57 nm^3	1.48X1.48X5.53 nm^3
16	1.50X1.50X5.58 nm^3	1.51X1.51X5.57 nm^3	1.38X1.38X 5.53 nm^3

Figure 5.10 shows the variation in the young`s modulus $E_{11}$ with $V_f$ = 2 to 16% for an armchair (5, 5) single wall carbon nanotube reinforced Natural rubber composites at an fixed aspect ratio (l/d=8). The results shows that the Young`s modulus E_{11} is increased as the volume fraction is increased. The value of the Young`s modulus is increased from 6.76 GPa to 64.41 GPa as the volume fraction increased from 2 to 16 % at fixed aspect ratio l/d=8. When 2% of CNT is added in NR, then the E_{11} is increased to 6.76 GPa and until the V_f increases up to 8% there is an increase in E_{11}. The value of E_{11} up to 8% volume fraction is 33.94% thereafter the rise in the E_{11} is minimal. The reason for the small rise in the E_{11} is due to the slippery nature of the CNT. Due to this slippery nature, no further improvement in the mechanical properties is assisted.

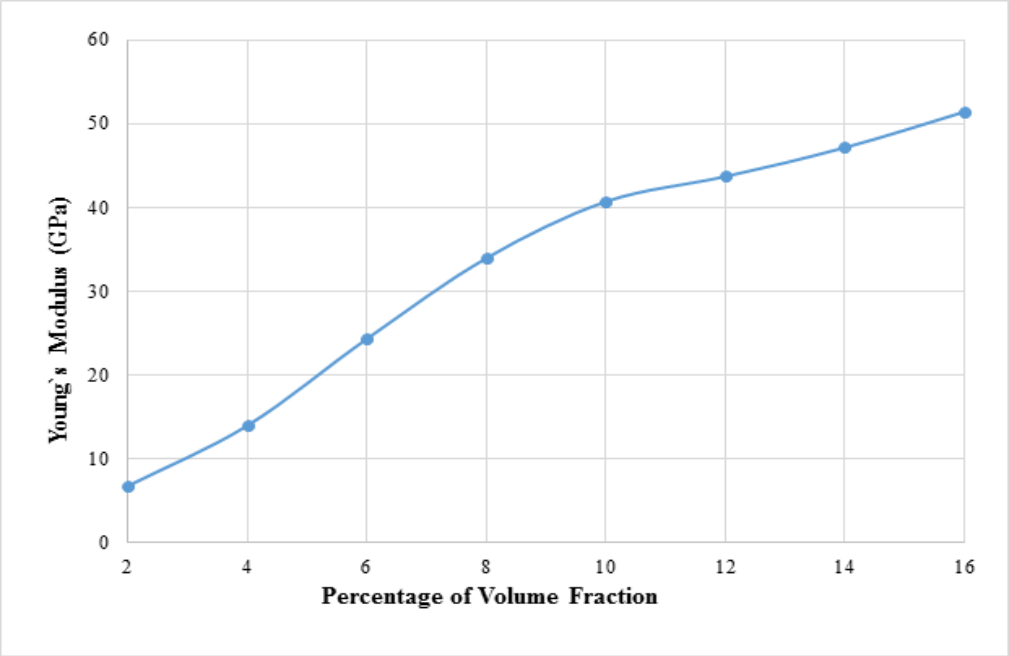

Figure 5.10 Variation in Young`s Modulus with varying Volume fraction Vf for an armchair (5,5) SWCNT/NR composite

Figure 5.11 shows the variation in the shear modulus, transverse modulus and bulk modulus of an armchair (5,5) SWCNT/NR composites. The shear modulus, bulk modulus and transverse modulus is increased as the volume fraction increases. Figure 5.12 shows the variation in the young`s modulus E_{11} with V_f = 0.02 to 0.16% for chiral (4,6) single Walled carbon nanotube reinforced Natural rubber composites at a fixed aspect ratio (l/d= 8).

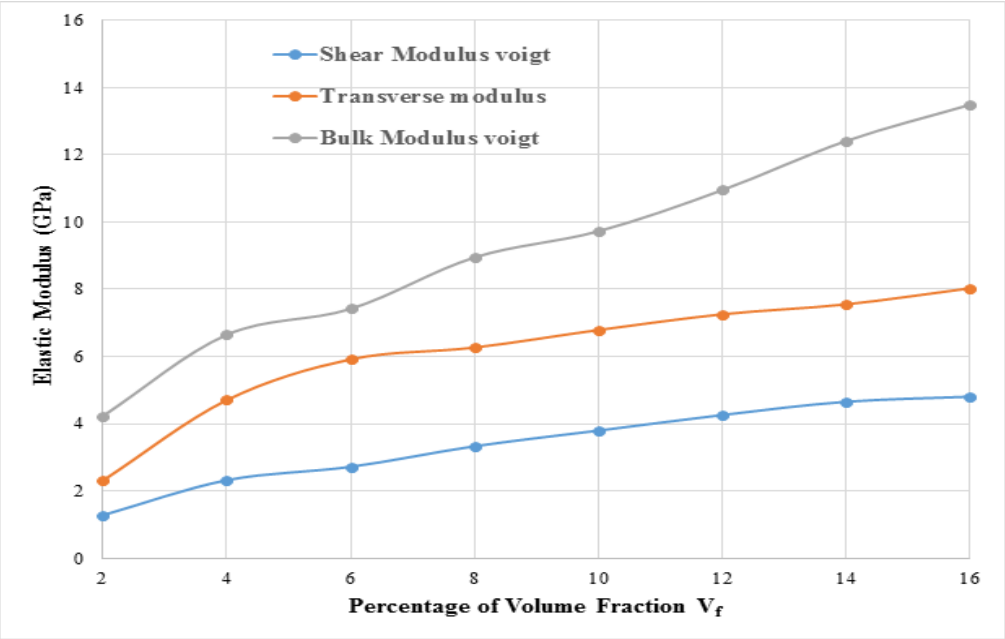

Figure 5.11 Variation in Shear Modulus, Transverse modulus and Bulk Modulus with varying volume fraction (Vf) of Armchair (5,5) SWCNT/NR composites

The results shows that the Young`s modulus E_{11} is increased as the volume fraction is increased. In case of a shear modulus, it can be observed that there is a faster rise in shear modulus up to the volume fraction of 8% then after, the percentage rise in the shear modulus slows down due to the aggregation of SWCNTs, slippery and curvy nature of the SWCNT. The E_{11} increase 51.41% with the increase in volume fraction from 0-16% but in case of a transverse modulus E_{22} as compared to the E_{11} there is an increase of only 8% as the volume fraction from 0-16%. The bulk modulus is also increase as the volume fraction increases. The value of the bulk modulus ranges from 4.2 GPa to 13.46 GPa. After the calculation of the armchair SWCNT/NR the same process is repeated for finding the Young`s Modulus of chiral (4,6) type SWCNT/NR composites. The value of the Young`s modulus is increased from 11.84 GPa to 41.91 GPa. As the volume fraction increased from 2 to 16 % at fixed aspect ratio l/d=8.

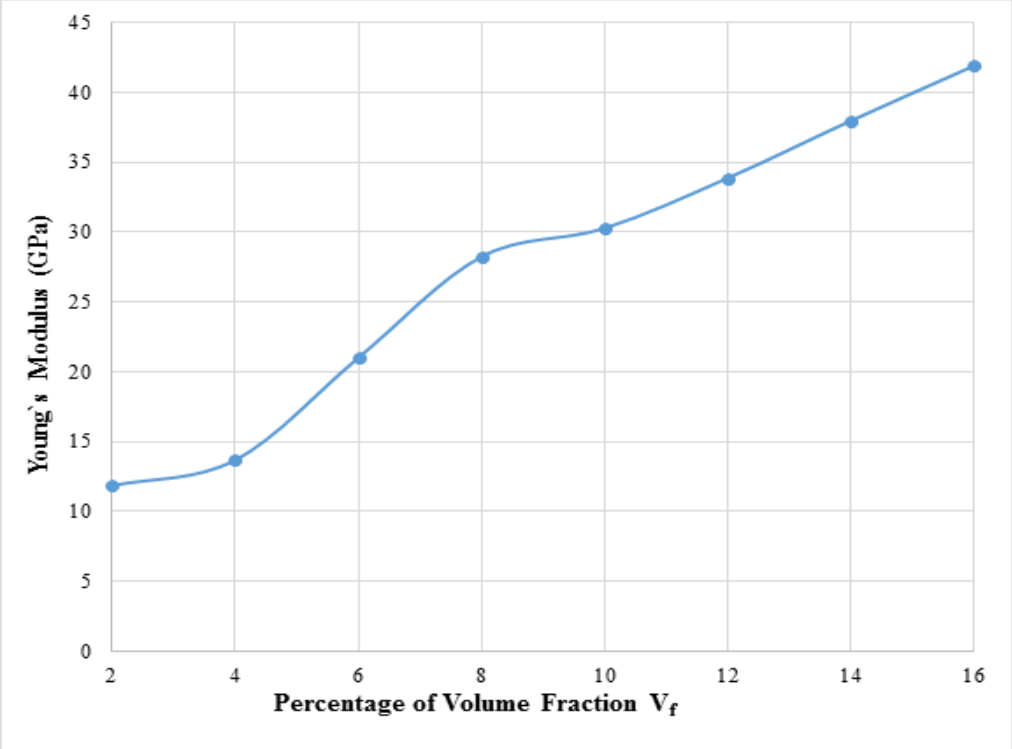

Figure 5.12 Variation in Young`s modulus E11with varying volume fraction Vf for chiral (4,6) SWCNT/NR composite

When 2% of CNT is added in NR, then the E_{11} is increased to 11.84 GPa and until the V_f increases up to 8% there is an increase in E_{11}. The value of E_{11} up to 8% volume fraction is 28.24% thereafter the rise in. the E_{11} is minimal. The reason for the small rise in the E_{11} is due to the slippery nature of the CNT. Due to this slippery nature, no further improvement in the mechanical properties is assisted. The value of young`s modulus obtained for chiral (4,6) is lower than that of the armchair (5,5) SWCNT/NR composite. In addition to young`s modulus Figure 5.13 shows the variation in the shear modulus, transverse modulus and bulk modulus of chiral (4, 6) SWCNT/NR composites. The bulk modulus have a slight increase in the value ranges from 6.38 GPa to 7.35 GPa with the increase in the volume fraction from 0-16% whereas the shear modulus and transverse modulus also increases but to a smaller extend as compared to Bulk modulus. The value of shear modulus ranges between 2.18 GPa to 3.62 GPa whereas transverse modulus E_{22} having an increase from 4.14 GPa to 5.73 GPa which is 86.3 % less than that of E_{11}.

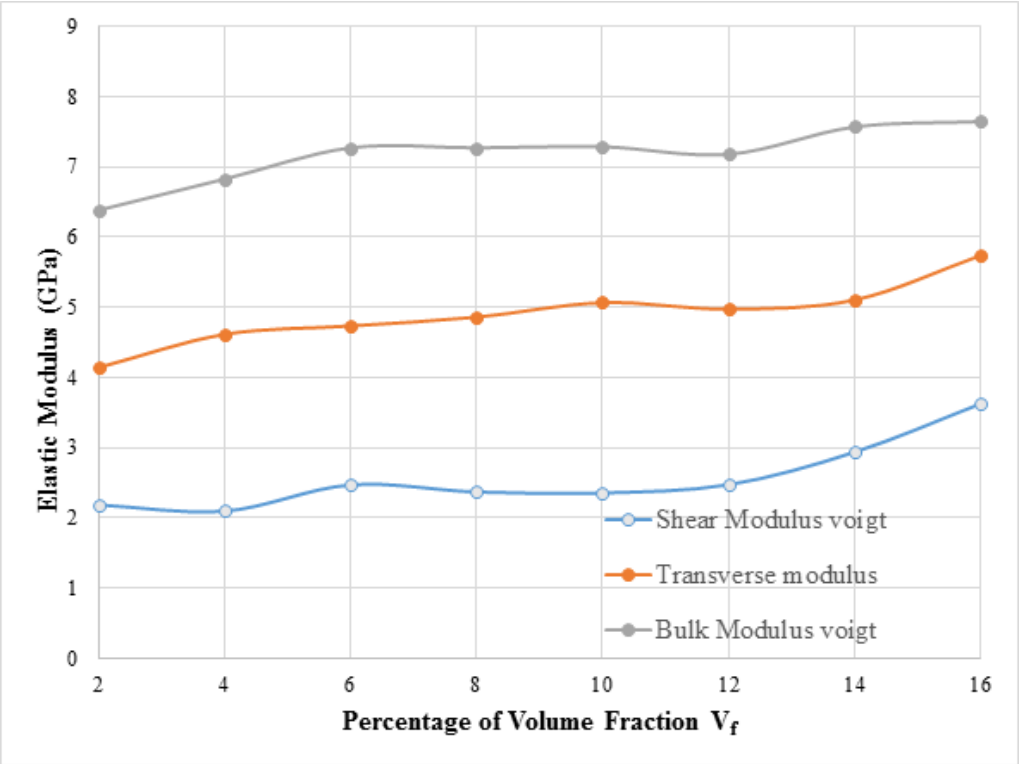

Figure 5.13 Variation in the shear modulus, transverse modulus and bulk modulus of a chiral (4, 6) SWCNT/NR composite with increase in volume fraction

Figure 5.14 shows the variation in the young`s modulus $E_{11}$ with $V_f$ = 0.02 to 0.16% for zigzag (8,0) single wall carbon nanotube reinforced Natural rubber composites at fixed aspect ratio l/d= 8. The process followed for calculating the elastic properties is same as we discussed earlier. The results shows that the Young`s modulus E_{11} is increased as the volume fraction is increased. The value of the Young`s modulus is increased from 10.40 GPa to 48.73 GPa. When 2% of CNT is added in NR, then the E_{11} is increased to 10.40 GPa. The value of E_{11} up to 8% volume fraction is 28.31% thereafter the rise in the E_{11} is minimal. The reason for the small rise in the E_{11} is due to the slippery nature of the CNT. The value of the young`s modulus $E_{11}$ is slightly better than that of chiral, but as compared with the armchair model the zigzag model have lower young`s modulus.

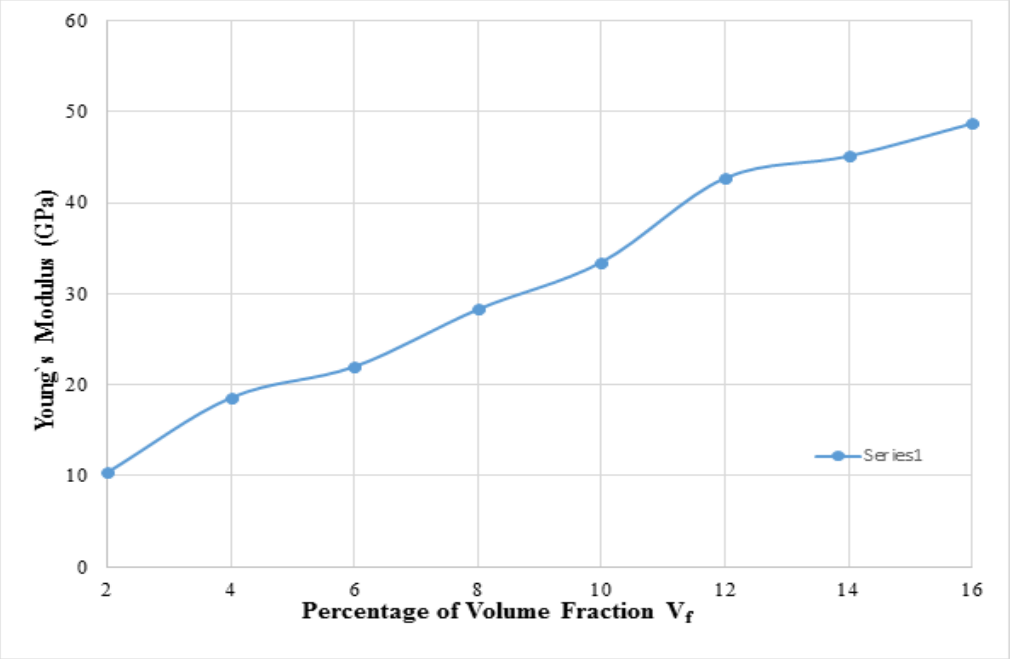

Figure 5.14 Variation in young`s modulus for zigzag (8,0) with varying volume fraction

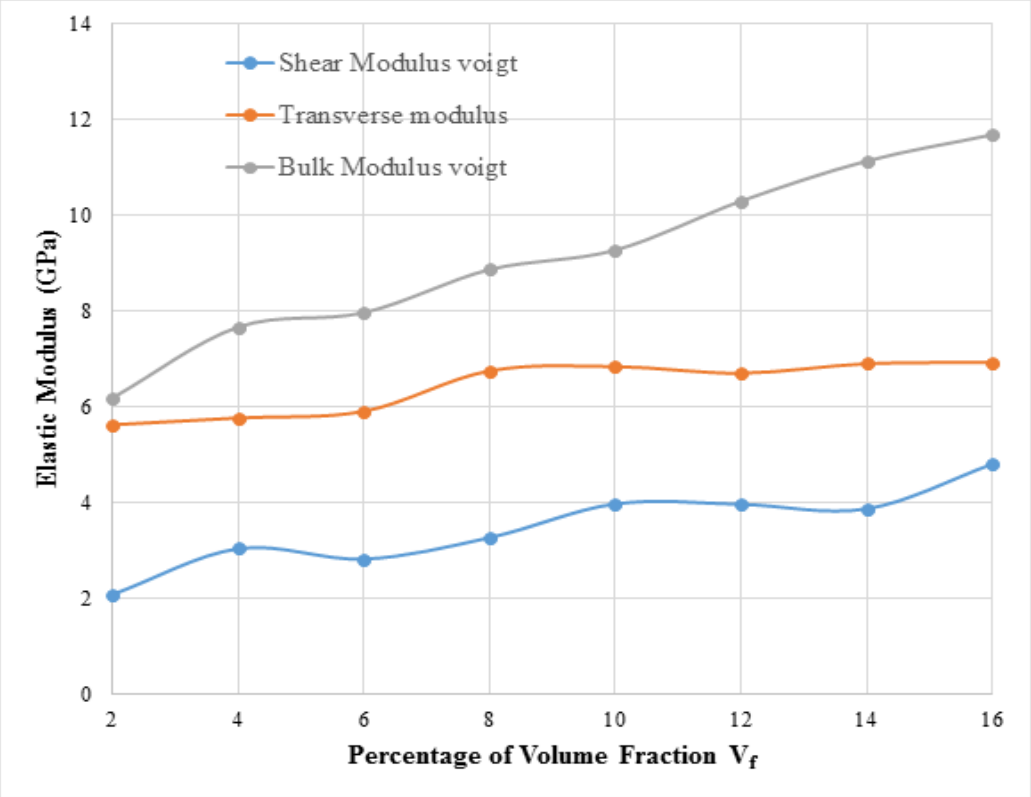

Figure 5.15 Variation in the shear modulus, transverse modulus and bulk modulus of Zigzag (8, 0) SWCNT/NR composite

Figure 5.15 shows the variation in the shear modulus, transverse modulus and bulk modulus of Zigzag (8, 0) SWCNT/NR composites. The shear modulus, bulk modulus and transverse modulus have been calculated as discussed in previous section and

observed that all elastic constant is slightly increased as the volume fraction V_f is increased from 0-16%.

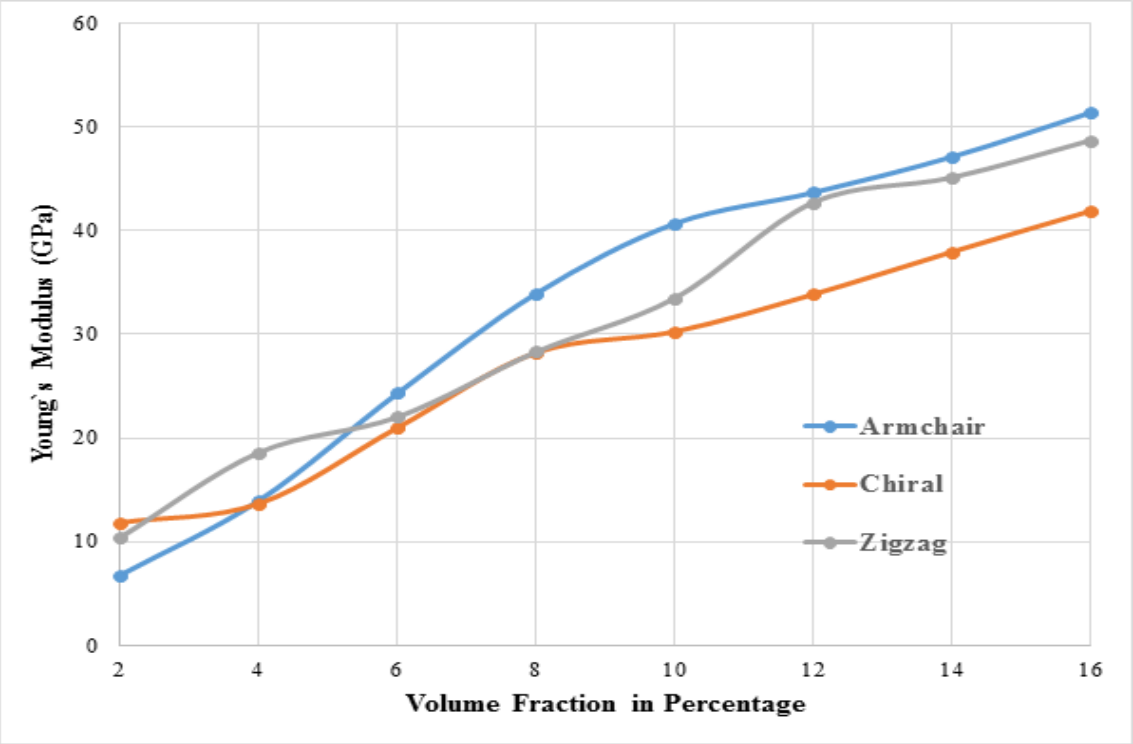

Figure 5.16 Comparison of Young`s modulus for different types of SWCNT/NR composites

Figure 5.16 shows the comparison of the young`s modulus between the different types of the CNT reinforced Natural rubber composites. After comparing the young`s modulus between all the three different types of SWCNT/NR composites we find that the armchair has a higher young`s modulus as compared to the chiral and zigzag. As the volume fraction increases from 0-16%, the value of young`s modulus for all different types of SWCNT/NR is increases. The armchair SWCNT/NR composites are preferred as compared to chiral and zigzag. The reason for having higher young`s modulus in case of armchair is due to the geometrical orientation of C-C bonds relative to nanotube axis as compared to zigzag. But in case of chiral SWCNT/NR composites which exhibits lower young`s modulus due to their curved nature of all the C-C sp-2 bonds.

Chapter 6

Effect of Stone-Wales and Vacancy Defects on Mechanical, Thermal and Interfacial Properties of CNT Reinforced Polymer Composites

CNTs having excellent mechanical properties when there was no defect present. During production and purification of the CNTs, some defects such as stone wales, vacancy, and hybridization may occur or we can introduce some defects deliberately using chemical treatment. In this study, the effect of stone wales and vacancy defects on the elastic moduli of single walled carbon nanotube reinforced Natural rubber composite has been investigated. A armchair (5,5) SWCNT/NR composite has been used and number of defects is varied from 1-10. Molecular Dynamics simulation has been used to study the effect of these defects on mechanical properties of SWCNT/NR.

6.1 Introduction

Defects can play an important role is decreasing the mechanical strength of the composites. The SW and vacancy defects have received considerable attention. To design and fabrication of strong components, reinforcing of CNTs with desirable mechanical properties for understating of mechanical behavior of single walled carbon nanotubes reinforced composites is required. In this study, the effects of number of defects on the single walled carbon nanotubes reinforced Natural rubber composites when subject to small strains had been studied.

6.2 Defects in CNTs

Defects may be introduced deliberately or during the synthesis, process may be decided into the categories.

(i) Stone wales defects comes under Topological defect.

(ii) Vacancy defects due to impurities.

(iii) Re-hybridization due to change in C-C bond due to deformation (sp^2 to sp^3)

- Stone Wales defects referred to the rotation of sp^2 bond to 90 degree. It is composed of 2 Heptagon - 2 Pentagon pairs. The Figure 6.1 shows the defect formation in the armchair (5, 5) hexagonal lattice.

- In case of vacancy defects, the removal of carbon atoms from the perfect hexagonal structure of CNT, due to the removal of atoms creates vacancy at the place of missing atoms is shown in Figure 6.2.

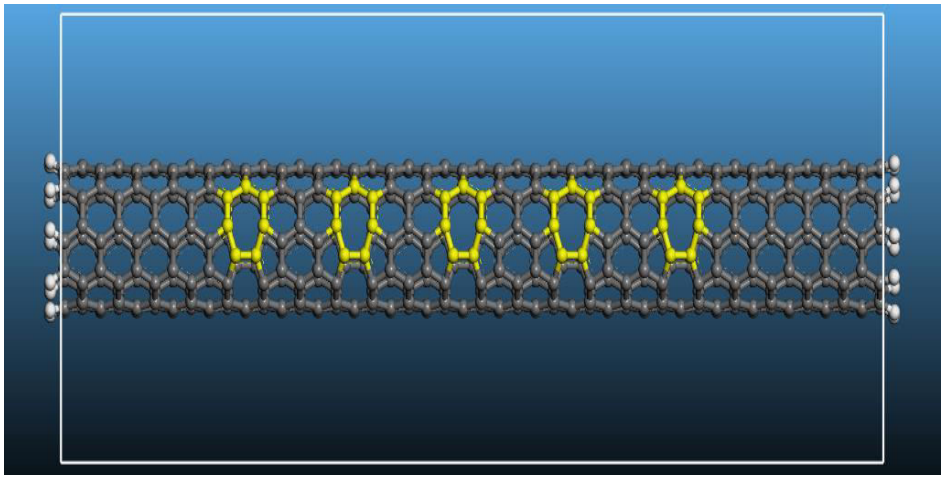

Figure 6.1 Schematic view of SWCNT with Stone-Wales Defect

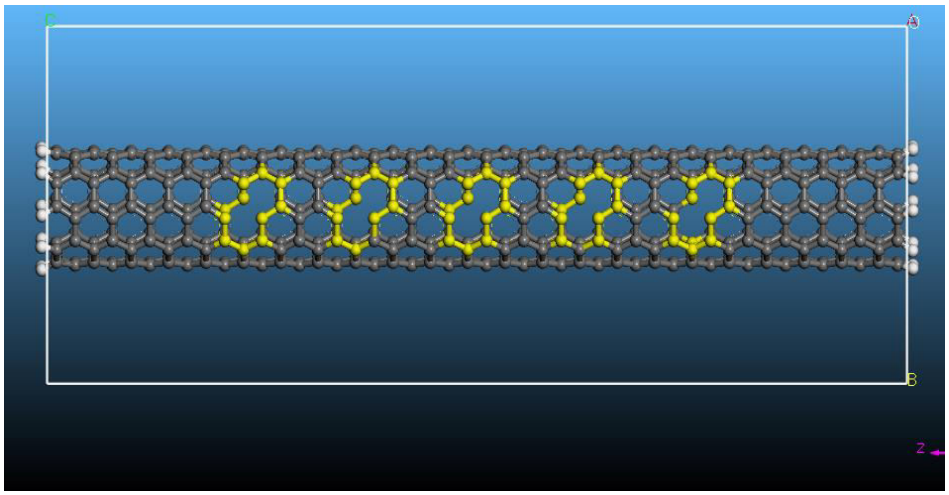

Figure 6.2 Schematic view of the SWCNT with Vacancy Defect

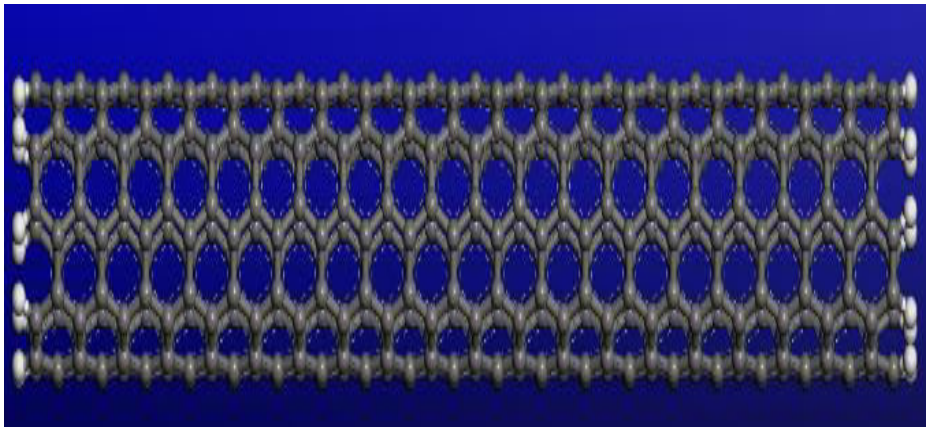

Figure 6.3 Armchair type (5, 5) SWCNT having both ends terminated by hydrogen atoms

6.3 Molecular Modelling SWCNT/NR Composites

In this chapter, we have performed computer simulation for finding the effect of defects on thermo-mechanical properties of single walled carbon nanotubes reinforced Natural rubber composite. For studying the molecular structure, "Material studio software 2017" is used and following steps have been performed for Molecular Dynamics simulation

Step 1: In this step, a (5, 5) armchair type SWCNT has been created using "build nanostructure" tool. Length and diameter for this SWCNT have been taken as 5.58nm and .678 nm respectively. The bond length of this non-periodic structure is .142nm. This armchair type SWCNT is of non-periodic structure and has been created using supercell. In this study, the nanotube is having 460 atoms and it is increased to 480 after adding hydrogen atoms on both the ends (Figure 6.3).

A Natural rubber has been created using "build polymer" tool. This homo-polymer structure is created using "Dienes" library, repeat unit has been taken as Natural rubber, and it is a single chain structure having chain length 10.

Step 2: In this step, a simulation cell of size 2.12nm×2.12nm×5.58nm has been created and SWCNT has been adjusted on it at the center (Figure 6.4). First, a Connolly surface has been created for SWCNT using "atoms volume and surfaces" tools and then isosurface has been created by creating segregation. For packing of Natural rubber around SWCNT "amorphous cell" module has been used and COMPASS have been selected as a force field. It is a most common force field for calculating inter and intra-molecular interaction forces. Density has been taken as 0.98 g/cc and has been packed in isosurface. For this packing process, quality has been chosen as the fine and summation method has been used for electrostatic as "Ewald" And for van der Waals as "Atom-based". After packing, total number of atoms has been observed as 2856.

Step 3: This step involves stabilization of the system. For optimizing the energy geometry optimization has been used and for this optimization "Forcite tools" has been used. For this step output of step 2 has been taken as input for this step. For this optimization process, the total number of iteration has been taken as 85000 and "smart algorithm" has been used. Force field has been selected for this process is COMPASS" and in this optimization process, motion groups have been considered as rigid.

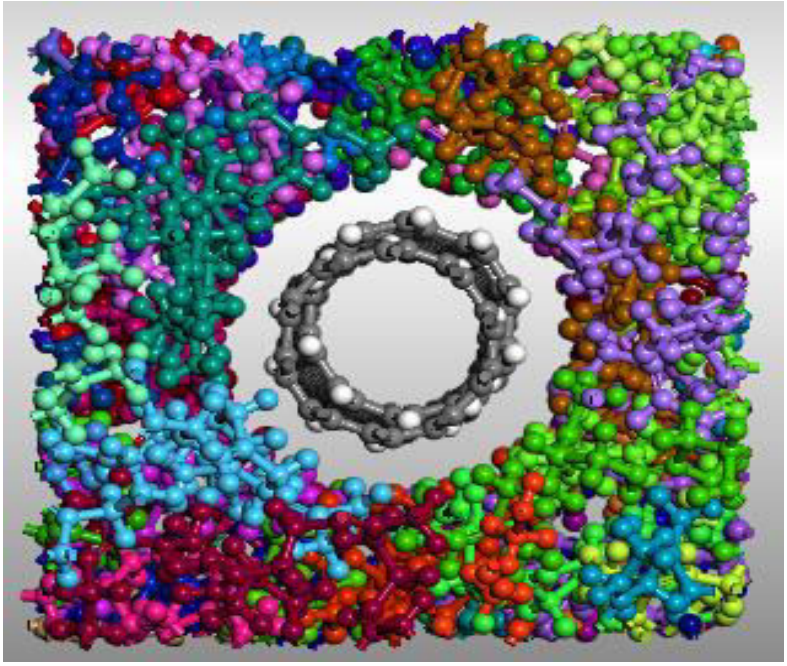

Figure 6.4 Packing of NR around SWCNT in a simulation cell

Step 4: In this step Dynamics has been performed using "Forcite" tools for SWCNT-Polymer composite system and this step helps in reducing the residual stress and obtaining the proper density by compressing the system. For this step to be done, the output of the first step has been considered as the input of this step. In this step, dynamics have been carried out by using NPT ensemble. NPT stands for constant temperature, constant pressure, and constant number of atoms. In this step, total simulation time has been taken as 60ps and time step has been taken as 1fs. For this process, Temperature has been considered as 298K. The thermostat has been chosen as "Nose" and Barostat as "Berenderson".

Step 5: This step again consists of geometry optimization process, optimization has been performed using "Forcite tools", and number of iteration steps has been taken as 85000. Input for this step has been taken as the output of the previous step.

Step 6: This step again consists of dynamic process and this dynamics has been performed using "Forcite" tools. In this step, dynamics has been performed using NVT i.e., (no. of atoms, volumes, and temperature are constant) ensemble at 298K. The thermostat has been selected as "Anderson", total simulation time for this step has been reduced to 40ps, and time step has been taken as 1fs. This step reduces the stress and gives proper structure. Input for this step has been taken as the output of the previous step.

Step 7: again, this step consists of geometry optimization process, optimization has been performed using "forcite" tools, and number of iteration steps has been taken as 85000. Input for this step has been taken as the output of the previous step.

Step 8: This is the final step involves "Mechanical property" calculation. In this step also, the output of the seventh step will be the input for this final step. In this step mechanical properties have been calculated using "forcite" tools and method for calculating mechanical property has been selected as "constant strain method". This step depends on the results of geometric optimization. The value of constant strain has been provided for calculating properties is 0.003. Fine quality has been chosen from the available options. After successful completion of this step, mechanical properties for the equilibrated system will be analysed.

6.4 Results and Discussions

The Section has been divided in to two parts. Firstly, the result of elastic moduli of the defective single walled carbon nanotube reinforced Natural rubber composite has been discussed. Secondly, the interfacial properties of the defective SWCNT/NR composite have been discussed. In this part of result and discussion, pull out force, interfacial shear stress and the surface density have been calculated. In addition, the thermal conductivity of the defective armchair single wall carbon nanotube reinforced Natural rubber composite has been evaluated

6.4.1 Elastic Moduli of the Defective SWCNT/NR Composite

Figure 6.5 shows the variation of the young`s modulus ($E_{11}$) in armchair (5,5) single walled reinforced Natural rubber composite with number of defects of stone wales and vacancy defects. The elastic moduli of the SWCNT/NR decrease as the number of defects increases. The young`s modulus of the stone wales defective SWCNT/NR decreases rapidly in comparison to the SWCNT/NR with vacancy defects. The percentage decrease in young`s modulus ($E_{11}$) in armchair (5,5) with the number of stone-wales defects is 36.85%, but in case of vacancy defects the percentage decrease in young`s modulus (E_{11}) in armchair (5,5) is 31.43%.

Figure 6.6 shows the variation of transverse modulus (E_{22}) in armchair (5,5) SWCNT/NR composite with the number of defects. In case of transvers modulus, the percentage decrease in E_{22} with the increase in number of defects for SW defects is 68.39%, whereas in case of vacancy defects the percentage decrease in E_{22} is 67.66%.

Therefore, the transverse modulus decreases with increase in number of defects nearly approaching 69%.

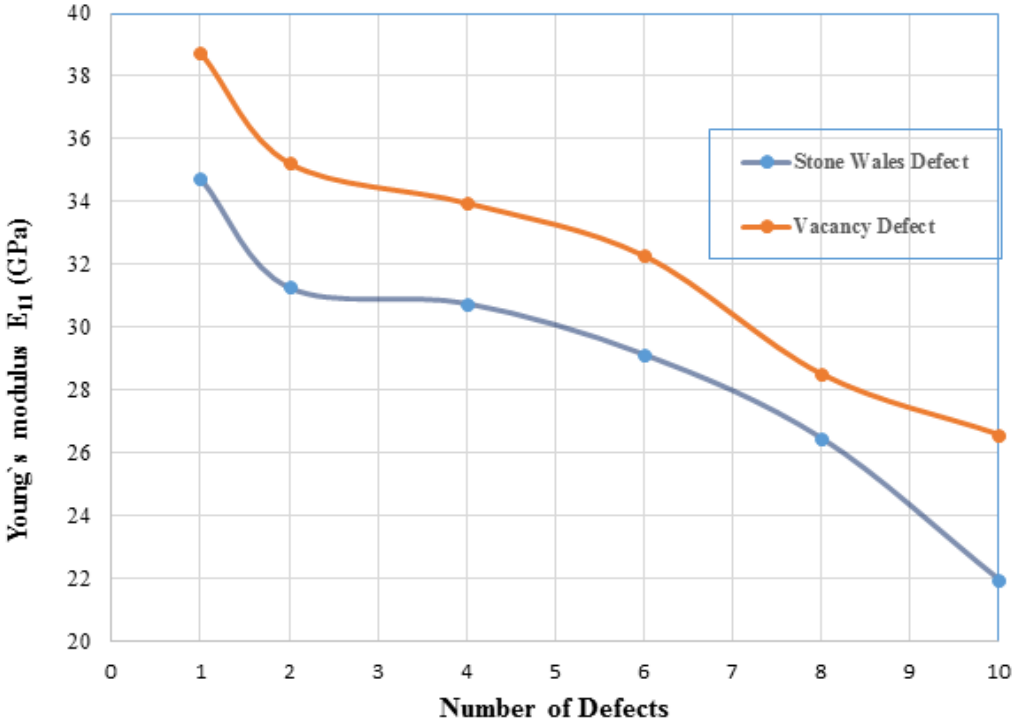

Figure 6.5 Variation of Young`s modulus (E_{11}) in (5,5) armchair SWCNT/NR composite with the number of defects

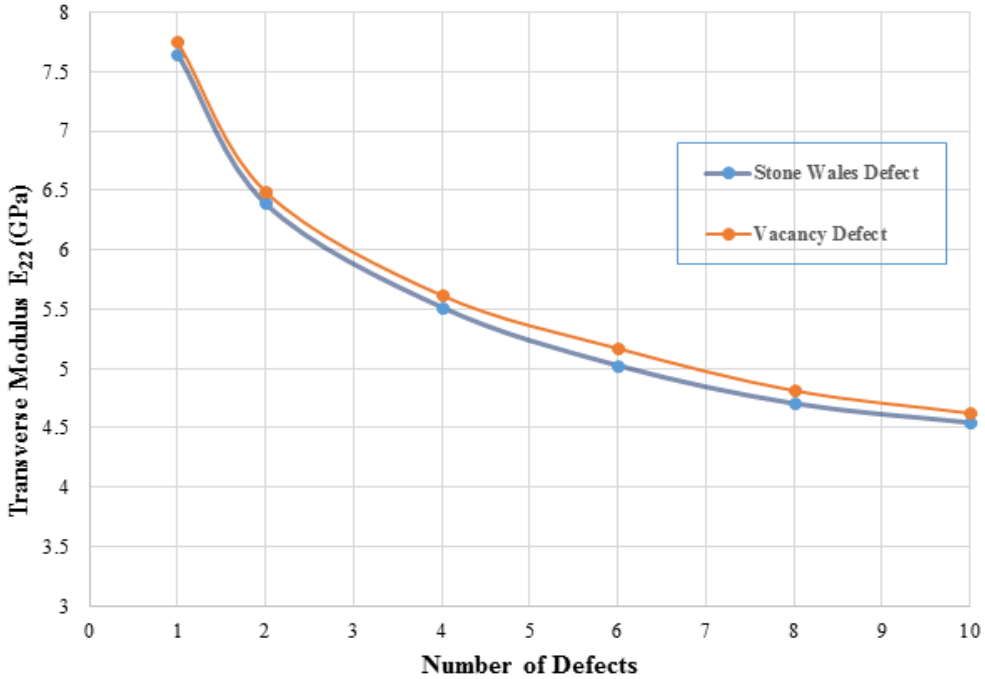

Figure 6.6 Variation in Transverse modulus (E_{22}) in (5,5) armchair SWCNT/NR composite with number of defects

Figure 6.7 shows the variation of shear modulus in armchair (5,5) SWCNT/NR composite with the increase in number of defects, In case of SW defects the percentage decrease of shear modulus is 18.25%, whereas in case of vacancy defects the shear modulus is 12%.

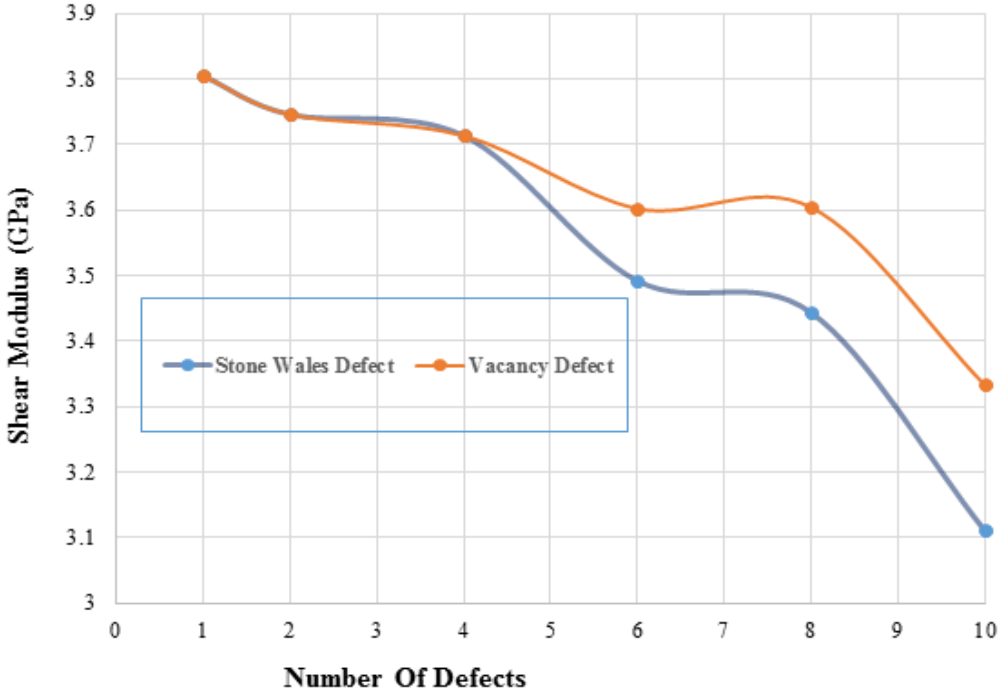

Figure 6.7 Variation in Shear modulus of (5,5) armchair SWCNT/NR composite with number of defects

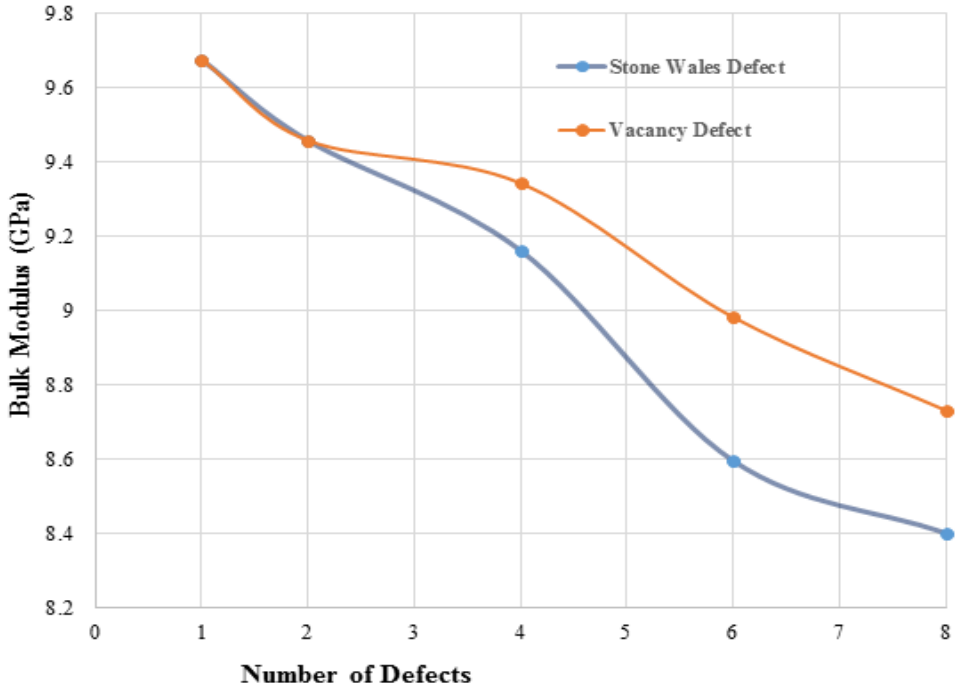

Figure 6.8 Variation in Bulk modulus in (5,5) armchair SWCNT/NR composite with number of defects

Figure 6.8 shows the variation of bulk modulus in armchair (5,5) SWCNT/NR composite with the increase in number of defects, In case of SW defects the percentage decrease of bulk modulus id 14%, whereas in case of vacancy defects the bulk modulus is 11%.

6.4.2 Pullout Force and Interfacial Shear Stress for the Defective SWCNT/NR

In this section the pull out force of SWCNT/NR composite has been done. The energy increment of each pull out step is equal to the work done by the pull out force. Therefore, this energy increment is helpful for finding the corresponding pullout force and interfacial shear stress (ISS). Interfacial shear stress and the interfacial bonding energy of the SWCNT/NR composites have been calculated by using the pull out simulations. The energy increment ΔE_{11} and pull out displacement Δx can be used for finding the pullout force with the help of Molecular Dynamics simulation. Pull out Forces cane be calculated from equation (6.1) given below:-

$$F_{11} = \frac{\Delta E_{11}}{\Delta x} \qquad (6.1)$$

The pullout force for the pristine SWCNT/NR and for the SW defective SWCNT/NR has been calculated by using the above equation. The SW defects pullout force follows the same trend as of pristine SWCNT/NR composite. The pull out forces decreases as we increase the number of SW defects. The figure 6.9 shows the variation in energy increment with the pullout displacement for the pristine and the SW defective SWCNT/NR composite with 1-10 number of defects. As the value of the summation of average energy, increment for the pristine is coming out to be 367 Kcal/mol and the value of the defective SWCNT/NR composite with increase in defects comes out to be less than that of pristine. The value of average energy increment with one defect is 334.22 Kcal/mol, with six defects is 331.168 Kcal/mol and with 10 number of defects is 306.41 Kcal/mol. The decrease in the average energy increment shows that the defects make an impact on the SWCNT/NR composite and the lower energy is required to pullout the single wall carbon nanotube from the Natural rubber polymer. Due to defects, the bond-bond interactions become weaker and less energy is required to pullout the SWCNT from the NR matrix. The pull out forces for the pristine and the SW defective SWCNT/NR composite are shown in the Table 6.1. The pull out force of the pristine is more as compared to the SW defective and the vacancy defective SWCNT/NR composite.

Table 6.1 Percentage decrease in pull out force of defective SWCNT from NR matrix as compared to pristine

Number of Defects	**Pull out force Kcal/(mol nm)**		**Percentage decrease in pull out force of defective SWCNT from NR matrix as compared to pristine (in %)**	
	SW Defects	Vacancy Defects	SW Defects	Vacancy Defects
Pristine	104.34	104.34	Pristine	Pristine
1	100.20	77.25	3.97	39.95
2	98.00	71.52	6.08	34.432
4	95.58	63.74	8.39	38.04
6	94.00	62.98	9.91	46.07
8	87.12	55.89	16.50	46.60
10	84.26	43.88	24.72	47.14

During the SWCNT pullout throughout the polymer matrix, the stress is generated and the generated stress is called as the ISS, which was induced by the pullout forces. As the results of simulation shown in the Figure 6.9 and Figure 6.10 gives us the clear idea that the energy increment ΔE_{11} fluctuates for the SW defects and the vacancy defects for different number of defects in comparison with the pristine and does not have a constant value during the pullout. The fluctuation in the energy is due to the non-uniformity of the polymer matrix (NR) chains and sues to the position sensitivity along the SWCNT walls.

Due to the fluctuation in the energy increment ΔE_{11}, several researchers assume that constant ISS with a uniform distribution over the embedded length of SWCNT. So as per the previous studies, it can be concluded that the ISS is mainly distributed at each end of embedded CNT within the range of a=1.0 nm as a pullout displacement, where the energy increments are large. Using the assumptions, the ISS `τ `was calculated as per equation.(6.2) [88, 89].

$$\tau = \frac{F_{II}}{2\pi D a} \qquad (6.2)$$

Where, D = Diameter of SWCNT (.67 nm), a = .1nm (as per the assumption)

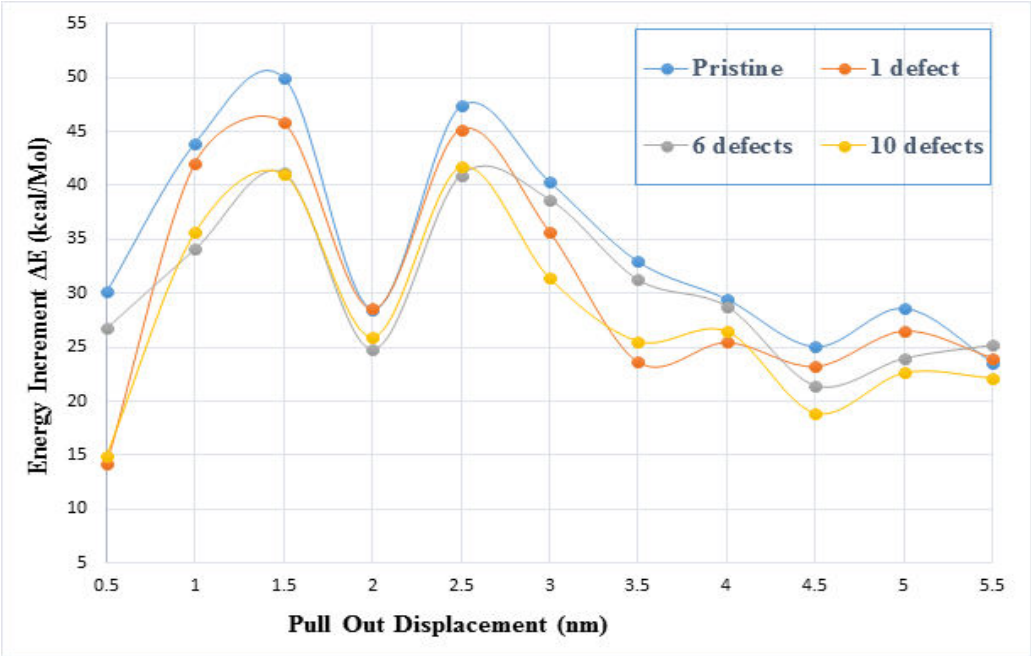

Figure 6.9 Variation of energy increment with pull out displacement of the pristine and SW defective SWCNT/NR composite

The results which can be obtained from the simulation and presented above can also be used to calculate the surface density γ , also known as the interfacial bonding energy, using Eq.(6.3) [88, 89].

$$\gamma = \frac{\Delta E}{2\pi D \Delta x} = \frac{F_{II}}{2\pi D} \qquad (6.3)$$

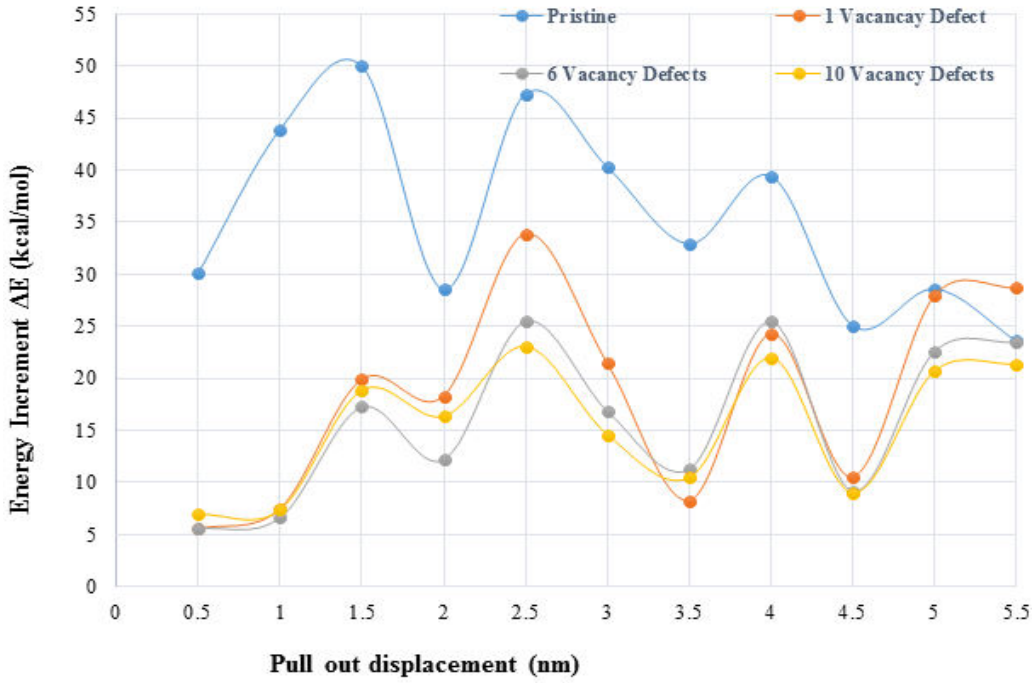

Figure 6.10 Variation of energy increment with Pull out Displacement of the pristine and vacancy defective SWCNT/NR composite

Figure 6.11 and Figure 6.12 represents the variation in ISS and the surface density with the increase in number of defects i.e. SW and Vacancy defects. As the value of ISS for the pristine SWCNT/NR composite is 245.06 MPa and for the SW defective SWCNT/NR composite the value of ISS is decreases to 197.88 MPa when the number of defects ranges from 1-10.

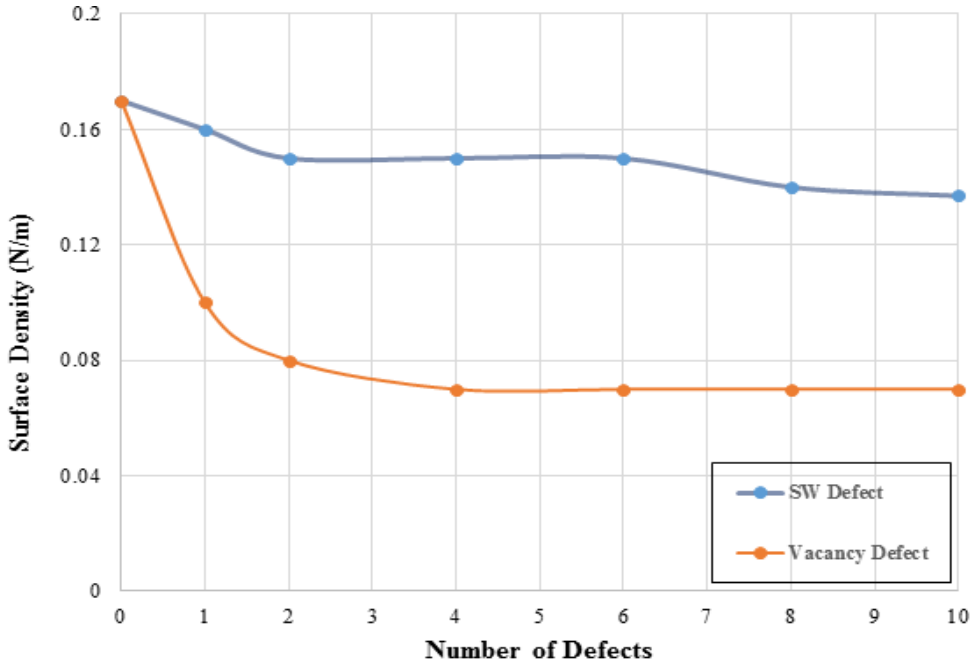

Figure 6.11 Variation in surface density with the increased number of Stone-Wales defects of the SWCNT/NR composite

Figure 6.12 Comparison in interfacial shear stress between SW and Vacancy defect of SWCNT/NR composite with increase in number of defects

However, the ISS for the vacancy defective SWCNT/NR with the defects ranges from 1-10 comes out to be 102.23 MPa. The value of the surface density with no defects is 0.170 N/m, as we introduce the defects in the SWCNT/NR composite the value of the surface density decreases. The value of surface density for the SW defective SWCNT/NR composite is 0.137 N/m and value of surface density for the Vacancy defective SWCNT/NR composite is 0.07 N/m. The table 6.2 represents the value of ISS and surface density with the increase in number of defects and the Percentage decrease in ISS and Surface density of defective SWCNT from NR matrix as compared to pristine. The value shows that in case of SW defective SWCNT/NR the percentage decrease in surface density ranges from 5.88% to 19.41% and in case of the vacancy defect the percentage decrease for surface density ranges from 41.17% to 58.82% with the increase in number of defects 1-10.

Table 6.2 Percentage decrease in ISS and surface density of defective SWCNT from NR matrix as compared to pristine

Number of Defects	**Value of ISS and Surface density**				**Percentage decrease in ISS and Surface density of defective SWCNT from NR matrix as compared to pristine**			
	Interfacial Shear		Surface Density		Surface Density		Interfacial Shear Stress	
	SW Defects (MPa)	Vacancy Defects (MPa)	SW Defects (N/m)	Vacancy Defects (N/m)	SW Defects	Vacancy Defects	SW Defects	Vacancy Defects
Pristine	245.06	245.06	0.17	0.17	-	-	-	-
1	235.33	147.16	0.16	0.10	5.88	41.17	3.97	39.95
2	230.15	126.82	0.15	0.08	11.76	52.94	6.08	48.24
4	224.48	104.05	0.15	0.07	11.76	58.82	8.39	57.53
6	220.76	102.30	0.15	0.07	11.76	58.82	9.91	57.44
8	204.61	103.27	0.14	0.07	17.64	58.82	16.50	57.85
10	197.88	102.23	0.137	0.07	19.41	58.82	19.25	57.99

Whereas the percentage decreases in ISS for the SW defective SWCNT/NR composite ranges from 3.97% to 19.25% and for vacancy defective SWCNT/NR composite ranges from 39.95% to 57.99%. The decrease in the ISS and surface density is due to the decrease in atomic interaction between the CNT and NR matrix. When the

number of vacancy defects increases, the ISS and the surface density value saturates due to tensile strength, which does not decreases further. In case of the SW defects, the value of ISS and surface density is more as compared to the vacancy defects. SW defects also called as geometrical defect has very little effect on ISS and surface density. It has been observed that sue to SW defects, the cross sectional area of CNT is changed, during pull out the proper connection between SWCNT and NR matrix does not occur that reduces the ISS and surface density

6.5 Thermal Conductivity of the Defective SWCNT/NR composite

Many researchers investigated the mechanical, physical, electrical and thermal properties of the single walled carbon nano tubes since the Iijima [2] discovered the CNT in 1991. Most of the researchers investigated the mechanical and physical properties either by computational method or by experimental method for the single walled carbon nanotube reinforced polymer composites. The thermal properties of the single walled carbon nanotube reinforced Natural rubber composite have not be calculated either by experimental or by computational method by the researchers. The thermal properties play an important role in addition to their mechanical stability. Therefore, the focus is to find out the effect of thermal conductivity for the SW and vacancy defective single walled carbon nanotube reinforced Natural rubber composite. Measurement of the thermal conductivity of SWCNT/NR composite with defects is based on the theoretical simulation and calculation, which gives us, scattered result. The thermal conductivity of SWCNT/NR composite depends upon the length, diameter of tube, number of stone-wales defects due to geometrical orientation and vacancy defects due to the impurities. The thermal conductivity also depends upon the atomic arrangement.

In the Molecular Dynamics simulation, the investigation of the thermal conductivity can be done by using non-equilibrium Molecular Dynamics (NEMD) or by equilibrium Molecular Dynamics (EMD). The “Direct method” and the “Green- Kubo” method are the two methods for finding the thermal conductivity. The direct method is based on temperature gradient which imposed across the simulation cell is an NEMD approach and analogous to experimental study. The Green-Kubo approach is based on the current fluctuation is an EMD approach.

Schelling et al. [111] in (2002) studied the effect of thermal conductivity by comparing the feature of “Direct” and “Green-Kubo” method. The authors observed

that in case of EMD, the thermal conductivity could be predicted in all directions using one simulation whereas in case of NEMD the thermal conductivity predicts by using a thermal gradient only in one direction. So NEMD is based on the Fourier`s law of conduction and the EMD is based on the fluctuation-dissipation Theorem. The exchange of the Kinetic energy of two particles is used in the reverse Non-equilibrium Molecular Dynamics method. In this method, the coldest particle is placed in hot layer and the hottest particle is placed in the cold layer. Also in this method, the ΔE energy is used and averaging over many exchanges. The Jund [112] in 1991 used the method in which the hot layer and cold layer particles are involved and the energy used is fixed. In the above methods, total energy and linear momentum of the system conserves means that no momentum is exchanged.

In this study for finding the thermal conductivity of the defective SWCNT/NR composite, the imposed flux method was used in the "Z" direction. Energy is being transferred from the one region to the other continuously. For defining the cold region and hot region, the velocities of the atoms are interchanged. The velocity of coldest atom in the hot region and the velocity of hot atom in the cold region were interchanged. The heat flux is generated while transferring the velocities. The flux generated is artificial and created from the cold to hot region.

$$J_z = \frac{1}{2tA} \sum \frac{m}{2} (v_{hot}^2 - v_{cold}^2) \qquad (6.4)$$

m=mass, t= time of simulation

A= cross sectional area of simulation cell, v_{hot} and v_{cold} are the velocities of atoms.

By using the Material studio 2017, a script was written for finding out the Thermal conductivity of the single walled carbon nanotubes reinforced Natural rubber composite. While writing the script some of settings for parameters are required for running the script. The number of the layers in the "Z" direction which id the direction flux was 40. The number of layers must be even. If we increase the number of layer, we obtain the more accuracy of the gradients but as we increase the number of layers this will lead to large fluctuation in the temperature of layers. After that the objects has been selected and the type of the objects was 'atoms' to exchange the velocity. Then another parameter has been selected for exchange methods. Two types of exchange method are available. One is 'FIXED' and other is 'VARIABLE'. The 'VARIABLE' method exchanges a variable energy between objects, one object in hot layer and one object in cold layer. In 'FIXED' method, constant energy has been exchanged between all the

objects in cold layers and hot layers. The value for the exchange energy in the fixed method was 1 Kcal/mol. The number of the exchanges performed for the equilibration was 500. The flux was calculated by the ratio of exchange energy and number of steps. The number of exchanges performed for production was 1000. A time step of 1fs was used and the number of steps between two exchanges was 100. The temperature for the thermostat was 298 K and the thermostat use was 'Berendsen'. If we decrease the number of steps between two exchanges this will leads to increase the higher flux and increase the temperature gradient. By using Molecular Dynamics simulation, the thermal conductivity for the Stone Wales defective SWCNT/NR composite and the Vacancy defective SWCNT/NR composite has been calculated with different number of defects.

6.5.1 Models to Calculate Thermal Conductivity

To find the effective thermal conductivity of single walled carbon nanotube reinforced Natural rubber composite based on theoretical and semi theoretical, lots of model are available. Two simple models such as series and parallel models have been used to validate the thermal conductivity, which were calculated using the Molecular Dynamics simulation techniques. The series model gives the lower bound whereas the parallel model gives the upper bound of the thermal conductivity. After the simulation using the Molecular Dynamics, the values obtained were validate if the values of thermal conductivity lie in between these two models. The descriptions of these two models are presented in this section.

Series Model: In the series model of the thermal conductivity applied to the laminated composites along the direction of the fiber. The effective thermal conductivity of the SWCNT/NR composite has been calculated by using the formula given below-

$$K = \frac{K_m * K_f}{K_f * (1 - V_f) + K_m * V_f} \qquad (6.5)$$

Where, K = Thermal conductivity of composite

K_f = Thermal conductivity of armchair

K_m = Thermal conductivity of Natural rubber matrix

V_f = Volume fraction

The series model gives the lowest bound for the thermal conductivity of composites.

In case of Parallel model, the thermal conductivity of single walled carbon nanotube reinforced Natural rubber polymer composite along the fiber alignment direction has been predicted. The parallel series method gives up the upper bound for the thermal conductivity of composites. So the value of thermal conductivity measured must falls between the lower bound of series method and the upper bound of the parallel model. For parallel method the thermal conductivity of composites has been calculated by using the formula given below.

$$K = \left(1 - V_f\right) * K_m + V_f * K_m \qquad (6.6)$$

Where, K = Thermal conductivity of composite

K_f = Thermal conductivity of armchair

K_m = Thermal conductivity of Natural rubber matrix

V_f = Volume fraction

6.6 Results and Discussions

Figure 6.13 shows the variation in the thermal conductivity of the armchair (5,5) defective SWCNT/NR composite with the increase in number of defects with volume fraction of 8%. In case of a Stone Wales defective single walled carbon nanotube reinforced Natural rubber composite, the thermal conductivity decreases as the number of defects increases, also in case of a vacancy defective single walled carbon nanotube reinforced Natural rubber composite, the thermal conductivity decreases as the number of defects increases. In comparison to thermal conductivity of both the defects, the vacancy defective SWCNT/NR composites decreases sharply as compared to stone wales defective SWCNT/NR composite.

Table 6.3 shows the percentage decrease in thermal conductivity of SW and vacancy defective SWCNT/NR composite in comparison to the pristine SWCNT/NR composite. The percentage decrease in thermal conductivity of SW defective single walled carbon nanotube reinforced with Natural rubber composite as compared to pristine, ranges from 19.30% to 34.50% with the number of defects increases from 1-10. In case of vacancy defective single walled carbon nano tube reinforce Natural rubber composite the percentage decrease in thermal conductivity in comparison to pristine ranges from 12.37% to 39.57% with the number of defects increases from 1-10. Figure 6.14 shows the comparison of results obtained by using Molecular Dynamics simulation for thermal conductivity of an armchair (5,5) defective single walled carbon nanotube reinforced

Natural rubber composite (V_f = 8%) with series and parallel model of thermal conductivity. The thermal conductivity values calculated using the Molecular Dynamics simulation with number of defects lies in between the series model, which gives lower bound values, and the parallel model, which gives the upper bound values. The thermal conductivity, which has been calculated by using the series model, was 0.14 and the thermal conductivity value, which has been calculated by using the parallel model, was 3.12.

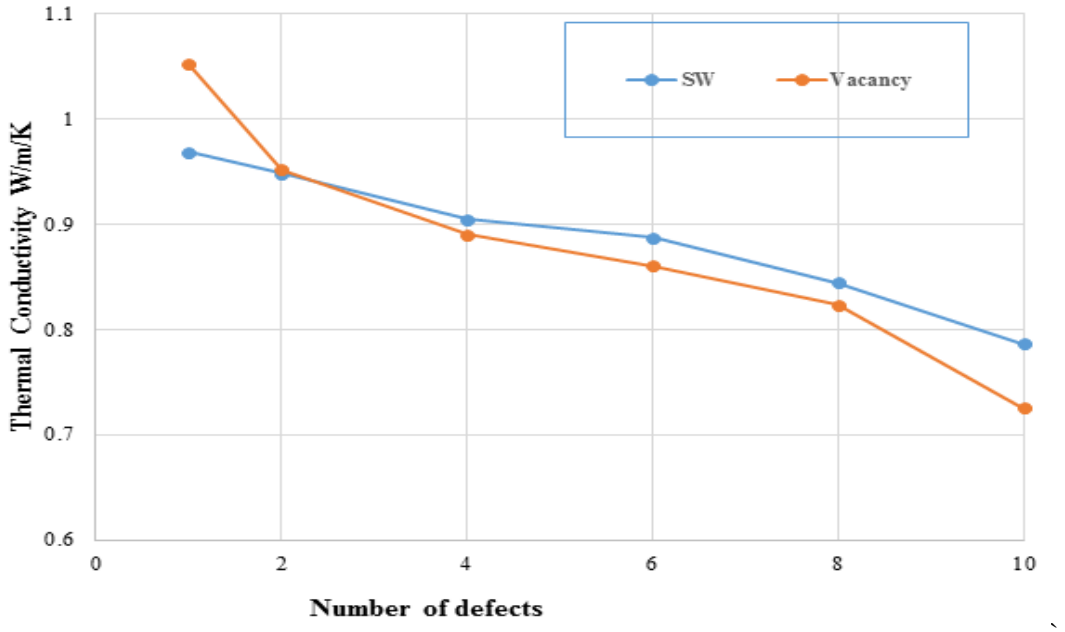

Figure 6.13 Variation in thermal conductivity of armchair (5,5) defective SWCNT/NR composite with number of defects

Table 6.3 Percentage decrease in Thermal conductivity of defective SWCNT from NR matrix as compared to pristine

Number of Defects	**Thermal Conductivity (W/m/K)**		**Percentage decrease in Thermal conductivity of defective SWCNT from NR matrix as compared to pristine**	
	SW Defects	Vacancy Defects	SW Defects	Vacancy Defects
Pristine	1.20	1.20	Pristine	Pristine
1	0.96	1.05	19.30	12.37
2	0.94	0.95	20.99	20.69
4	0.90	0.89	24.61	25.83
6	0.88	0.86	26.08	28.28
8	0.84	0.82	29.67	31.39
10	0.78	0.72	34.50	39.57

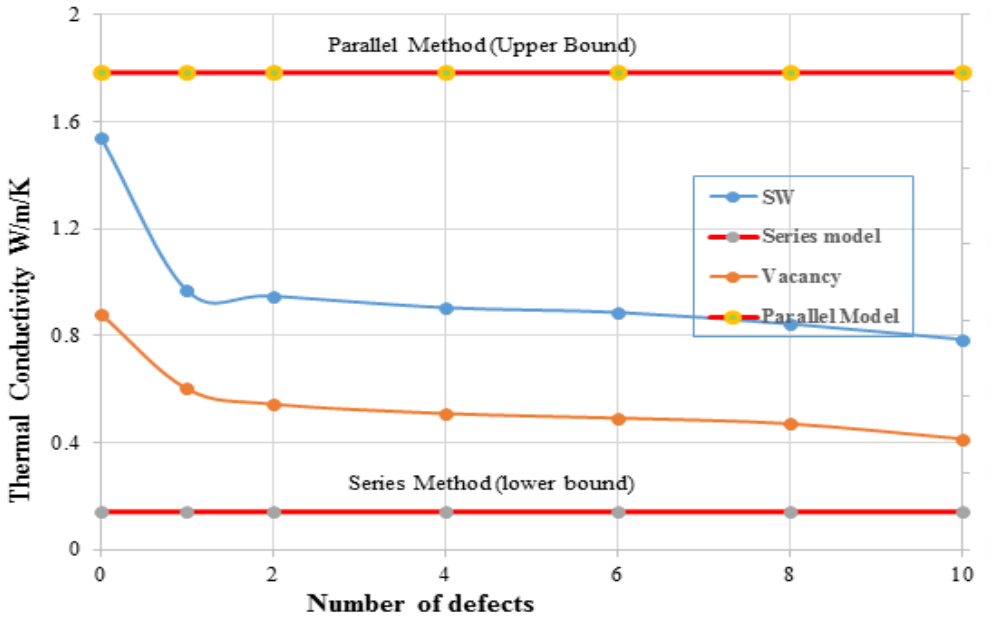

Figure 6.14 Comparison of the results of Molecular Dynamics for armchair (5,5) defective SWCNT/NR composite with Vf = 8 % for thermal conductivity with the series and parallel models

Table 6.4 Comparison of thermal conductivity results of MD for armchair (5,5) defective SWCNT/NR composite with V_f =8 % with the series and parallel models.

Number of Defects	**Comparison of thermal conductivity results of MD for armchair (5,5) defective SWCNT/NR composite with V_f = 8 % with the series and parallel models (W/m/K)**			
	SW Defects	Vacancy Defects	Series Model (Lower bound)	Parallel Model (Upper Bound)
Pristine	1.20	1.20	0.14	3.12
1	0.96	1.05		
2	0.94	0.95		
4	0.90	0.89		
6	0.88	0.86		
8	0.84	0.82		
10	0.78	0.72		

The values obtained shown in Table 6.4 for thermal conductivity of defective SWCNT/NR composite by MD simulation was in the range of 0.96 to 0.78 W/m/k with stone walls defect for V_f = 8% and for the vacancy defect, the value of thermal conductivity ranges in between 1.05 to 0.72 W/m/K. The values of the thermal conductivity depend upon the chirality because heat transfer depends purely on the band gaps present in the CNTs.

Chapter 7

Effect of functionalization of CNT on Mechanical and Thermal properties of CNT Reinforced Polymer Composites

7.1 Introduction

By now, CNTs have already attracted many researchers because of their eminent physical properties that include mechanical, thermal as well as electrical properties. CNTs were unknown three decades ago. It was year 1991 when CNTs were discovered by Iijima [2]. An expansive scope of warm, basic and electronic properties has been appeared by the CNT. A broad range of thermal, structural and electronic properties has been shown by the CNT. These properties vary with the nanotube types, which are not just confined to SWCNT or MWCNT, but types are numerous based on their length, aspect ratio, functional group attached or angle of twist etc. Addition of additional functional groups to the surface of any material is called functionalization. In other words, it is the process of adding new features, functions, properties, or capabilities to a material by changing the surface properties of the material. It is a basic technique used throughout materials science, chemistry, biological engineering, and nanotechnology. Carbon nanotubes (CNTs)/rubber composites have aroused a tremendous attraction in the past decade due to the excellent mechanical and electrical properties of CNTs [113]. In the form of functionalization, carbon or hydrogen atoms introduced to form covalent bonds with carbon atoms on the CNT. These atoms may affect the properties of CNTs [114]. Covalent bonds, which have been developed due to specific functional groups onto the surface of SWCNT, such as carboxyl, amine, fluorine, hydroxyl etc., provide strong covalent bond between tubes and polymer so that load-transfer capability was significantly enhanced. With the increase in the functionalization the young`s modulus of CNT decreases. Sumit Sharma *et al.* [82] in 2016 used Molecular Dynamics simulation to analyse functionalized SWNCT-polymer nanocomposites. Researcher showed that both dynamics as well as mechanical properties of SWNT with varying functional groups. Armchair (5,5) SWNT was chosen and molecular simulation was done with proper consideration of practical environment conditions. Aspect ratio was

fixed to 10. Apart from the good mechanical properties of CNT/polymers, thermal properties also plays a very important role in the stability of the CNTs. CNTs are of excellent electrical conductivity, thermal stability and conductivity. Thermal conductivity is useful to find the amount of heat dissipation from surfaces. Thermal conductivity are technological important and interesting property [115]. H. Liu et al [116] in 2014 showed that with the increase of carbon amount the thermal conductivities were increased. Savas Berber et al in 2000 [117] shows that carbon nanotubes having an unusually high thermal conductivity value of 37000 W/m K. The thermal conductivity of a material is determined by the transportation of phonons. In graphite, phonons dominate the thermal conductivity at temperatures above 20 K, and it increases markedly as the temperature decreases [118]. Thermal conductivities in the CNT/polymer composites are critically depend on the dispersion state, aspect ratio and the interfacial interactions between the CNTs and the polymer matrix. The thermal conductivities of SWCNTs were much more influenced by chemical or covalent functionalization than physical or noncovalent functionalization. Shenogina *et al.* in 2005 [119] modelled the contact between CNTs in which author concluded that due to weak van der Walls forces binding CNTs the heat flow by CNT-CNT direct contact is very ineffective resulting a significant thermal resistant. Moisala *et al.* in 2006 [120] experimentally studied the thermal conductivity and found a thermal conductivity less than 0.30 W/mK for MWCNT/epoxy composite with 0.5 wt.% MWCNT loading. Song and Youn in 2006 [121] evaluated the effective thermal conductivity of the carbon nanotube/polymer composites by control volume finite element method. In this study Molecular Dynamics simulation is used to find the thermal conductivity and the mechanical properties of SWCNT-NR composites, when SWCNT is functionalized with various groups like -OH, -COOH, -$COOCH_3$ with the help of Materials studio 2017.

7.2 Calculation of Mechanical Properties

First step is the modeling of the SWCNT using 'Build' tool, a (5,5) armchair SWCNT of diameter 0.67 nm and length of 5.58 nm was built. Hydrogen atoms were terminated from both the ends to avoid the effects of unsaturated boundary conditions. Functional groups were added by attaching the atoms of different functional groups of carboxylic (COOH), ester ($COOCH_3$) and hydroxyl (OH) to the surface of SWCNT and

all groups were added symmetrically by using the "sketch Atoms" tools of Material studio software shown in Figure 7.1 to Figure 7.3.

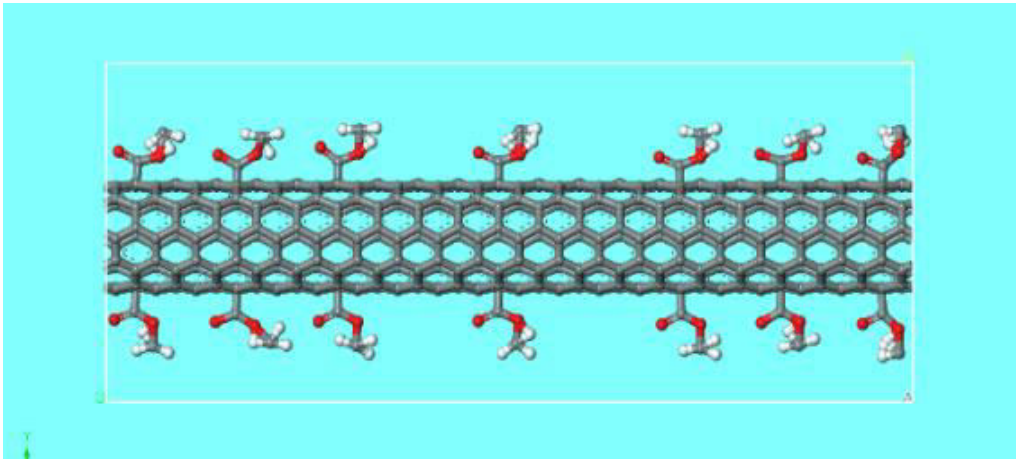

Figure 7.1 Functionalized SWCNT of $COOCH_3$

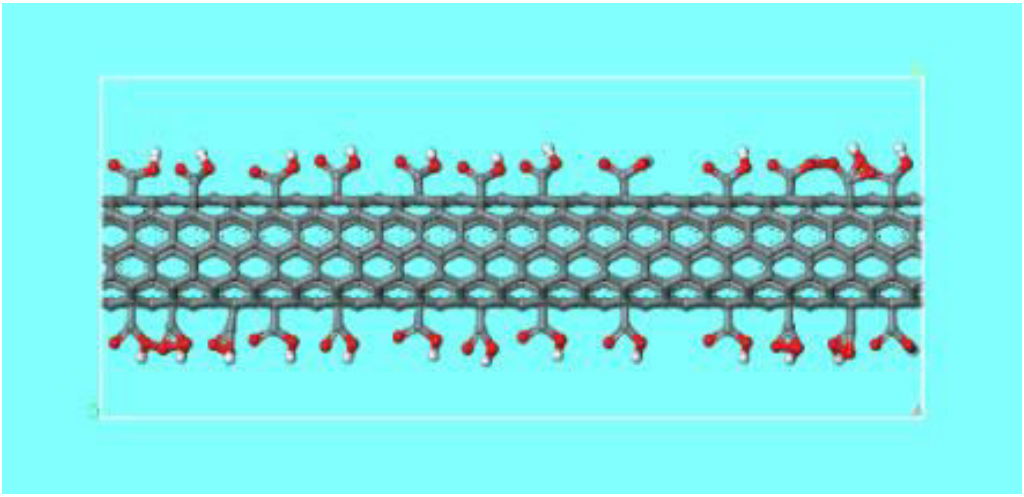

Figure 7.2 Functionalized SWCNT of COOH

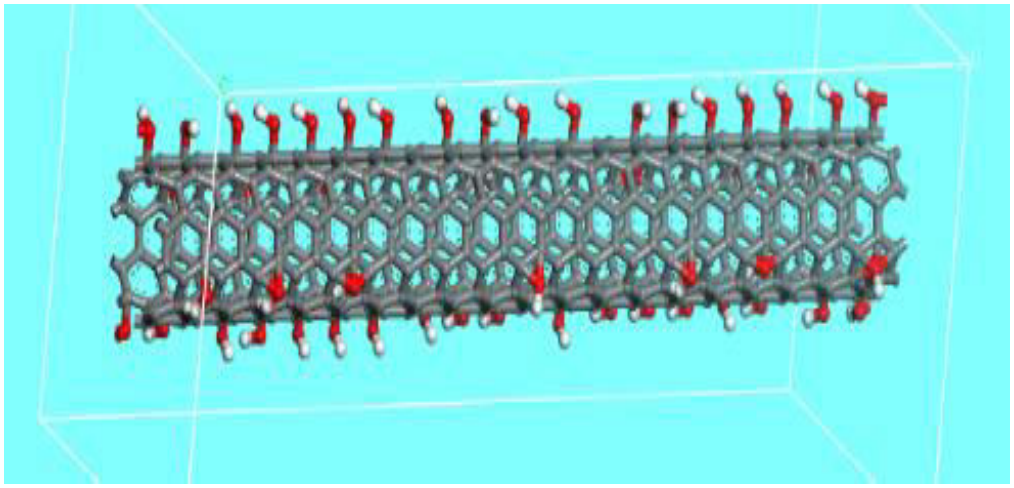

Figure 7.3 Functionalized SWCNT of OH

A final structure consists of 498 atoms. In the next step packing of a composite system using “amorphous cell module” in which a single chain of Natural rubber consists of 10 repeated units has been used as input in the simulation cell module at an initial density of 0.98g/cm3. For describing the Intra and Intermolecular atomic interactions the most common force field, i.e. Condensed Phase Optimized Molecular Potential for Atomistic Simulation Studies (COMPASS) has been used [86]. The size of the simulation cell was 2.42 X 2.42 nm X 4.70 nm consists of 2874 atoms shown in Figure 7.4 and Figure 7.5 which provided the volume fraction (Vf) of ~ 8%.

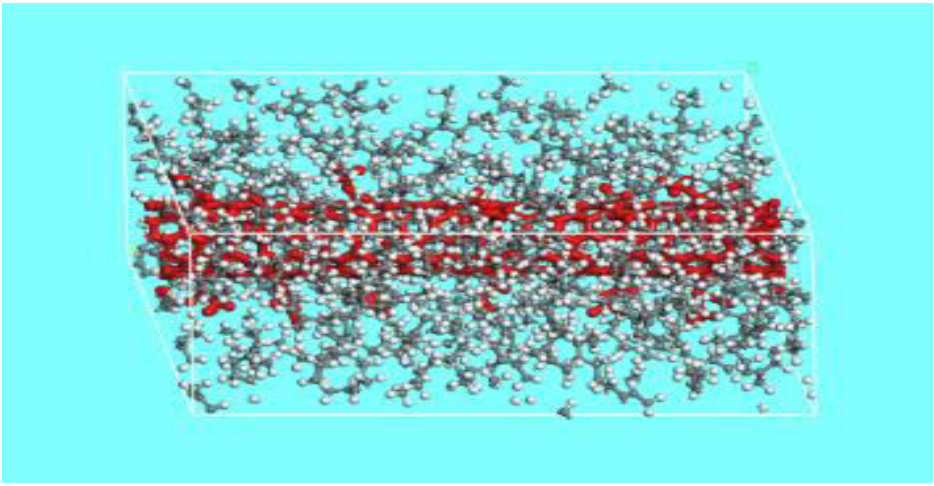

Figure 7.4 CNT packed with NR

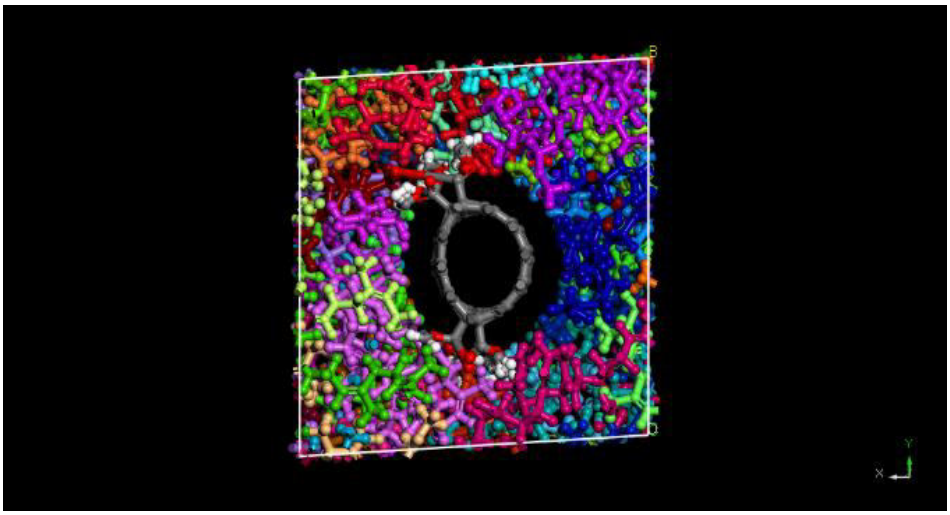

Figure 7.5 Simulation cell consists of 2874 atoms

After the completion of the simulation cell packing, two steps to be followed for the equilibration process for calculating the young`s modulus. The first step is “Geometric Optimization” using forcite tools. This step is crucial because configurations in the

beginning is in the higher state of energy and thus needs to be minimized. Many optimization methods are available in material studio and steepest descent method [95] was particularly chosen for this study. The next step is "Dynamics" using forcite tools, Using NPT (Constant pressure, constant temperature), "Nose" as a thermostat and "Berenderson" as a Barostat, which is used to compress the system, to obtain proper density, and low residual stresses. The total time provided for the simulation was 60 ps with the time step of 1 fs [89, 98]. After this dynamic run repeats the Geometric optimization, using the output of dynamics as input. The output comes will further use as an input for the NVT ensemble (constant number of atoms, volume, and temperature) which provide the equilibrated system at 40 ps and proper structure with low stresses [122]. Before and after each Dynamics run, the structure was optimized with steepest descent algorithm again with 90000 steps. For calculating the mechanical properties of the composite, a constant strain of 0.003 was applied, and number of strains was kept constant at 6. The structure was pre-optimized before performing mechanical properties calculations.

7.3 Calculation of Thermal Properties

Thermal conductivity can be computed in MD simulation by either using equilibrium MD (EMD) or non-equilibrium MD (NEMD). In the "direct method" (MEMD), temperature gradient was imposed across the simulation cell which was similar to the experimental situation. In "Green-Kubo" approach (EMD), fluctuation dissipation theorem was used to compute thermal conductivity in which current fluctuates. Hone et al in 2000 [123] identified that the thermal conductivity of the SWCNT is over 200W/m/k at room temperature. Zhou *et al.* in 2004 [124] found that the axial thermal conductivity at room temperature of the annealed SWCNT fiber spun was 19 W/m/K. A simple formula for the thermal conductivity enhancement in carbon nanotube composites is presented on the conventional effective medium model and this model shows that a remarkable enhancement in the effective thermal conductivity of the composites by addition of small amount of CNTs [125]. The thermal conductivity of epoxy with 1 wt. % SWCNT is about 0.5 W/m/K at room temperature, while the thermal conductivity of the control epoxy without SWCNT was about 0.2 W/m/K [126]. Energy exchanged in the reverse non-equilibrium MD (RNEMD) method was carried with the help of exchanging the kinetic energy of the two particles. For finding the thermal conductivity imposed flux method was used. A script was written in Materials

Studio 2017 using the available scripting option. The number of layer for finding the thermal conductivity was fixed at 40 in the direction of flux. As accuracy of the gradients depend upon the number of layers, increase number of layers may increase the accuracy but leads to the large fluctuation in the temperature of layers. The exchange method used in this study was "Variable" which helps in exchange of variable energy between objects in cold layer and hot layer. "Fixed" exchange variable was used for exchange in constant energy between all hot objects and cold objects in their respective layers. The amount of energy to exchange was 1Kcal/mol. The number of exchanges performed for equilibration was taken as 500 and the number of exchanges performed for production was 1000. Constant Energy (NVE) was used for production stage and the time step for simulation was 1fs. The number of time steps between two exchanges was 100. Change in number of steps leads to change in fluxes and changes the temperature gradient. Too small values were avoided as these introduce nonlinear effects and may affect performance.

7.4 Results and Discussion

7.4.1 Young's Modulus of Hydroxyl (-OH) Functionalized SWCNT/NR Composite

Variation of Young's modulus with the variation in concentration of hydroxyl groups is shown in Figure 7.6. With the increase in the concentration of hydroxyl in SWCNTs, the Young's modulus decreases continuously. A total reduction of around 28% in Young's modulus is observed in SWCNT composites as we move from 1 percent -OH concentration 20 percent -OH concentration.

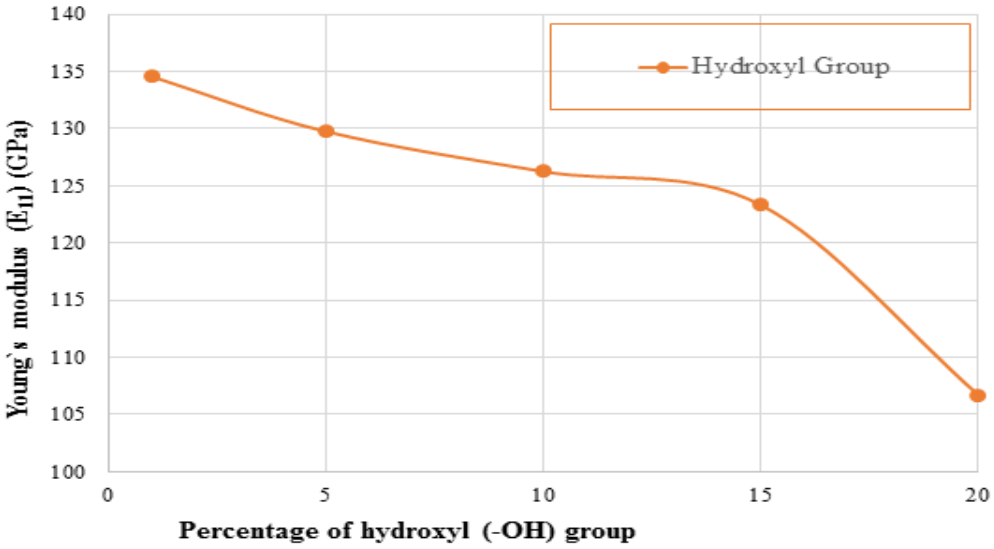

Figure 7.6 Variation in Young`s modulus of armchair (5,5) SWCNT/NR composite with increase in hydroxyl group (-OH)

Thus, higher the percentage of -OH functional group, higher will be the un-stability of the composite. Now, this functional group conforms to the expectations, i.e. Young's modulus decreases with increase in concentration of the hydroxyl group.

7.4.2 Young's Modulus of Carboxyl (-COOH) Functionalized SWCNT/NR Composite

Variation of Young's modulus with the variation in concentration of carboxyl groups is shown in Figure 7.7. With the increase in the concentration of carboxyl in SWCNTs, the Young's modulus decreases continuously. A total reduction of around 16% in Young's modulus is observed in SWCNT composites as we move from 1% of -COOH concentration to 20% -COOH concentration. Thus, higher the percentage of functional groups, higher will be the un-stability of the composite. Now, this functional group conforms to the expectations, i.e. Young's modulus decreases with increase in concentration of the carboxyl group.

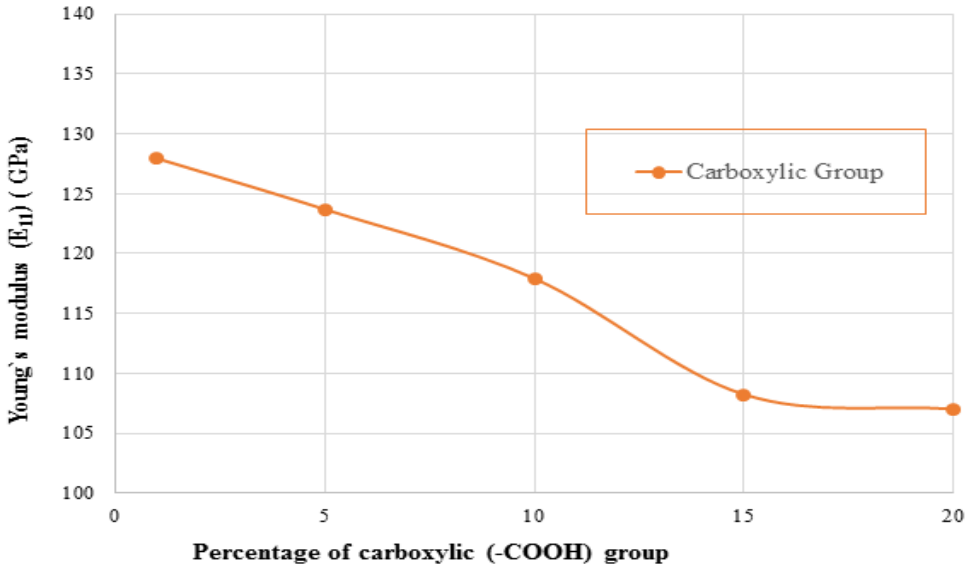

Figure 7.7 Variation in Young`s modulus of armchair (5,5) SWCNT/NR composite with increase in carboxyl group (-COOH)

7.4.3 Young's Modulus of Ester (-$COOCH_3$) Functionalized SWCNT/NR Composite

Variation of Young's modulus with the variation in concentration of ester groups is shown in Figure 7.8. With the increase in the concentration of ester in SWCNTs, the Young's modulus decreases continuously. A total decrement of around 7% in Young's modulus is observed in SWCNT composites as we move from 1 percent $COOCH_3$ concentration 20 percent $COOCH_3$ concentration. Thus, higher the percentage of functional groups, higher will be the un-stability of the composite. Now, this

functional group also conforms to the expectations, i.e. Young's modulus decreases with increase in concentration of the ester group.

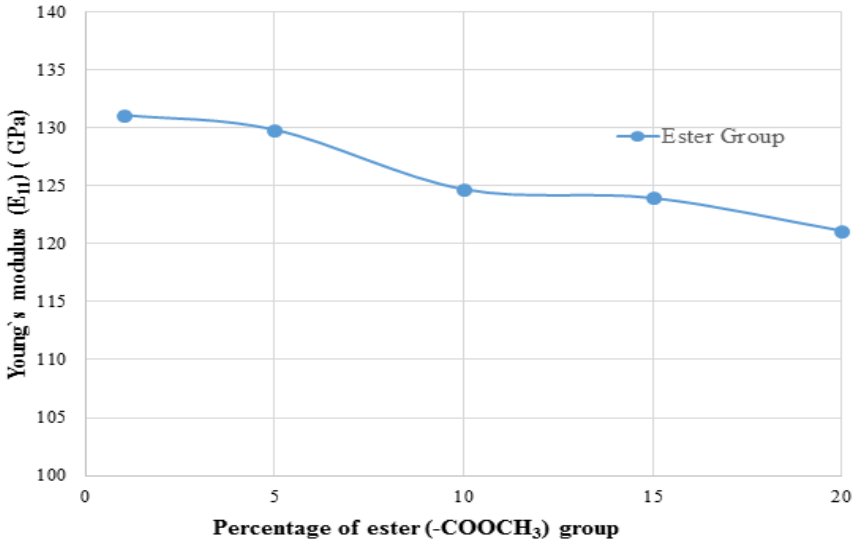

Figure 7.8 Variation in Young`s modulus of armchair (5,5) SWCNT/NR composite with increase in ester group (-$COOCH_3$)

7.4.4 Comparison of all the Functional Groups

It is evident from this research that it is not predictable that whether or not there will be increment or reduction in the Young's modulus of CNT/NR composite with introduction of the functional groups to the pristine CNT, It solely depend on the type of functional groups as well as their concentration in the composite. A comparative analysis among three type's functional groups is shown in Figure 7.9.

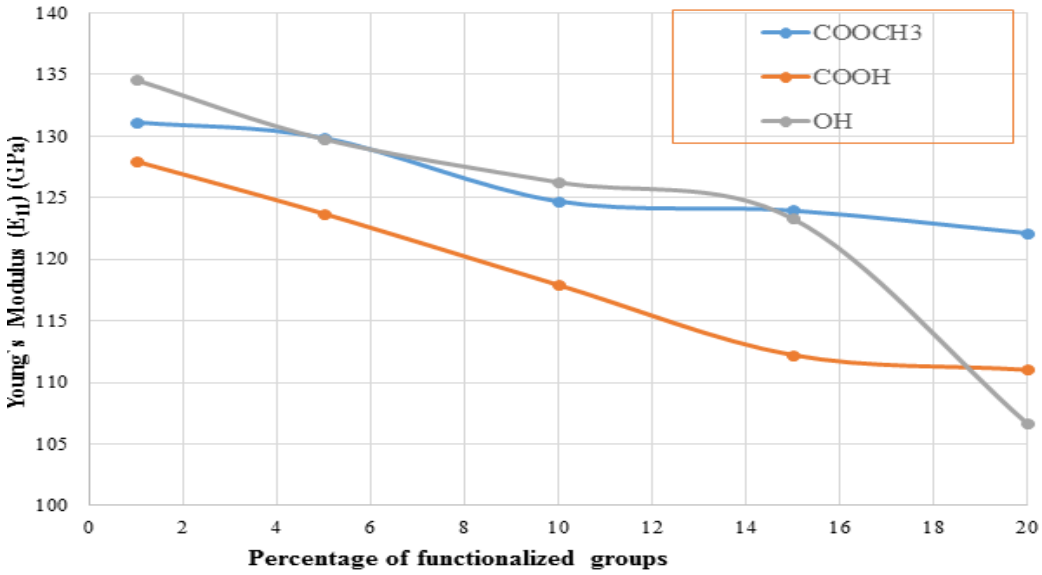

Figure 7.9 Comparison of Young`s modulus for Armchair (5,5) SWCNT/NR composite between different types of functionalised group

As concluded by Sharma et al [23] that chemical functionalization degrades most of the macroscopic elastic stiffness components of the composite materials, it is the same case in this research also. The Young's modulus is decreased by the addition of functionalization of -OH and -COOH functional groups. Little variations among the results because the polymer matrix is different and different configuration (n, n) taken for SWCNT. Very similar pattern can be obtained from other researches [127-133]. A general trend of reduction in Young's modulus with increasing rate of functionalization is observed. A total reduction of 20% in Young's modulus is observed in this research when we move from pristine SWCNT to 20% functionalized with -COOH group, which is same as obtained by Sharma *et al.* [83], and Priyal *et al.* [129]. At low percentage of functionalized group, results are in validation with Yang *et al.* [128], Ling *et al.* [130], and Milowska *et al.* [131]. A total reduction of 28 % in Young's modulus is observed in this research when we move from pristine SWCNT to 20% functionalized with -OH group. It is about 20% reduction when functionalization percentage is around 10%, the same is the result obtained by Priyal *et al.* [129] at 10% of functionalization with hydroxyl (-OH) group. In this work around 10% of total reduction is observed when the functional group is ester (-$COOCH_3$) which can be validated by Sumit *et al.* [83], and Odegard *et al.* [134] shown in Table 7.1.

Table 7.1 Reduction in Young`s modulus of armchair (5,5) SWCNT/NR composite with variation in functional groups attached in percentage

Authors	**Reduction in Young`s modulus with variation in functional groups**					
	Our Work			Sharma *et al.*	Priyal *et al.*	
	Functional group attached in percentage					
Functional Group	5%	10%	15%	16%	5%	10%
-COOH	10% Reduction	15 % Reduction	20% Reduction	21% Reduction	5 % Reduction	10 % Reduction
-$COOH_3$	9 % Reduction	20% Reduction	28% Reduction	17% Reduction	10 % Reduction	21 % Reduction
-OH	07% Reduction	09% Reduction	10% Reduction	09 % Reduction	10 % Reduction	20 % Reduction

The comparison among various studies is shown in Table 7.3. In Table 7.2, we have summarized similar results reported in the literature obtained using various functional groups at varying percentage of functionalization along with the major results of the present study. Thus, we can now easily understand the effect of functionalization on CNT or CNT composites. Table 7.3 provides for various methods used by the respective authors for their simulation or experimental works. A combined analysis of both the Table 7.3 and Table 7.4 helps for better understanding the effects of functionalization on Young's modulus and mechanical characterization on functionalized SWCNT/NR composites as whole.

Table 7.2 Work done in past by various researchers with different functionalised groups using different methods

Author	Year	Functional Group	Method Used
F.V. Ferreira et al	2017	-COOH, -DDA	X-ray spectroscopy, TEM
Sharma et al	2016	-COOH, -OH, $-COOCH_3$	Molecular Dynamics
Yang et al	2014	-COOH	Molecular Dynamics
Priyal et al	2014	-OH, -COOH, $-NH_2$	Molecular Mechanics
Milowska et al	2013	-OH, -COOH, $-NH_2$	DFT, MM in TINKER
Ling et al	2012	-OH, -COOH, $-NH_2$	Molecular Mechanics
Kuang et al	2009	$-C_2H_3$	Molecular Mechanics
Zhang et al	2008	-H	AFEM
Odegard et al	2005	-OH, $-COOCH_3$	Molecular Dynamics

Figure 7.10 shows the variation in the thermal conductivity of armchair (5,5) SWCNT/NR composite with different functional groups with volume fraction of 8%. The thermal conductivity of functionalized SWCNT/NR composite increases as the percentage of functional group increases. It has been observed that thermal conductivity of the functionalized SWCNT/NR composite of hydroxyl (-OH) group is more as compared to the thermal conductivity of the Ester ($-COOCH_3$) and carboxyl group (-COOH) group. However, as compared to the pristine SWCNT/NR composite the thermal conductivity of the functionalized SWCNT/NR composite reduces. The thermal conductivity of un-functionalized SWCNT/NR composite is 1.2 W/m/K but when the functionalised group is attached to SWCNT/NR composite, its value reduces to 0.26 W/m/K.

Table 7.3 Comparison of results obtained for functionalised armchair (5,5) SWCNT/NR composite with results obtained by other researchers with different matrix.

Authors →	**Sharma et al**	**Odegard et al**	**Yang et al**	**Priyal et al**		**Ling et al**	**Milowska et al**		**Kuang et al**		**Zhang et al**		**Our Work**		
%age →				5%	10%		6%	10%	8%	21%	10%	20%	5%	10%	15%
Group ↓															
-COOH	21%	11%	15%	10%	21%	15%	9%	14%					10 %	15%	20%
-OH	17%			10%	20%	16%	9%	14%					9%	20%	28%
$-COOCH_3$	9%	11%											7%	9%	10%
Others				10% $-NH_2$	20%	14%	9%	12%	16% $-C_2H_3$	31%	6% -H	12%			

Table 7.4 Variation in thermal conductivity with Percentage increase of functional groups

Thermal Conductivity (W/m/K)			
Percentage of groups	Ester group ($-COOCH_3$)	Carboxylic group (-COOH)	Hydroxyl group (-OH)
1%	0.14	0.20	0.21
5%	0.24	0.21	0.22
10%	0.24	0.23	0.26
20%	0.26	0.23	0.29

The decrease in percentage of thermal conductivity of functionalized SWCNT/NR composite as compared to the un–functionalized SWCNT/NR composite varies from 75% to 88%. The table 7.5 shows the decrease in percentage of the thermal conductivity of the functionalized SWCNT/NR composite.

Table 7.5 Percentage decrease in Thermal conductivity of functionalized SWCNT/NR matrix as compared to un-functionalized SWCNT/NR

Percentage of Functionalized groups attached	**Thermal Conductivity W/m/K**			**Percentage decrease in Thermal conductivity of functionalized SWCNT/NR matrix as compared to un-functionalized SWCNT/NR**		
	$-COOCH_3$	-COOH	-OH	$-COOCH_3$	-COOH	-OH
Un-functionalized	1.20	1.20	1.20	-	-	-
1%	0.14	0.2	0.21	88.33%	83.33%	82.50%
5%	0.24	0.21	0.22	80.00%	82.50%	81.67%
10%	0.24	0.23	0.26	80.00%	80.83%	78.33%
20%	0.26	0.23	0.29	78.33%	80.83%	75.83%

The reason for reduction in thermal conductivity is due to the generation of the defects on the walls of nanotubes during the oxidation procedure and increase the interfacial thermal resistance. The thermal conductivity increases with the increase in percentage of functionalized groups from 1-20. The value ranges from 0.2 to 0.29 W/m/K, but as compared to the un-functionalized SWCNT/NR composite, the thermal conductivity decreases up to 88%.

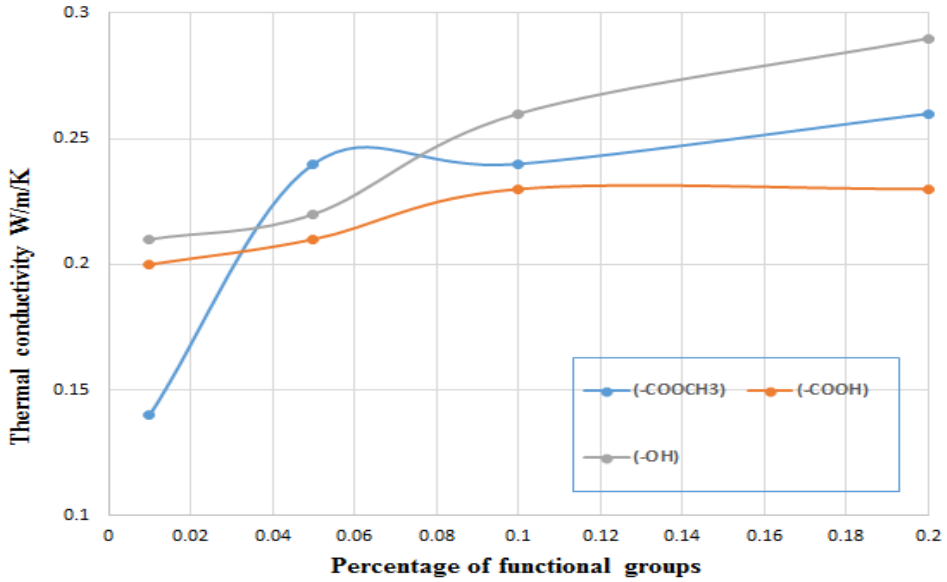

Figure 7.10 Comparison of thermal conductivity for armchair (5,5) SWCNT/NR composite with different functional groups

Figure 7.11 shows the comparison between the results obtained by Molecular Dynamics simulation for armchair (5,5) functionalized SWCNT/NR composite with different groups of functionalization for thermal conductivity with the series and parallel models of thermal conductivity.

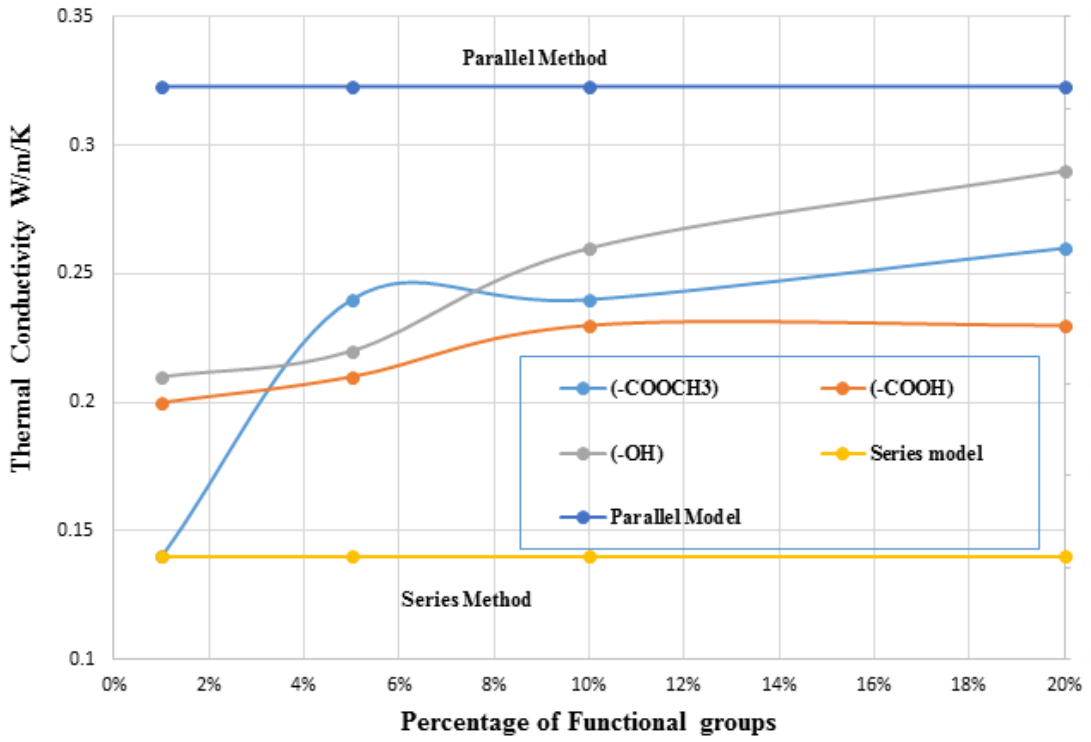

Figure 7.11 Comparison of the results of MD for armchair (5,5) functionalized SWCNT/NR composite with V_f = 8 % for thermal conductivity with the series and parallel models

The thermal conductivity values calculated using the Molecular Dynamics simulation with number of defects lies in between the series model, which gives lower bound values, and the parallel model, which gives the upper bound values. The thermal conductivity value, which has been calculated by using the series model, was 0.14 and the thermal conductivity value, which has been calculated by using the parallel model, was 3.12. The values obtained shown in Table 7.6 for thermal conductivity of functionalized SWCNT/NR composite by MD simulation was in the range of 0.14 to 0.26 W/m/k with Ester group ($-COOCH_3$) attached to the armchair (5,5) single walled carbon nanotube reinforced Natural rubber composite with V_f = 8% is 1-20.

Table 7.6 Comparison of the results of MD for armchair (5,5) functionalized SWCNT/NR composite with V_f = 8 % for thermal conductivity with the series and parallel models

Percentage of Functional groups	**Comparison of the results of MD for armchair (5,5) functionalized SWCNT/NR composite with V_f = 8 % for thermal conductivity with the series and parallel models**				
	$-COOCH_3$	-COOH	-OH	Series Model (Lower bound)	Parallel Model (Upper Bound)
1	0.14	0.2	0.21	0.141	3.12
5	0.24	0.21	0.22		
10	0.24	0.23	0.26		
20	0.26	0.23	0.29		

The values of the thermal conductivity depend upon the chirality because heat transfer depends purely on the band gaps present in the CNTs. The thermal conductivity of functionalized SWCNT/NR composite by MD simulation was in the range of 0.20 to 0.23 W/m/k with Carboxyl group (-COOH) attached to the armchair (5,5) single walled carbon nanotube reinforced Natural rubber composite with V_f = 8% is 1-20. The thermal conductivity of functionalized SWCNT/NR composite by MD simulation was in the range of 0.21 to 0.29 W/m/k with Hydroxyl group (-OH) attached to the armchair (5,5) single walled carbon nanotube reinforced Natural rubber composite with V_f = 8% is 1-20. In case of a series and parallel models, a perfect interface is assumed when two phases are in contact and each phase independently contribute to thermal resistant and conductance. The interactions between the filler are neglecting, due to this series model gives underestimation of composites and predicts the lower bound of the thermal conductivity of composites. However, in case of a parallel series the upper bound of the reinforced composites predicts due to the overestimation of the thermal conductivity of composites because of assumption of perfectly contact between the particles. Therefore, the results obtained with Molecular Dynamics simulation for thermal conductivity of the single walled carbon nanotube reinforced Natural rubber composite lies between the upper bound and the lower bound of the composites.

Chapter 8

Effect of Volume Fraction, Aspect Ratio, Defects and Functionalization on the Damping Characteristics of CNT Reinforced Polymer Composites

8.1 Introduction

Carbon Nanotubes are thin, as well as long hollow cylinders of carbon. It was the year 1991 when CNTs were discovered by Iijima [2]. As of late, greater fervor has been started for their comprehension and a lot of study has been performed. Right now, the physical properties are yet being found and debated. An expansive scope of warm, basic and electronic properties has been appeared by the CNT. Broad ranges of thermal, structural and electronic properties have been shown by the CNT. Despite the different types of theoretical studies conducted on the macroscopic elastic behavior of CNTs, there remain the controversial issues regarding damping characteristics. Very less effort has been put by the researchers in finding the damping of the single walled carbon nanotubes reinforced polymer composites. Many of the researchers have worked in finding the damping characteristics of the CNTs by using the experimental studies. Buldum and lu in 1999 [135] studied the stick slip motion of nanotubes and investigated the orientational locking based on the potential energy calculation. The author also found the interfacial sliding and rolling characteristics of the carbon nanotubes. Zhou *et al.* in 2004 [124] observed that there is a significant change increase in damping ratio with the addition of 1% SWCNT in the polymeric composites. The author also proposed a micromechanical model based on stick-slip frictional motion between the nanotubes and resin. Suhr et al in 2004 [136] observed an increase in mechanical damping due to the energy dissipation at the CNT-polymer interface caused by interfacial sliding and the energy dissipation cue to the stick-slip sliding between CNT-CNT interfaces.

Based on the experimental data of the previous studies the damping characteristics of the polymer composites enhanced a lot by the addition of the small amount of the CNTs. Very less theoretical studies has been explored for finding the damping properties of single wall carbon nanotubes reinforced polymer. Therefore, based on previous literature our goal is to find the damping characteristics of

SWCNT/NR composite. None of the previous research shows the damping properties of the SWCNT/NR composites. This is the first time to explore the damping properties of the SWCNT/NR using the Molecular Dynamics simulations. In this study for finding, the damping properties of the SWCNT/NR composites using the approach based on the dissipated energy. The energy stored in the material during the cyclic loading and during un-loading some of the energy is recovered has been observed. The energy dissipated has been calculated by finding the area between the loading and unloading cycle. The calculated dissipated energy is divided by the area under the cures shown in figure 8.1 gives us the loss factor.

8.2 Damping of Single Walled Carbon Nanotubes (SWCNT)

Now days the understanding of vibration in structure is more important because due to the transient or dynamic loading the structure experience a vibration which causes a noise, wear and unsafe conditions to the operator. Therefore, to eliminate the vibrations from the structure understating of the vibration is necessary. High damping capacity materials are required to remove the vibrations. Damping capacity means the ability of the material to dissipate energy during vibration. Damping capacity can be improved by the addition of the CNTs to the material even in small amount. In this study, for finding the damping properties of the single walled carbon nanotubes reinforced with Natural rubber composites Molecular Dynamics simulation has been performed by using the software Material Studio 2017. In this process of MD simulation for calculating the mechanical properties of the single walled carbo nanotubes reinforced Natural rubber by using the `Forcite calculation` and the "constant strain approach" method. Before starting the process of calculating the mechanical properties, the optimization of the structure is necessary for minimizing the energy and the strain is applied in each configuration to obtain a strained structure. After the completion of the mechanical properties, the dissipated energy can be obtained. For measuring the damping loss factor (η_{11}), dissipated energy obtained after calculation divided by the energy obtained before the unloading. In Material Studio 2017 software, after the completion of the mechanical properties two energy frames developed. The energy obtained during the loading cycle comes under the first energy frame whereas

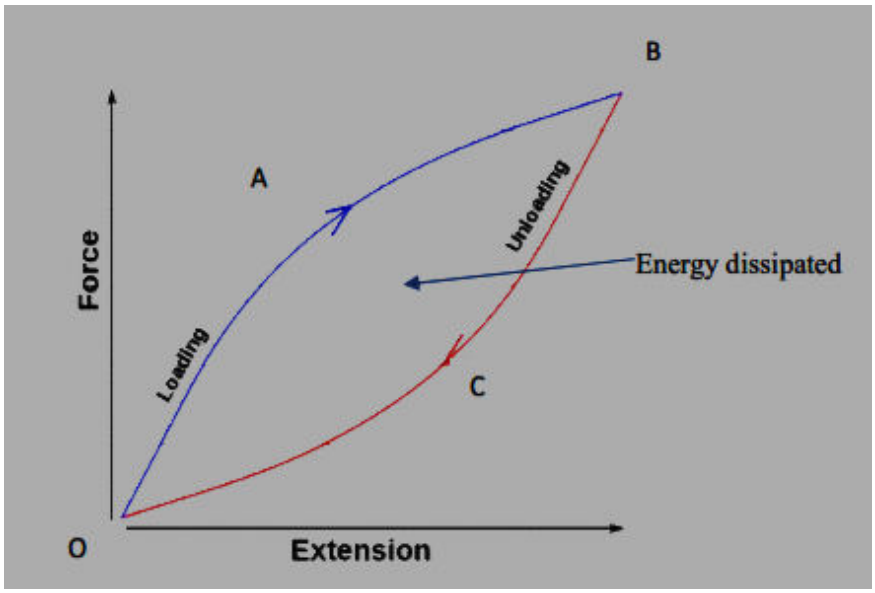

Figure 8.1 Energy dissipation during loading and unloading cycle

the energy during unloading comes under the last energy frame. The difference between the energies obtained in first frame and last frame gives the dissipated energy. Then after the dissipate energy obtained must be divided by the energy obtained during loading gives us the damping loss factor (η_{11}). The dissipation of the energy is depends upon the two mechanism which could lead to the damping in the SWCNT/NR composite at molecular level.

i. Due to the interfacial sliding at nanotubes and Natural rubber interface, cause energy dissipated.
ii. Due to interfacial stick-slip phenomena at CNT-CNT interface, causes energy dissipated.

The elongation starts in composite after tensile stress is applied to the SWCNT/NR composite. Due to this, shear stress is applied on the CNTs developed by the matrix and transferring the load to the CNTs. Whenever stress is applied, the strain is appearing in the CNTs. When the applied stress is small, then the matrix and the CNTs doesn't debonds and move together due to sticking phenomena and when the applied stress is increased the deboning of the CNT and matrix stars. The constant strain applied on the CNT is constant. When the strain is increased further in the SWCNT/NR composites then no load is transfer between carbon nanotube and matrix, due to the occurrence of slippage between them energy dissipated starts.

8.3 Results and Discussions

Figure 8.2 shows the variation of damping loss factor (η_{11}) with the increase in volume fraction of different single walled carbon nanotubes reinforced Natural rubber composite. It has been observed that with the increase in volume fraction of the SWCNT/Nr composite the loss factor (η_{11}) decreases. The loss factor (η_{11}) having inversely relation with the young`s modulus ($E_{11}$). As discussed in the previous section the young`s modulus of the different SWCNT/NR composites increases with the increase in volume fraction therefore the loss factor (η_{11}) decreases with the increase of volume fraction from 1-20%. It has been observed that up to 10% of the volume fraction the loss factor (η_{11}) decreases sharply but after the 10% of volume fraction the loss factor (η_{11}) reduces steadily. This is because of the stick-slip phenomena and due to slippery and curvy nature of single walled carbon nanotube reinforced Natural rubber composite, which does not help to reduce the damping properties further. The damping loss factor (η_{11}) ratio is higher for all the configurations of SWCNT/NR composites up to the 10% of volume fraction and then after the percentage of damping ratio is less.

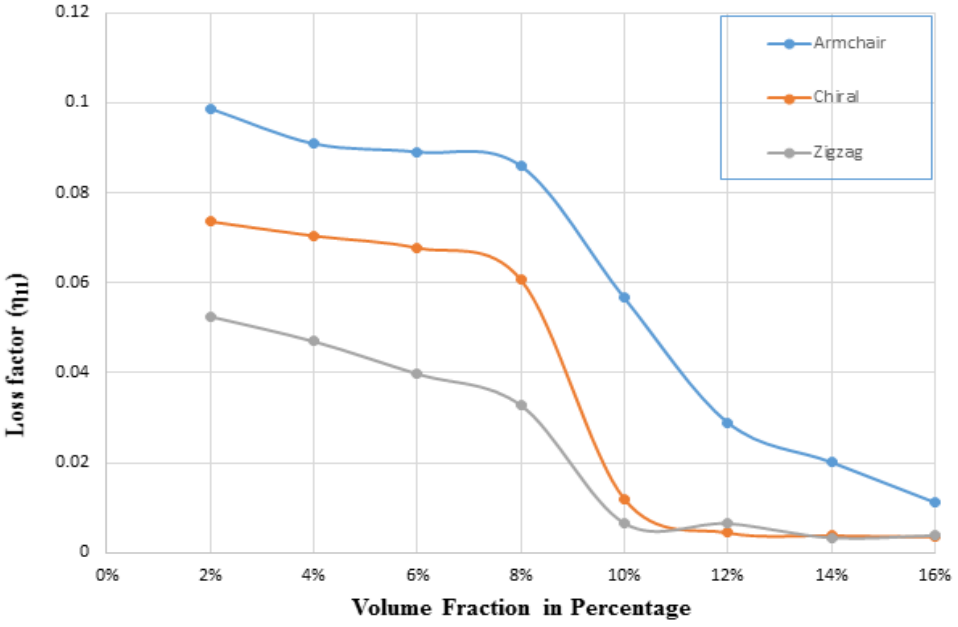

Figure 8.2 Variation in damping loss factor (η_{11}) for different configuration of SWCNT/NR composite with volume fraction for fixed aspect ratio

Figure 8.3 shows, the variation of damping loss factor (η_{11}) with different aspect ratio (l/d) of different configurations of single walled carbon nanotubes reinforced composites. It has been observed that the loss factor (η_{11}) decreases with the increase in aspect ratio. The reasons for decrease in loss factor (η_{11}) is due to the inverse relationship between the young`s modulus ($E_{11}$). The young`s modulus for the

SWCNT/NR composites increases with the increase in aspect ratio as already discussed in the previous chapters. In the armchair SWCNT/NR composite the loss factor (η_{11}) decrease and ranges from 4.18% to 1.63%. In case of the chiral SWCNT/NR composite the loss factor (η_{11}) also decrease and ranges between 2.99% to 0.94% where as in case of zigzag SWCNT/NR composite the loss factor (η_{11}) decrease and ranges from 0.86% to 0.59%.

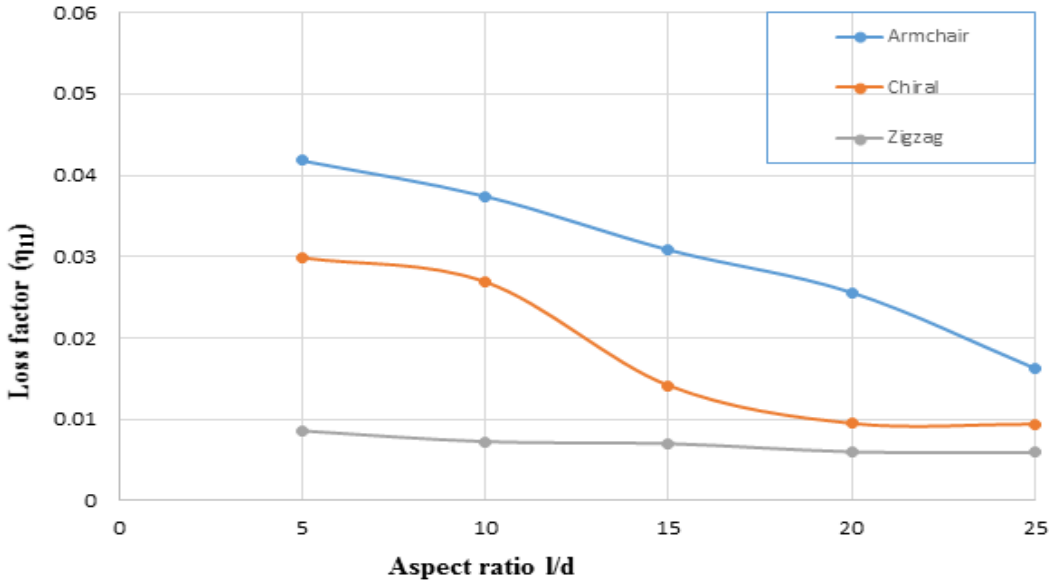

Figure 8.3 Variation in damping loss factor (η_{11}) for different configuration of SWCNT/NR composite with aspect ratio for fixed volume fraction

Figure 8.4 shows the variation in damping loss factor (η_{11}) with the increase in number of the Stone-Wales and vacancy defects in the armchair (5,5) single walled carbon nanotubes reinforced Natural rubber composite. The damping loss factor (η_{11}) for the SW defective armchair SWCNT/NR composite increases with the increase in number of defects increases from 1-10. The increase in percentage of the damping loss factor (η_{11}) is 4.18% to 7.51% whereas in case of the vacancy defects the damping loss factor (η_{11}) also decreases and the percentage increase is 4.6% to 8.18%. Therefore, the vacancy defects dissipate more energy as compared to Stone wales defects due to the stick slip phenomena and the damping loss factor (η_{11}) is inversely proportional to the young`s modulus (E_{11}).

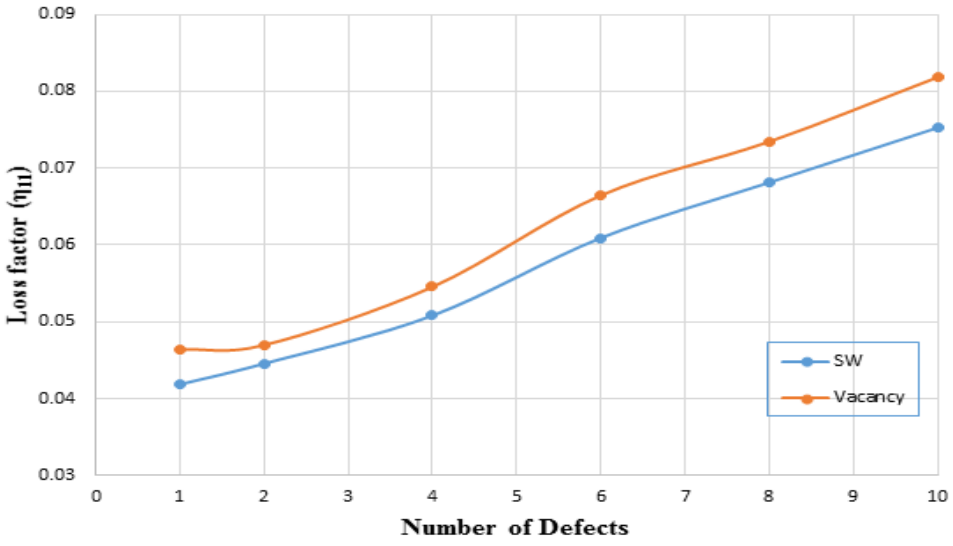

Figure 8.4 Variation in damping loss factor (η_{11}) for Defective armchair (5,5) SWCNT/NR composite with number of defects

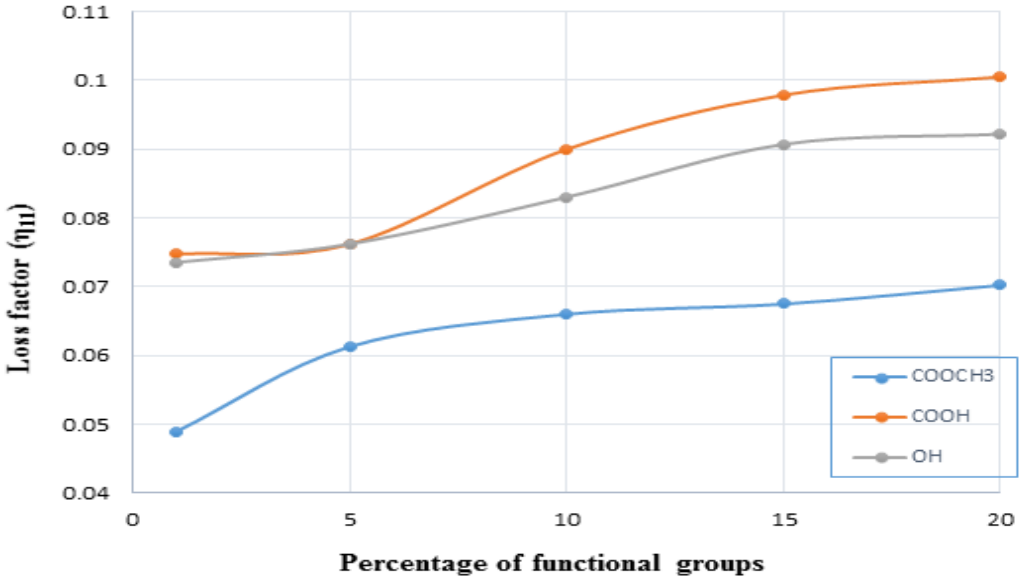

Figure 8.5 Variation in damping loss factor (η_{11}) for different functional groups attached to armchair (5,5) SWCNT/NR composite number of functional groups

Figure 8.5 shows the variation in loss factor (η_{11}) with increase in percentage of different functional group attached to the armchair (5,5) single walled carbon nanotube reinforced Natural rubber composite with the fixed volume fraction of 0.08%. The damping loss factor (η_{11}) is more when carboxyl group is attached to the SWCNT/NR composite as compared to the ester and hydroxyl group attached to SWCNT/NR composite. So according to the inverse relation between loss factor (η_{11}) and young`s modulus, as the young`s modulus decreases with the increase in functional groups attached gives us the decrease in damping loss factor (η_{11}).

Chapter 9

Executive Summary and Future Scope

CNTs play an important role in enhancing the properties of the elastomers, polymers, fibers nanocomposites materials. CNTs based composites have the potential to provide extremely tough and ultra-light new material. From last few years, academic researcher, as well as industrial researcher, worked hard to understand the improvement in the properties of the new materials. Fabrication of the CNT composite is still challenging and expensive process. For predicting the nanocomposite reinforced polymer properties is limited in the micromechanical approach. In micromechanical, approach the molecular interaction between the CNTs and polymer matrix as well as between polymer-polymer itself not taken into the considerations. Analytical models are difficult to construct at the nanoscale and complicated to conduct an experiment. Therefore, to overcome this difficulty, modelling and computer simulations could be done by using a software on a desktop computer. For finding the properties of the single walled carbon nanotube reinforced polymer based on volume fraction, aspect ratio, number of the functional groups attached and defects present in the CNT-polymer, strong computational tools are required. For achieving the characterization and mechanical properties of the CNT-based composites at the critical controlled parameter of the SWCNT/NR composites a Molecular Dynamics simulations have been performed using Material Studio 2017.

Molecular Dynamics simulation is a strong tool for predicting the properties and analyse the characterization of the carbon nanotube composites. The MD methods concept is very straightforward and logical. Newton's equation of motion is used for governing the motion of molecules. This method is based on computer simulation for microscopic analysis MD simulation were based on Newton's equations of motion in which the molecular interaction plays an important part for solving the polymer-polymer and polymer-nanocomposites interacting system.

In this study, the interfacial property of the single walled carbon nanotube reinforced Natural rubber composite has been evaluated using the MD simulation. An effort has been made to predict the mechanical properties, loss factor and thermal

conductivity for the different configurations of the SWCNT/NR composite. The following systems have been used to evaluate their properties using MD simulations.

(i) SWCNT/NR composite with varying diameter, length and volume fraction.

(ii) SWCNT/NR composite consists of different defects.

(iii) SWCNT/NR composite attached with different functional groups.

The following are the major findings of this study:-

1. In regard to study the effect of chirality, nanotube length and diameter on the interfacial properties of CNT reinforced polymer (NR) composites a series of SWCNT pull out simulations from the NR matrix were performed using the MD simulation. The effect of CNT length and diameter on energy increment (ΔE) was studied. ISS and surface energy density (γ) are the main outputs of this study. It was concluded that the incremental energy increased sharply to a peak value at a specified displacement in the first stage and then in the stage second there the increment energy remains steady between specified peak values. The average energy increment in the second stage ($\Delta E11_)$ was independent of the nanotube length. ΔE_{11} and the pullout energy $\Sigma\Delta E$ increased linearly with an increase in the nanotube diameter (D). ISS and surface energy density (γ) decreased with an increasing SWCNT diameter and converged at some value. The ISS and surface energy density converged at 113.5 MPa and 0.1 N/m.
2. In regard to the dynamic properties of the single walled carbon nanotube reinforced Natural rubber composite of different configurations. It was concluded that the Young's modulus (E_{11}) of armchair (5,5) SWCNT/NR composite is increased from 24.1 GPa to 84.03 GPa as the aspect ratio (l/d) increased from 0-25.The transverse modulus (E_{22}) of armchair (5,5) SWCNT/NR composite is increased from 6.33 GPA to 7.14 GPa. Similarly, the E_{11} and E_{22} of chiral and zigzag SWCNT/NR composite have been evaluated. The E_{11} of chiral SWCNT/NR composite is increased from 22.69 GPa to 44.9 GPa and for zigzag SWCNT/NR composite is increased from 22.07 GPa to 53.94 GPa as the aspect ratio increased from 0-25. The E_{22} of chiral and zigzag SWCNT/NR composite is decreased from 6.68 GPa to 3.093 GPa and 8.13 GPa to 05.96 GPa respectively as the aspect ratio increased from 0-25. The major reason for having higher E_{11} of the armchair is due to the geometrical orientation of C-C bond relative to the nanotube axis. The shear modulus for the different configuration of SWCNT/NR is decreased as the aspect ratio increased. Therefore, the armchair is preferred

over the zigzag and chiral SWCNT/NR composite. The effect of volume fraction has been calculated for different configurations of SWCNT/NR composite. The E_{11} increases with the increase in volume fraction. The E_{11} for armchair SWCNT/NR increases from 6.76 GPa to 64.41 GPa whereas E_{11} for the chiral and zigzag SWCNT/NR composite increases from 11.84 GPa to 41.91 GPa and 10.40 GPa to 48.73 GPa respectively as the volume fraction increase from 02% to 16%. The value of E_{11} is increasing sharply up to 8% of volume fraction then the rise is minimal due to the slippery nature of the CNTs.

3. In regard to study the effect of the defective SWCNT/NR composite on the thermo mechanical properties of SWCNT/NR composite. The defects taken into the consideration was SW and vacancy defects, it was concluded that with the increase in the number of defects for armchair (5,5) SWCNT/NR composite the Young's modulus (E_{11}) decreases rapidly in case of SW defects as compared to vacancy defects. The E_{11} in SW defective SWCNT/NR composite is decreases more up to 36.85% as compared to 31.43% of vacancy defects. The E_{22} in SW defective SWCNT/NR composite is also decreases up to 68.39% whereas E_{22} for the vacancy defects decreases up to 31.43%. The shear modulus and bulk modulus is also reduced up to 18.25% and 14% in case of SW defective SWCNT/NR composite where as in case of vacancy defect it is reduced up to 14% and 11% respectively. The thermal conductivity of the armchair SWCNT/NR composite with defects as compared to pristine has been evaluated. The percentage decrease in thermal conductivity of SW defective single walled carbon nanotube reinforced with Natural rubber composite as compared to pristine ranges from 19.30% to 34.50% with the number of defects increases from 1-10. In case of vacancy defective single walled carbon nanotube reinforced Natural rubber composite the percentage decrease in thermal conductivity in comparison to pristine ranges from 12.37% to 39.57% with the number of defects increases from 1-10.
4. While studying the effect of functionalization on the armchair (5,5) SWCNT/NR composite and the thermal conductivity of the functionalized SWCNT/NR composite, it was concluded that the young`s modulus E_{11} of the armchair (5,5) SWCNT/NR with different functional groups have been evaluated. The E_{11} has been reduced to 25% when the hydroxyl group (-OH) is attached with single walled carbon nanotube reinforced Natural rubber composite. The E_{11} for the ester group (-$COOCH_3$) and the carboxyl group (-COOH) is also reduced by 7% and

16% respectively. It was also concluded that the thermal conductivity reduced with the addition of the functional groups. The thermal conductivity of the (-OH) group is reduced less in comparison to the (-COOH) and (-$COOCH_3$) groups as compared to the un-functionalized SWCNT/NR composite. The reduction in –OH group is 82.50% to 75.83% , in –COOH group reduction ranges from 83.33% to 80.83 % and in $COOCH_3$ the reduction in thermal conductivity ranges from 88.33 % to 78.33% as the number of functionalized groups is increased.

5. For evaluating the damping loss factor (η_{11}) of the different single walled carbon nanotubes reinforced Natural rubber, the author concluded that η_{11} decreases with the increase in aspect ratio. In the case of armchair SWCNT/NR composite, the η_{11} decreases up to 1.63% whereas in case of chiral and zigzag the η_{11} decreases more, up to 0.94% and 0.59%. The decrease in η_{11} is due to the stick-slip phenomena.

Future scope

In the field of single walled carbon nanotube reinforced polymer composite wide spreading work has been done using the micromechanical approach. MD simulation of SWCNT/NR composite is a new field. Using Natural rubber as a matrix in this study is the novel approach of modeling of the CNTs. This study can be further extended to-

(i) Effect of increase in temperature on the mechanical and thermal properties of the SWCNT/NR composites is yet to be explored.

(ii) MWCNT/NR can be simulated by MD for analysis of effects of defects on elastic moduli of the carbon nanotube.

(iii) By using Molecular Dynamics, the optical properties can also be evaluated. In addition, the new technique Density functional theory (DFT) can also be used for evaluating the mechanical properties.

(iv) Study the effect of the thermal on the interfacial shear stress and damping loss factor of SWCNT/composites.

(v) Study the effect of the functionalization on the interfacial properties of the SWCNT/Polymer composites.

(vi) The experimental work can be performed to substantiate the results of the MD simulation.

Bibliography

[1] B. K. Kaushik and M. K. Majumder, "Carbon nanotube: Properties and applications," in *Carbon Nanotube Based VLSI Interconnects*: Springer, 2015, pp. 17-37.

[2] S. Iijima, "Helical microtubules of graphitic carbon," *Nature,* vol. 354, no. 6348, p. 56, 1991.

[3] N. Hamada, S. Sawada, and A. Oshiyama, "New one-dimensional conductors: Graphitic microtubules," *Phys Rev Lett,* vol. 68, no. 10, pp. 1579-1581, Mar 9 1992.

[4] R. Saito, M. Fujita, G. Dresselhaus, and u. M. Dresselhaus, "Electronic structure of chiral graphene tubules," *Appl Phys Lett,* vol. 60, no. 18, pp. 2204-2206, 1992.

[5] J. Seitz, "The estimation of mechanical properties of polymers from molecular structure," *J Appl Polym Sci,* vol. 49, no. 8, pp. 1331-1351, 1993.

[6] K. Tanaka *et al.*, "Electronic properties of carbon nanotube," *Chem Phys Lett,* vol. 223, no. 1-2, pp. 65-68, 1994.

[7] T. Ebbesen and T. Takada, "Topological and sp3 defect structures in nanotubes," *Carbon,* vol. 33, no. 7, pp. 973-978, 1995.

[8] J. Mintmire and C. White, "Electronic and structural properties of carbon nanotubes," *Carbon,* vol. 33, no. 7, pp. 893-902, 1995.

[9] C. Cornwell and L. Wille, "Elastic properties of single-walled carbon nanotubes in compression," *Solid State Commun,* vol. 101, no. 8, pp. 555-558, 1997.

[10] A. Krishnan, E. Dujardin, T. Ebbesen, P. Yianilos, and M. Treacy, "Young's modulus of single-walled nanotubes," *Phys Rev B,* vol. 58, no. 20, p. 14013, 1998.

[11] E. Mickelson *et al.*, "Solvation of fluorinated single-wall carbon nanotubes in alcohol solvents," *J Phys Chem B,* vol. 103, no. 21, pp. 4318-4322, 1999.

[12] E. Hernandez, C. Goze, P. Bernier, and A. Rubio, "Elastic properties of single-wall nanotubes," *J Appl Phys,* vol. 68, no. 3, pp. 287-292, 1999.

[13] M. B. Nardelli, J.-L. Fattebert, D. Orlikowski, C. Roland, Q. Zhao, and J. Bernholc, "Mechanical properties, defects and electronic behavior of carbon nanotubes," *Carbon,* vol. 38, no. 11-12, pp. 1703-1711, 2000.

[14] Z. Yao, C.-C. Zhu, M. Cheng, and J. Liu, "Mechanical properties of carbon nanotube by molecular dynamics simulation," *Comput Mater Sci,* vol. 22, no. 3-4, pp. 180-184, 2001.

[15] S. Frankland, A. Caglar, D. Brenner, and M. Griebel, "Molecular simulation of the influence of chemical cross-links on the shear strength of carbon nanotube–polymer interfaces," *J Phys Chem B,* vol. 106, no. 12, pp. 3046-3048, 2002.

[16] Y. P. Sun, K. Fu, Y. Lin, and W. Huang, "Functionalized carbon nanotubes: properties and applications," *Acc Chem Res,* vol. 35, no. 12, pp. 1096-104, Dec 2002.

[17] H. Peng, L. B. Alemany, J. L. Margrave, and V. N. Khabashesku, "Sidewall carboxylic acid functionalization of single-walled carbon nanotubes," *J Am Chem Soc,* vol. 125, no. 49, pp. 15174-82, Dec 10 2003.

[18] C. Li and T.-W. Chou, "Elastic moduli of multi-walled carbon nanotubes and the effect of van der Waals forces," *Compos Sci Technol,* vol. 63, no. 11, pp. 1517-1524, 2003.

[19] B. Kim and W. M. Sigmund, "Functionalized multiwall carbon nanotube/gold nanoparticle composites," *Langmuir,* vol. 20, no. 19, pp. 8239-42, Sep 14 2004.

[20] H. Jiang, X.-Q. Feng, Y. Huang, K. Hwang, and P. Wu, "Defect nucleation in carbon nanotubes under tension and torsion: Stone–Wales transformation," *Comput Method Appl M,* vol. 193, no. 30-32, pp. 3419-3429, 2004.

[21] M. Paiva, B. Zhou, K. Fernando, Y. Lin, J. Kennedy, and Y.-P. Sun, "Mechanical and morphological characterization of polymer–carbon nanocomposites from functionalized carbon nanotubes," *Carbon,* vol. 42, no. 14, pp. 2849-2854, 2004.

[22] N. O. V. Plank and R. Cheung, "Functionalisation of carbon nanotubes for molecular electronics," *Microelectron Eng,* vol. 73, pp. 578-582, 2004.

[23] N. Chandra, S. Namilae, and C. Shet, "Local elastic properties of carbon nanotubes in the presence of Stone-Wales defects," *Phys Rev B,* vol. 69, no. 9, p. 094101, 2004.

[24] Q. Lu and B. Bhattacharya, "Effect of randomly occurring Stone–Wales defects on mechanical properties of carbon nanotubes using atomistic simulation," *Nanotechnology,* vol. 16, no. 4, p. 555, 2005.

[25] S. L. Mielke *et al.*, "The role of vacancy defects and holes in the fracture of carbon nanotubes," *Chem Phys Lett,* vol. 390, no. 4-6, pp. 413-420, 2004.

[26] Y.-R. Jeng, P.-C. Tsai, and T.-H. Fang, "Effects of temperature and vacancy defects on tensile deformation of single-walled carbon nanotubes," *J Phys Chem Solids,* vol. 65, no. 11, pp. 1849-1856, 2004.

[27] L. Liu, A. H. Barber, S. Nuriel, and H. D. Wagner, "Mechanical properties of functionalized single-walled carbon-nanotube/poly (vinyl alcohol) nanocomposites," *Adv Funct Mater,* vol. 15, no. 6, pp. 975-980, 2005.

[28] T. Ramanathan, F. Fisher, R. Ruoff, and L. Brinson, "Amino-functionalized carbon nanotubes for binding to polymers and biological systems," *Chem Mater,* vol. 17, no. 6, pp. 1290-1295, 2005.

[29] S. Zhang *et al.*, "Mechanics of defects in carbon nanotubes: atomistic and multiscale simulations," *Phys Rev B,* vol. 71, no. 11, p. 115403, 2005.

[30] Y. Wang, X.-x. Wang, X.-g. Ni, and H.-a. Wu, "Simulation of the elastic response and the buckling modes of single-walled carbon nanotubes," *Comput Mater Sci,* vol. 32, no. 2, pp. 141-146, 2005.

[31] A. Bródka, J. Kołoczek, A. Burian, J. C. Dore, A. C. Hannon, and A. Fonseca, "Molecular dynamics simulation of carbon nanotube structure," *J Mol Struct,* vol. 792, pp. 78-81, 2006.

[32] H. Fan, K. Zhang, and M. M. Yuen, "Effect of defects on thermal performance of carbon nanotube investigated by molecular dynamics simulation," in *Electronic Materials and Packaging, 2006. EMAP 2006. International Conference on*, 2006, pp. 1-4: IEEE.

[33] J. Liu *et al.*, "Sidewall functionalization of single-wall carbon nanotubes (SWNTs) through aryl free radical addition," *Chem Phys Lett,* vol. 430, no. 1-3, pp. 93-96, 2006.

[34] R. Jain, U. K. Vaidya, and A. Haque, "Processing and characterization of carbon-carbon nanofiber composites," *Adv Compos Mater,* vol. 15, no. 2, pp. 211-241, 2006.

[35] Q. Wang, W. Duan, N. Richards, and K. Liew, "Modeling of fracture of carbon nanotubes with vacancy defect," *Phys Rev B,* vol. 75, no. 20, p. 201405, 2007.

[36] W. Hou and S. Xiao, "Mechanical behaviors of carbon nanotubes with randomly located vacancy defects," *J Nanosci Nanotechnol,* vol. 7, no. 12, pp. 4478-85, Dec 2007.

[37] K. Tserpes and P. Papanikos, "The effect of Stone–Wales defect on the tensile behavior and fracture of single-walled carbon nanotubes," *Compos Struct,* vol. 79, no. 4, pp. 581-589, 2007.

[38] R. W. Haskins *et al.*, "Tight-binding molecular dynamics study of the role of defects on carbon nanotube moduli and failure," *J Chem Phys,* vol. 127, no. 7, p. 074708, Aug 21 2007.

[39] A. Al-Ostaz, G. Pal, P. R. Mantena, and A. Cheng, "Molecular dynamics simulation of SWCNT–polymer nanocomposite and its constituents," *J Mater Sci,* vol. 43, no. 1, pp. 164-173, 2008.

[40] X. Hao, H. Qiang, and Y. Xiaohu, "Buckling of defective single-walled and double-walled carbon nanotubes under axial compression by molecular dynamics simulation," *Compos Sci Technol,* vol. 68, no. 7-8, pp. 1809-1814, 2008.

[41] J. Yuan and K. M. Liew, "Effects of vacancy defect reconstruction on the elastic properties of carbon nanotubes," *Carbon,* vol. 47, no. 6, pp. 1526-1533, 2009.

[42] P. Singh, S. Campidelli, S. Giordani, D. Bonifazi, A. Bianco, and M. Prato, "Organic functionalisation and characterisation of single-walled carbon nanotubes," *Chem Soc Rev,* vol. 38, no. 8, pp. 2214-30, Aug 2009.

[43] S. Nisar Hossain Rubaiyat, "Study of carbon nanotubes with defects under tensile and compressive loads using molecular dynamics simulation," *PhD diss,* 2009.

[44] M. ARJMAND, A. SHOKUHFAR, and M. A. SARABI, "Effect of unit cell length on young's modulus of zigzag single walled carbon nanotubes," *Olomouc Czech Repub Eur,* 2010.

[45] R. Menzel, M. Q. Tran, A. Menner, C. W. Kay, A. Bismarck, and M. S. Shaffer, "A versatile, solvent-free methodology for the functionalisation of carbon nanotubes," *Chem Sci,* vol. 1, no. 5, pp. 603-608, 2010.

[46] S. C. Chowdhury, T. Okabe, and M. Nishikawa, "Effects of vacancy defects on the interfacial shear strength of carbon nanotube reinforced polymer composite," *J Nanosci Nanotechnol,* vol. 10, no. 2, pp. 739-45, Feb 2010.

[47] S. C. Chowdhury and S. N. H. Rubaiyat, "Investigation of Mechanical Behavior of Defective Carbon Nanotubes Using Molecular Dynamics Simulation," *JEST,* vol. 8, no. 1, pp. 20-24, 2010.

[48] T. Dinadayalane, J. S. Murray, M. C. Concha, P. Politzer, and J. Leszczynski, "Reactivities of sites on (5, 5) single-walled carbon nanotubes with and without a Stone-Wales defect," *J Chem Theory Comput,* vol. 6, no. 4, pp. 1351-1357, 2010.

[49] M. Davoudabadi and S. Farahani, "Investigation of Vacancy Defects on the Young's Modulus of Carbon Nanotube Reinforced Composites in Axial Direction via a Multiscale Modeling Approach," *J Solid,* vol. 2, no. 3, pp. 248-256, 2010 2010.

[50] V. Parvaneh and M. Shariati, "Effect of defects and loading on prediction of Young's modulus of SWCNTs," *Acta Mech* vol. 216, no. 1-4, pp. 281-289, 2011.

[51] A. Liu, K. Wang, and C. E. Bakis, "Effect of functionalization of single-wall carbon nanotubes (SWNTs) on the damping characteristics of SWNT-based epoxy composites via multiscale analysis," *Compos Part A Appl Sci Manuf,* vol. 42, no. 11, pp. 1748-1755, 2011.

[52] L. Deng, S. J. Eichhorn, C.-C. Kao, and R. J. Young, "The effective Young's modulus of carbon nanotubes in composites," *ACS Appl Mater Interfaces,* vol. 3, no. 2, pp. 433-440, 2011.

[53] K. Talukdar and A. K. Mitra, "Molecular dynamics simulation study on the mechanical properties and fracture behavior of single-wall carbon nanotubes," in *Carbon Nanotubes-Synthesis, Characterization, Applications*: InTech, 2011.

[54] H. Zeng, J. Zhao, J. Wei, and H. Hu, "Effect of N doping and Stone-Wales defects on the electronic properties of graphene nanoribbons," *Eur Phys J B,* vol. 79, no. 3, pp. 335-340, 2011.

[55] H. Chen *et al.*, "Functionalization of single-walled carbon nanotubes enables efficient intracellular delivery of siRNA targeting MDM2 to inhibit breast cancer cells growth," *Biomed Pharmacother,* vol. 66, no. 5, pp. 334-8, Jul 2012.

[56] M. Yuan, Y. Yang, and Z. Xia, "Modeling of push-out test for interfacial fracture toughness of fiber-reinforced composites," *Adv Compos Mater,* vol. 21, no. 5-6, pp. 401-412, 2012.

[57] J. Wernik, B. Cornwell-Mott, and S. Meguid, "Determination of the interfacial properties of carbon nanotube reinforced polymer composites using atomistic-based continuum model," *Int J Solids Struct,* vol. 49, no. 13, pp. 1852-1863, 2012.

[58] K. Sharma, K. K. Saxena, and M. Shukla, "Effect of multiple Stone-Wales and Vacancy defects on the mechanical behavior of carbon nanotubes using Molecular Dynamics," *Procedia Eng,* vol. 38, pp. 3373-3380, 2012.

[59] K. K. Saxena and A. Lal, "Comparative Molecular Dynamics simulation study of mechanical properties of carbon nanotubes with number of stone-wales and vacancy defects," *Procedia Eng,* vol. 38, pp. 2347-2355, 2012.

[60] K. Talukdar and A. Mitra, "Molecular dynamics simulation of elastic properties and fracture behavior of single wall carbon nanotubes with vacancy and Stone–Wales defect," *Adv Compos Mater,* vol. 20, no. 1, pp. 29-38, 2011.

[61] S. Yang, S. Yu, and M. Cho, "Influence of Thrower–Stone–Wales defects on the interfacial properties of carbon nanotube/polypropylene composites by a molecular dynamics approach," *Carbon,* vol. 55, pp. 133-143, 2013.

[62] J. J. Yeo, Z. Liu, and T. Y. Ng, "Comparing the effects of dispersed Stone–Thrower–Wales defects and double vacancies on the thermal conductivity of graphene nanoribbons," *Nanotechnology,* vol. 23, no. 38, p. 385702, 2012.

[63] S. Sharma, R. Chandra, P. Kumar, and N. Kumar, "MOLECULAR DYNAMICS SIMULATION OF CARBON NANOTUBES," *J Nanosci Nanotechnol,* vol. 4, no. 1, 2013.

[64] F. Dai-Li, F. Yan-Hui, C. Yang, L. Wei, and Z. Xin-Xin, "Effects of doping, Stone—Wales and vacancy defects on thermal conductivity of single-wall carbon nanotubes," *Chin Phys B,* vol. 22, no. 1, p. 016501, 2013.

[65] M. Mahboob, M. Z. Islam, R. L. Lowe, and S. E. Bechtel, "Molecular dynamics and atomistic finite element simulation studies of the effect of Stone-Wales defects on the mechanical properties of carbon nanotubes," *Nanosci Nanotech Let,* vol. 5, no. 9, pp. 941-951, 2013.

[66] M. M. S. Fakhrabadi, P. K. Khorasani, A. Rastgoo, and M. T. Ahmadian, "Molecular dynamics simulation of pull-in phenomena in carbon nanotubes with Stone–Wales defects," *Solid State Commun,* vol. 157, pp. 38-44, 2013.

[67] B. Arash and Q. Wang, "Molecular separation with carbon nanotubes," *Comput Mater Sci,* vol. 90, pp. 50-55, 2014.

[68] I. V. Lara, I. Zanella, and S. B. Fagan, "Functionalization of carbon nanotube by carboxyl group under radial deformation," *J Chem Phys,* vol. 428, pp. 117-120, 2014.

[69] J. Xiao, J. Staniszewski, and J. Gillespie Jr, "Tensile behaviors of graphene sheets and carbon nanotubes with multiple Stone–Wales defects," *Materials Science and Engineering: A,* vol. 527, no. Mat Sci Eng A, pp. 715-723, 2010.

[70] S. Sharma, R. Chandra, P. Kumar, and N. Kumar, "Effect of Stone–Wales and vacancy defects on elastic moduli of carbon nanotubes and their composites using molecular dynamics simulation," *Comput Mater Sci,* vol. 86, pp. 1-8, 2014.

[71] X.-Y. Sun, R. Wu, R. Xia, X.-H. Chu, and Y.-J. Xu, "Effects of Stone-Wales and vacancy defects in atomic-scale friction on defective graphite," *Appl Phys Lett,* vol. 104, no. 18, p. 183109, 2014.

[72] M. Brcic, M. Canadija, and J. Brnic, "Influence of waviness and vacancy defects on carbon nanotubes properties," *Procedia Eng,* vol. 100, pp. 213-219, 2015.

[73] R. Rafiee and M. Mahdavi, "Molecular dynamics simulation of defected carbon nanotubes," *P I Mech Eng L-J Mat,* vol. 230, no. 2, pp. 654-662, 2016.

[74] P. Nayebi and E. Zaminpayma, "A molecular dynamic simulation study of mechanical properties of graphene–polythiophene composite with Reax force field," *Phys Lett A,* vol. 380, no. 4, pp. 628-633, 2016.

[75] S. Sharma, R. Chandra, P. Kumar, and N. Kumar, "Molecular level analysis of carbon nanofiber reinforced polymer composites," *J Compos Mater,* vol. 50, no. 13, pp. 1787-1804, 2016.

[76] S. Sharma, R. Chandra, P. Kumar, and N. Kumar, "Thermo-mechanical characterization of multi-walled carbon nanotube reinforced polycarbonate composites: A molecular dynamics approach," *Cr Mecanique,* vol. 343, no. 5-6, pp. 371-396, 2015.

[77] N. Taniguchi, T. Nishiwaki, and H. Kawada, "Tensile strength of unidirectional CFRP laminate under high strain rate," *Adv Compos Mater,* vol. 16, no. 2, pp. 167-180, 2007.

[78] Z. A. Mohammadi, S. F. Aghamiri, A. Zarrabi, and M. R. Talaie, "A comparative study on non-covalent functionalization of carbon nanotubes by chitosan and its derivatives for delivery of doxorubicin," *Chem Phys Lett,* vol. 642, pp. 22-28, 2015.

[79] E. V. Basiuk *et al.*, "Solvent-free functionalization of carbon nanotube buckypaper with amines," *Appl Surf Sci,* vol. 357, pp. 1355-1368, 2015.

[80] N. Kong, M. R. Shimpi, J. H. Park, O. Ramström, and M. Yan, "Carbohydrate conjugation through microwave-assisted functionalization of single-walled carbon nanotubes using perfluorophenyl azides," *Carbohydrate research,* vol. 405, pp. 33-38, 2015.

[81] V. D. Punetha *et al.*, "Functionalization of carbon nanomaterials for advanced polymer nanocomposites: a comparison study between CNT and graphene," *Prog Polym Sci,* vol. 67, pp. 1-47, 2017.

[82] G. Tian, H. Li, W. Ma, and Y. Wang, "Substituent Effects in pi-Stacking of Histidine on Functionalized-SWNT and Graphene," *Comput Theor Chem,* vol. 1062, pp. 44-49, Jun 15 2015.

[83] S. Sharma, R. Chandra, P. Kumar, and N. Kumar, "Molecular dynamics simulation of functionalized SWCNT–polymer composites," *J Compos Mater,* p. 0021998316628973, 2016.

[84] F. Aghadavoudi, H. Golestanian, and Y. T. Beni, "Investigation of CNT Defects on Mechanical Behavior of Cross linked Epoxy based Nanocomposites by Molecular Dynamics," *Int J Adv Design Manuf Technol,* vol. 9, no. 1, pp. 137-146, 2016.

[85] X. Peng and S. Meguid, "Molecular dynamics simulations of the buckling behavior of defective carbon nanotubes embedded in epoxy nanocomposites," *Eur Polym J,* vol. 93, pp. 246-258, 2017.

[86] H. Sun, "COMPASS: an ab initio force-field optimized for condensed-phase applications overview with details on alkane and benzene compounds," *J Phys Chem B,* vol. 102, no. 38, pp. 7338-7364, 1998.

[87] H. Sun, P. Ren, and J. Fried, "The COMPASS force field: parameterization and validation for phosphazenes," *Comput Theor Polym S,* vol. 8, no. 1-2, pp. 229-246, 1998.

[88] Y. Li, Y. Liu, X. Peng, C. Yan, S. Liu, and N. Hu, "Pull-out simulations on interfacial properties of carbon nanotube-reinforced polymer nanocomposites," *Computational Materials Science,* vol. 50, no. 6, pp. 1854-1860, 2011.

[89] S. Haghighatpanah and K. Bolton, "Molecular-level computational studies of single wall carbon nanotube–polyethylene composites," *Computational materials science,* vol. 69, pp. 443-454, 2013.

[90] R. Chawla and S. Sharma, "Molecular dynamics simulation of carbon nanotube pull-out from polyethylene matrix," *Composites Science and Technology,* vol. 144, pp. 169-177, 2017.

[91] P. M. Ajayan, L. S. Schadler, C. Giannaris, and A. Rubio, "Single-walled carbon nanotube–polymer composites: strength and weakness," *Advanced materials,* vol. 12, no. 10, pp. 750-753, 2000.

[92] E. Thostenson, W. Li, D. Wang, Z. Ren, and T. Chou, "Carbon nanotube/carbon fiber hybrid multiscale composites," *Journal of Applied physics,* vol. 91, no. 9, pp. 6034-6037, 2002.

[93] O. S. N. Ghosh, S. Gayathri, P. Sudhakara, S. Misra, and J. Jayaramudu, "Natural Rubber Nanoblends: Preparation, Characterization and Applications," in *Rubber Nano Blends*: Springer, 2017, pp. 15-65.

[94] T. Sabu, J. Jithin, and C. Chin Han, "Natural rubber materials, volume 2-composites and nanocomposites," ed: London: Royal Society of Chemistry, 2014.

[95] M. Levitt and S. Lifson, "Refinement of protein conformations using a macromolecular energy minimization procedure," *J Mol Biol,* vol. 46, no. 2, pp. 269-279, 1969.

[96] R. Fletcher and C. M. Reeves, "Function minimization by conjugate gradients," *The computer journal,* vol. 7, no. 2, pp. 149-154, 1964.

[97] O. Ermer, "Calculation of molecular properties using force fields. Applications in organic chemistry," in *Bonding forces*: Springer, 1976, pp. 161-211.

[98] J. Gou, B. Minaie, B. Wang, Z. Liang, and C. Zhang, "Computational and experimental study of interfacial bonding of single-walled nanotube reinforced composites," *Computational Materials Science,* vol. 31, no. 3, pp. 225-236, 2004.

[99] K. Liao and S. Li, "Interfacial characteristics of a carbon nanotube–polystyrene composite system," *Appl Phys Lett,* vol. 79, no. 25, pp. 4225-4227, 2001.

[100] Q. Zheng, D. Xia, Q. Xue, K. Yan, X. Gao, and Q. Li, "Computational analysis of effect of modification on the interfacial characteristics of a carbon nanotube–polyethylene composite system," *Appl Surf Sci,* vol. 255, no. 6, pp. 3534-3543, 2009.

[101] Y. Li *et al.*, "Molecular mechanics simulation of the sliding behavior between nested walls in a multi-walled carbon nanotube," *Carbon,* vol. 48, no. 10, pp. 2934-2940, 2010.

[102] N. Hu, Y. Li, and S. Liu, "Molecular Mechanics Investigations on Interfacial Properties in Nano-Materials due to Van der Waals and Electrostatic Coulombic Interactions," in *Engineering Asset Management and Infrastructure Sustainability*: Springer, 2012, pp. 391-415.

[103] S. Bal and S. Samal, "Carbon nanotube reinforced polymer composites-A state of the art," 2007: Indian Academy of Sciences.

[104] M. Wong, M. Paramsothy, X. Xu, Y. Ren, S. Li, and K. Liao, "Physical interactions at carbon nanotube-polymer interface," *Polymer,* vol. 44, no. 25, pp. 7757-7764, 2003.

[105] P. Collins, "Oxford Handbook of Nanoscience and Technology," ed: Oxford University Press USA, 2010.

[106] P. Ajayan, "PM Ajayan, V. Ravikumar, and J.-C. Charlier, Phys. Rev. Lett. 81, 1437 (1998)," *Phys Rev Lett,* vol. 81, p. 1437, 1998.

[107] L. Liu and Z. Huang, "A note on Mori-Tanaka's method," *Acta Mech Solida Sin,* vol. 27, no. 3, pp. 234-244, 2014.

[108] J. D. Eshelby, "The determination of the elastic field of an ellipsoidal inclusion, and related problems," *Proc Royal Soc A,* vol. 241, no. 1226, pp. 376-396, 1957.

[109] G. P. Tandon and G. J. Weng, "The effect of aspect ratio of inclusions on the elastic properties of unidirectionally aligned composites," *Polym Composite,* vol. 5, no. 4, pp. 327-333, 1984.

[110] Y. Benveniste, "A new approach to the application of Mori-Tanaka's theory in composite materials," *Mech Mater,* vol. 6, no. 2, pp. 147-157, 1987.

[111] P. K. Schelling, S. R. Phillpot, and P. Keblinski, "Comparison of atomic-level simulation methods for computing thermal conductivity," *Phys Rev B,* vol. 65, no. 14, p. 144306, 2002.

[112] P. Jund and R. Jullien, "Molecular-dynamics calculation of the thermal conductivity of vitreous silica," *Phys Rev B,* vol. 59, no. 21, p. 13707, 1999.

[113] L. Qiu, Y. Chen, Y. Yang, L. Xu, and X. Liu, "A study of surface modifications of carbon nanotubes on the properties of polyamide 66/multiwalled carbon nanotube composites," *J Nanomater,* vol. 2013, p. 2, 2013.

[114] D. Stojkovic, P. Zhang, and V. H. Crespi, "Smallest nanotube: breaking the symmetry of sp(3) bonds in tubular geometries," *Phys Rev Lett,* vol. 87, no. 12, p. 125502, Sep 17 2001.

[115] R. S. Ruoff and D. C. Lorents, "Mechanical and thermal properties of carbon nanotubes," *Carbon,* vol. 33, no. 7, pp. 925-930, 1995.

[116] C. Liu, H. Huang, Y. Wu, and S. Fan, "Thermal conductivity improvement of silicone elastomer with carbon nanotube loading," *Appl Phys Lett,* vol. 84, no. 21, pp. 4248-4250, 2004.

[117] S. Berber, Y. K. Kwon, and D. Tomanek, "Unusually high thermal conductivity of carbon nanotubes," *Phys Rev Lett,* vol. 84, no. 20, pp. 4613-6, May 15 2000.

[118] R. A. Buerschaper, "Thermal and electrical conductivity of graphite and carbon at low temperatures," *J Appl Phys,* vol. 15, no. 5, pp. 452-454, 1944.

[119] N. Shenogina, S. Shenogin, L. Xue, and P. Keblinski, "On the lack of thermal percolation in carbon nanotube composites," *Appl Phys Lett,* vol. 87, no. 13, p. 133106, 2005.

[120] A. Moisala, Q. Li, I. Kinloch, and A. Windle, "Thermal and electrical conductivity of single-and multi-walled carbon nanotube-epoxy composites," *Compos Sci Technol,* vol. 66, no. 10, pp. 1285-1288, 2006.

[121] Y. S. Song and J. R. Youn, "Evaluation of effective thermal conductivity for carbon nanotube/polymer composites using control volume finite element method," *Carbon,* vol. 44, no. 4, pp. 710-717, 2006.

[122] M. Dhawan, S. Sharma, and R. Chawla, "Variation of interfacial properties during carbon nanotube pullout from natural rubber," *Compos Interfaces,* pp. 1-13, 2018.

[123] J. Hone *et al.*, "Electrical and thermal transport properties of magnetically aligned single wall carbon nanotube films," *Appl Phy lett,* vol. 77, no. 5, pp. 666-668, 2000.

[124] W. Zhou *et al.*, "Single wall carbon nanotube fibers extruded from super-acid suspensions: Preferred orientation, electrical, and thermal transport," *J Appl Phys,* vol. 95, no. 2, pp. 649-655, 2004.

[125] C.-W. Nan, Z. Shi, and Y. Lin, "A simple model for thermal conductivity of carbon nanotube-based composites," *Chem Phys Lett,* vol. 375, no. 5-6, pp. 666-669, 2003.

[126] M. Biercuk, M. C. Llaguno, M. Radosavljevic, J. Hyun, A. T. Johnson, and J. E. Fischer, "Carbon nanotube composites for thermal management," *Appl Phys Lett,* vol. 80, no. 15, pp. 2767-2769, 2002.

[127] G. M. Odegard, S.-J. V. Frankland, and T. S. Gates, "Effect of nanotube functionalization on the elastic properties of polyethylene nanotube composites," *Aiaa J,* vol. 43, no. 8, pp. 1828-1835, 2005.

[128] Q.-S. Yang, B.-Q. Li, X.-Q. He, and Y.-W. Mai, "Modeling the mechanical properties of functionalized carbon nanotubes and their composites: design at the atomic level," *Adv Cond Matter Phys.,* vol. 2014, 2014.

[129] P. H. Shah and R. C. Batra, "Effect of covalent functionalization on Young's modulus of a single-wall carbon nanotube," in *Modeling of carbon nanotubes, graphene and their composites*: Springer, 2014, pp. 111-134.

[130] C. C. Ling, Q. Z. Xue, and X. Y. Zhou, "Mechanical properties of functionalized carbon nanotube as reinforcements," in *Adv Mater Res*, 2012, vol. 583, pp. 22-26: Trans Tech Publ.

[131] K. Z. Milowska, "Influence of carboxylation on structural and mechanical properties of carbon nanotubes: composite reinforcement and toxicity reduction perspectives," *J Phys Chem C,* vol. 119, no. 47, pp. 26734-26746, 2015.

[132] Y. Kuang and X. He, "Young's moduli of functionalized single-wall carbon nanotubes under tensile loading," *Compos Sci Technol,* vol. 69, no. 2, pp. 169-175, 2009.

[133] Z. Q. Zhang, B. Liu, Y. L. Chen, H. Jiang, K. C. Hwang, and Y. Huang, "Mechanical properties of functionalized carbon nanotubes," *Nanotechnology,* vol. 19, no. 39, p. 395702, Oct 1 2008.

[134] G. M. Odegard, S.-J. V. Frankland, and T. S. Gates, "Effect of nanotube functionalization on the elastic properties of polyethylene nanotube composites," *Aiaa Journal,* vol. 43, no. 8, pp. 1828-1835, 2005.

[135] A. Buldum and J. P. Lu, "Atomic scale sliding and rolling of carbon nanotubes," *Phys Rev Lett,* vol. 83, no. 24, p. 5050, 1999.

[136] J. Suhr, N. Koratkar, P. Keblinski, and P. Ajayan, "Viscoelasticity in carbon nanotube composites," *Nat Mater,* vol. 4, no. 2, pp. 134-7, Feb 2005.